A Hydrometallurgical Comparison between the Caustic and Sulphuric Acid Cracking of Steenkampskraal (SKK) Monazite

By:

U.A.Q Ahmed

Submitted in fulfilment for the award of the degree of Master of Science in Chemical Engineering

March 2017

Supervisor:

Prof. J Petersen

Co-supervisor:

Mr. W Zimba

University of Cape Town

The copyright of this thesis vests in the author. No quotation from it or information derived from it is to be published without full acknowledgement of the source. The thesis is to be used for private study or non-commercial research purposes only.

Published by the University of Cape Town (UCT) in terms of the non-exclusive license granted to UCT by the author.

University of Cape Town

ABSTRACT

The demand for rare earth elements (REEs) is continuously increasing since all high-tech products contain them. The Steenkampskraal (SKK) mine holds the full spectrum of REEs including high-value neodymium (Nd) used in the manufacture of high strength magnets, computers and hard drives.

The REEs and thorium (Th) deposit at the SKK mine in the Western Cape has been confirmed to be the highest grade in the world, at an average of 14.4% Total Rare Earth Oxide (TREO) and 2.14% ThO_2 respectively, with some locations of the ore body having as high as 45% TREO. These rare earths are hosted in the dominant mineral called monazite. In order to free the REEs from the monazite crystal, it requires "cracking" from the lattice such that it may be soluble in aqueous solution from which it undergoes purification. Two methods of cracking are usually employed in processing of monazite concentrate: caustic and sulphuric acid cracking. The aim of this study was to decide which route was more suitable to the SKK monazite in terms of factors which are usually considered in the setting up of such a processing plant, such as: recovery, capital expenditure (CAPEX); operating expenditure (OPEX); Safety, Health, Radiation, Environment and Quality (SHREQ); and lastly the effects on downstream processes.

Experiments were firstly done to develop a flow sheet based on the optimum conditions at which each of these processes were to be carried out. These results would firstly indicate the recovery obtained from each of the processes and additionally impact on our choice of equipment (hence CAPEX), the amount of reagents and power (thus OPEX) and other factors such as SHREQ and effects on downstream processes.

It was found that the TREO recovery from the caustic crack was 89% and that of the sulphuric acid crack 90%. However, the sulphuric acid crack required more process stages since the test results implied that the feed to the crack required drying and the product from the crack required conversion from a sulphate into a hydroxide salt. This resulted in a CAPEX of R 13,54M as opposed to the lower value of R 10,03M in the caustic circuit. Also, based on approximately 3 tons of feed to the hydrometallurgical circuit

it was found that the sulphuric acid crack required almost twice the amount of OPEX since the power requirement was double that of the caustic cracking method and the reagent requirements were approximately 22% greater. Both of the CAPEX and OPEX mentioned, indicate that the project NPV for the caustic cracking route is ~12.5% higher (~R200M) when treating SKK monazite.

The effect on downstream processes was also more negative in the sulphuric acid crack since there was a 5% loss during the double salt precipitation (DSP), 70% of which was Y. Were Y to be recovered at a later stage, its recovery, necessitating further process steps, would have further implications in the plant's CAPEX and OPEX. In addition to this, Th splits at an almost 1:1 ratio after the DSP step and would require an introduction of two new processing legs.

The SHREQ aspects that were considered identified minimal impact in the caustic crack route. These, however, were quite extreme in the acid crack route, due to the latter containing high volumes of chemically altered effluents as well as the handling of fine dust particles resulting from its numerous drying stages. In addition to this, the main motivation to favour the caustic cracking route was to avoid the SO_3 gas emissions that occurred when using the sulphuric acid cracking route.

Hence, it was concluded that the caustic cracking was superior to the sulphuric acid cracking route when treating SKK monazite.

Keywords: Steenkampskraal; Monazite; Rare Earth Elements; Caustic Crack; Sulphuric Acid Crack

DECLARATION

I, **Uwais Al Qarn Ahmed**, hereby declare that the work on which this dissertation/thesis is based is my original work (except where acknowledgements indicate otherwise) and that neither the whole work nor any part of it has been, is being, or is to be submitted for another degree in this or any other university.

I know the meaning of plagiarism and declare that all the work in the document, save for that which is properly acknowledged, is my own. This thesis has been submitted to the Turnitin module and I confirm that my supervisor has seen my report and any concerns revealed by such have been resolved with my supervisor.

I empower the university to reproduce for the purpose of research either the whole or any portion of the contents in any manner whatsoever.

Signed by candidate

Signature: _____

Date: **7 August 2017**

EBE Faculty: Assessment of Ethics in Research Projects

Any person planning to undertake research in the Faculty of Engineering and the Built Environment at the University of Cape Town is required to complete this form before collecting or analysing data. When completed it should be submitted to the supervisor (where applicable) and from there to the Head of Department. If any of the questions below have been answered YES, and the applicant is NOT a fourth year student, the Head should forward this form for approval by the Faculty EIR committee: submit to Ms Zakiya Chikte (Zakiya.chikte@uct.ac.za); New EBE Building, Ph 021 650 5739).

Please note – It is important to keep a signed copy of this form as students must include a copy of the completed form with the dissertation/thesis when it is submitted for examination.

Name of Principal Researcher/Student: Uwais Ahmed **Department:** Chemical engineering

If a Student: **Degree:** MSc **Supervisor:** Dr. J. Petersen

If a Research Contract indicate source of funding/sponsorship:

Research Project Title: A hydrometallurgical comparison on the behavioural response of the Steenkampskraal monazite ore between the caustic & sulphuric acid crack

Overview of ethics issues in your research project:

Question 1: Is there a possibility that your research could cause harm to a third party (i.e. a person not involved in your project)?	YES	~~NO~~
Question 2: Is your research making use of human subjects as sources of data? If your answer is YES, please complete Addendum 2.	YES	~~NO~~
Question 3: Does your research involve the participation of or provision of services to communities? If your answer is YES, please complete Addendum 3.	YES	~~NO~~
Question 4: If your research is sponsored, is there any potential for conflicts of interest? If your answer is YES, please complete Addendum 4.	YES	~~NO~~

If you have answered YES to any of the above questions, please append a copy of your research proposal, as well as any interview schedules or questionnaires (Addendum 1) and please complete further addenda as appropriate.

I hereby undertake to carry out my research in such a way that

- there is no apparent legal objection to the nature or the method of research; and
- the research will not compromise staff or students or the other responsibilities of the University;
- the stated objective will be achieved, and the findings will have a high degree of validity;
- limitations and alternative interpretations will be considered;
- the findings could be subject to peer review and publicly available; and
- I will comply with the conventions of copyright and avoid any practice that would constitute plagiarism.

Signed by:

	Full name and signature	Date
Principal Researcher/Student:	Signed by candidate UWAIS AL QARN AHMED	22/03/2016

This application is approved by:

Supervisor (if applicable):	Signed by candidate	23/03/2016
HOD (or delegated nominee): Final authority for all assessments with NO to all questions and for all undergraduate research.	Signed by candidate	23/03/2016
Chair : Faculty EIR Committee For applicants other than undergraduate students who have answered YES to any of the above questions.		

ACKNOWLEDGEMENTS

I would firstly like to thank my Creator for granting me the opportunity to expand my horizon of knowledge. At the same time, I thank God, The Almighty, that I'm a product of my parents Mr Aboobaker and Nazira Ahmed and that they infected me with their intelligence and energy for life, with their thirst for knowledge and their love. I am grateful that I know where I come from.

I would like to express my special appreciation and thanks to my advisor Professor Dr. Jochen Petersen, who has been a tremendous mentor for me. Despite the distance and thus limited face to face contact, your feedback and comments had me prompted into the right direction at the right moments. Thank you for allowing me the freedom of thought and helping me grow as a research scientist.

Undoubtedly, every field has an icon to which it's researchers look up to. In the case of rare earth elements it is to Witker Zimba that had inspired me to write this thesis. Witker, I don't really know how to express my gratitude to the help that you offered, and how special you are to me from an academic point of view. Simply putting it, I hope it suffices to say that, as I grow older I aim to be more like you- A walking encyclopaedia of knowledge!

A special thanks to the technical director of Steenkampskraal-Robbie Louw, who (despite his busy schedule) has grown me in terms of technical knowledge and whom I take as my "Guru" in the real world.

I would like to thank Steenkampskraal Monazite Mine, and especially Trevor Blench (the chairman of Steenkampskraal Holdings Ltd.) for allowing me to use the available experimental data to produce this thesis. Trevor, your humility and kindness radiates over great distances.

Lastly, to my beloved younger brother and friend- Abdullah Mahamed. Thank you for your continous support through this task of authoring my thesis. From day one you allowed me hundreds of opportunities to blabber my ideas despite not understanding a word I said. Your mere presence in my life has grown me into the person I am. Thank you!

TABLE OF CONTENTS

LIST OF TABLES

LIST OF FIGURES

NOMENCLATURE

LIST OF ABBREVIATIONS

Capital expenditure	CAPEX
Back-scattered Electron	BSE
Double Salt Precipitation	DSP
Fluid Cracking Catalysts	FCCs
Fibre Reinforced Plastic	FRP
Grams	g
Heavy Rare Earth Elements	HREEs
Hours	h
Ion Exchange	IX
Light Rare Earth Elements	LREEs
Middle Rare Earth Elements	MREEs
Mineral Liberation Analyzer	MLA
Mixed Rare Earth	MRE
Operating Expenditure	OPEX
Preliminary Economic Assessment	PEA
Process Flow Diagram	PFD
Rare Earth Elements	REEs
Rare Earth Extraction Company	RARECO
Rare Earth Oxide	REO
Run of Mine	ROM
Safety, Health, Radiation, Environment & Quality	SHREQ
Solid -Liquid	S/L
Specific Gravity	SG
Steenkampskraal	SKK
Steenkampskraal Monazite Mine	SMM
Temperature	T
Tons	t
Tons per hour	tph
Tri sodium phosphate	TSP
Total Rare Earth Oxide	TREO
United Kingdom	UK
X-Ray Diffraction	XRD
Pregnant Leach Solution	PLS

LIST OF ELEMENTS AND COMPOUNDS

Carbon monoxide	CO
Aluminium	Al
Barium	Ba
Calcium	Ca
Calcium phosphate	$Ca_3(PO_4)_2$
Cerium	Ce
Copper	Cu
Dysprosium	Dy
Hydrochloric acid	HCl
Iron	Fe
Lanthanoids	Ln
Lanthanum	La
Magnesium	Mg
Neodymium	Nd
Nitric Acid	HNO_3
Phosphorus	P
Praseodymium	Pr
Rare earth Chloride	$RECl_3$
Rare earth Hydroxide	$RE(OH)_3$
Rare Earth Sodium Sulphate	$RENaSO_4$
Scandium	Sc
Silicon	Si
Silver chloride	AgCl
Sodium	Na
Sodium hydroxide	NaOH
Sodium metabisulfite	SMBS
Sodium sulphate	Na_2SO_4
Strontium	Sr
Sulphur	S
Sulphuric Acid	H_2SO_4
Thorium	Th
Titanium	Ti
Uranium	U
Yttrium	Y

CHAPTER 1

1 BACKGROUND & INTRODUCTION

1.1 BACKGROUND

The Rare Earth Elements (REEs) are a group of 17 chemically similar elements consisting of the lanthanides, yttrium (Y) and scandium (Sc). Their unique properties have made them essential in the state-of-the-art technologies involving magnets, catalysts, batteries, various electronics application etc. REEs generally present in minerals such as monazite ((REE)PO_4), xenotime (Y(PO_4)) and bastnaesite (REE)CO_3F, though other REE bearing minerals do occur. The Steenkampskraal Monazite Mine (SMM), situated in the Western Cape is proven to have the highest grade of REEs as well as thorium (Th) in the world (Carlsen *et al,* 2014). In particular, the mine possesses extremely high grades of neodymium (Nd) and praseodymium (Pr) and both the latter have significant uses in the development of high tech products, particularly that of high strength magnets and various alloys. Additionally, Th can also be exploited as fuel for new generation nuclear reactors. With this in mind, the development of a mining operation with such a high grade of monazite has prompted the development of a flow sheet suitable to recover REEs from the monazite, particularly in terms of the applicable hydrometallurgical treatment routes (either that of caustic or sulphuric acid cracking).

Monazite mines across the world mostly use either sulphuric acid or caustic cracking of the monazite as the primary reaction stage when recovering the REEs. The choice made when selecting either one of these processes depends on several factors such as that of the recoveries obtained from each; the capital expenditure (CAPEX) and operating expenditure (OPEX) of the selected process; safety, health, radiation, environment and quality (SHREQ) factors; and lastly that of its effect on resultant downstream processing.

Generally, both the caustic and sulphuric acid processes yield satisfactory recoveries of the REEs, however, the notable differences in choice arise when one considers the grade of the ore. Usually, ores which are low grade and cannot be upgraded (to 50% TREO) are treated with sulphuric acid simply due to the majority of gangue being silicacious, which, when treated with caustic soda, will tend to form a gelatinous paste which tends to cause severe processing difficulties (particularly in the context of filtration). Additionally, silica would consume much of the relatively expensive reagent i.e. caustic soda. Ores which can be upgraded (to ~50% TREO), on the contrary, are treated with caustic soda simply as caustic consuming minerals are in minor quantities and thus filtration is easily done. An added advantage to the caustic process is that the expensive caustic soda may be regenerated and recycled, which may lead to a significant reduction in the plant's OPEX. Furthermore, there are various other factors that need to be considered in selecting either route, such as Safety, Health, Radiation, Environment and Quality (SHREQ) factors and subsequent downstream processes.

The Steenkampskraal mine is located in the Western Cape province of South Africa, approximately 330 km due north of Cape Town and 90 km east of the Atlantic Ocean shoreline. Steenkampskraal Ltd. was formerly known as Rare Earth Extraction Company Ltd. (RARECO). It was acquired by a Norwegian entity i.e. the Thorium Foundation in September 2015.

The Steenkampskraal Mine was operated by Anglo American subsidiary Monazite and Mineral Ventures (Pty) Ltd. from 1952 to 1963. During this time monazite concentrate was exported to, inter alia, Thorium Ltd. in the UK, where it was treated using the caustic cracking process. The deposit was subsequently the subject of several technical studies and mineral resource estimates. These include a study by RARECO in 2002 that formed the basis of approval of the Industrial Development Corporation (IDC) for funds to reopen the mine. Following the

acquisition of the mine by Great Western Minerals Group (GWMG) in 2010, a preliminary economic analysis (PEA) was completed by Snowden in December 2012 which demonstrated the economic viability of the project. Following this, Venmyn Deloitte completed a National Instrument (NI) 43-101 (Standards of Disclosure for Mineral Projects within Canada) Independent Technical Report (ITR) on the results of a feasibility study for the Steenkampskraal REEs project based on the price of REEs at the time. This ITR deviated from all previous work in three major respects: the production of the mine was increased from 2,700 tons to 5,000 tons of rare earth oxides (REOs) per year; it proposed a trackless mine based on the development of new underground infrastructure; and it proposed a sulphuric acid treatment process instead of the caustic soda process. The approach had to be changed due to the drop in prices of REEs from $76.69/kg (which excludes La, Ce, Ho, Er, Tm and Yb) to the current price of $17.80/kg. The project is now based on returning to a projected output of 2,700 tpa, optimum utilization of the existing mining infrastructure and the use of the caustic soda cracking process as opposed to the sulphuric acid cracking process. It is envisaged that this return to the original design will substantially reduce the capital and operating costs and de-risk the project in many significant ways- more specifically with regards to the method of cracking.

Thus, this study is aimed at comparing the caustic and sulphuric acid cracking methods when treating the Steenkampskraal monazite ore deposit.

1.2 Problem Statement

Although both the caustic and sulphuric acid cracking of monazite are proven technologies, the applicability of one over the other differs from ore to ore. Previously the company had designed the plant to use the sulphuric acid crack. However, due to the current price of REEs and new ownership, the caustic crack is now being considered as stated above. Thus a comparison of these two technologies is to be carried out

on the SKK monazite ore in order to establish the overall most economic process route to follow.

1.3 Objectives

This study aims to:

- Identify the various factors influencing the cracking of SKK monazite when using the caustic and sulphuric acid method.
- Once established, draw up a flow sheet for each route based on these optimum conditions and parameters investigated.
- Carry out a techno-economic comparison between the caustic and sulphuric acid cracking flow sheets on the SKK monazite ore in terms of their REE recoveries, CAPEX, OPEX, SHREQ aspects.
- Make a decision as to which cracking route best suits the SKK monazite.

1.4 Scope and Limitations of Study

The concentration of SKK monazite will briefly be illustrated in the relevant section of the literature study. Beside this, no beneficiation work to pre-concentrate the ore will be discussed. This study is focused only on the actual cracking of monazite by using the caustic and sulphuric acid methods and hence, the optimum conditions at which these are established will be reported in detail. These conditions will then be translated into a flow sheet depicting only the major equipment and conditions such that a comparison may be done in terms of the REE recoveries, CAPEX, OPEX, SHREQ aspects and the effects on downstream processes.

CAPEX and OPEX will be summarised for both methods of cracking on the basis of a 3 tph plant throughput for each circuit, thus assuming the same throughput to establish a fair comparative study.

1.5 Layout of thesis

The next chapter in this thesis is the literature study covering rare earths and their importance as well as the background of this project

and its economic importance in the current world market. In order to put the different cracking steps into context, a brief overview of monazite processing is dealt with together with the relevant advantages and disadvantages associated with each.

Chapter 3 deals with the Steenkampskraal Monazite Mine and its specifics associated with the mine, its location, current infrastructure and overall processing. The information presented in this chapter forms the basis of the elements of many of the results in chapter 5 and 6.

Chapter 4 deals with the experimental procedure for both the caustic and sulphuric acid cracking of monazite.

In chapter 5 and 6, the results from each of the above (the caustic and sulphuric acid cracking respectively) are reported upon and these results are then used to develop a flow sheet for each of the cracking methods. These flow sheets are simply the results drawn up from the experiments and are each scrutinised with regard to their implications upon which this thesis was based i.e. which one of the methods reports superior recoveries, CAPEX, OPEX, SHREQ and their associated effects downstream.

Chapter 7 reports the conclusions obtained above in the form of a trade off study between the caustic and sulphuric acid cracking in tabular form based on the studied factors mentioned earlier on.

CHAPTER 2

2 LITERATURE REVIEW

This chapter aims to elucidate the background to this thesis, from the beginning – as to what are rare earths and why they are important as demonstrated by their uses; market analyses of REE; the sources of REEs in the world with their associated projects; and lastly the general overall processing of REEs from monazite.

2.1 RARE EARTH ELEMENTS

2.1.1 GENERAL

Rare Earth Elements (REEs), sometimes referred to as Rare Earth Metals or simply Rare Earths, are a group of 17 chemically strongly related elements that comprise of scandium (Sc), yttrium (Y), and the 15 so-called lanthanides (Ln) which are the elements lanthanum (La), cerium (Ce), praseodymium (Pr), neodymium (Nd), promethium (Pm), samarium (Sm), europium (Eu), gadolinium (Gd), terbium (Tb), dysprosium (Dy), holmium (Ho), erbium (Er), thulium (Tm), ytterbium (Yb) and lutetium (Lu) (Voncken, 2015).

Traditionally, the REEs are sub-divided into light REEs (LREEs) Middle Rare Earth Elements (MREEs) and heavy REEs (HREEs) (Van Gosen *et al*, 2014). The LREEs occur in greater quantities than the HREEs. Commonly the LREEs are La, Ce, Nd and Pr while the HREEs are Tb, Dy, Ho, Er, Tm, Yb, Lu and Y (Jackson & Christiansen, 1993). Those elements occurring between these two groups i.e. Sm, Eu and Gd are known as the MREEs. The exact point of sub-division has become somewhat contentious, but is traditionally based on criteria which include the electronic structure of the element. Cerium is present in concentrations similar to those of copper. Scandium exhibits some chemical properties that are similar to REEs, but it is rarely found in the same minerals deposits as the lanthanides (British Geological Survey, 2011).

The name “Rare Earths” is certainly one which is misleading because they are not per se rare as, in the abundance tables (in the field of geochemistry); they are indicated as relatively abundant. However, this is a theoretical number. This, in no way reflects any proof of an economic exploitation. The common message that REEs are more abundant in the earth’s crust than gold or platinum is a common misleading aspect and of no economic use. In fact, rare earths *are* rare in a sense that, because the geochemical properties of REEs are specific, and thus they are characteristically dispersed throughout the crust and consequently, are rarely found in economically exploitable concentrations (Zepf, 2013).

REEs were in fact quite in a “low profile” until 2009 when, suddenly the general public started taking great interest in them due to China (claiming 97% of the worlds production) introduced production quotas, export quotas and export taxes, enforced environmental legislations, and granted no new rare earth mining licenses. This caused anxiety around the globe. This was simply due to the fact that high tech equipment such as hard-disk drives, smart phones, flat screen TVs and monitors, household and automotive rechargeable batteries and a list of other applications are simply not feasible without rare earths. This period (from 2009) was termed as “The Rare Earth Crisis” and awareness was created regarding this group of elements (Voncken, 2015). This also spawned a lot of renewed interest in re-commissioning existing REE mines around the world as well as exploiting new ones. This is expected to continue as long as the demand for REEs remains high and will be discussed later on.

Rare earths are used in many modern high technology applications as shown in section 2.1.2. Rare earths are also indispensable for many sustainable energy technologies, including energy production and increased energy efficiency due to their use in permanent magnets for applications such as in wind-turbine generators.

TABLE 1: APPLICATIONS OF RARE EARTHS.

	Wind Turbines	**Vehicles**		**Lighting**
Material	**Magnets**	**Magnets**	**Batteries**	**Phosphors**
Lanthanum			X	X
Cerium			X	X
Praseodymium	X	X	X	
Neodymium	X	X	X	
Samarium	X	X		
Europium				X
Terbium				X
Dysprosium	X	X		
Yttrium				X

2.1.2 USES OF RARE EARTHS

2.1.2.1 MAGNETS

Neodymium, praseodymium and dysprosium make up 24.1% of the mass of the rare earths in the SKK ore and 85% of the economic value.

Neodymium, praseodymium and dysprosium are the REEs that are used in the manufacture of permanent magnets. Nd and Pr form the basis of neodymium-iron-boron (NdFeB) magnets. Dy is of particular interest in magnet manufacturing as it allows NdFeB magnets to operate at high temperatures.

The market for NdFeB magnets has been growing at between 5% and 10% per year for many years. These magnets are used in a wide range of products ranging from miniature speakers in smart phones to wind turbines.

Because of their superior magnetic flux density, NdFeB magnets are in high demand for motors and generators. Small (servo) motors power disc drives in computers, electric windows in automobiles and multitudes of other everyday applications. Large motors, such as those in electric cars, use up to 200 g of Nd and 30 g of Dy per motor. Wind turbine generators can contain up to 500-600 kg of Nd per megawatt of electricity generation capacity (Constantinides, 2016).

Listed below are the major uses of Nd magnets in the manufacture of:

- **Hybrid and electric cars and trucks:**
  - It is estimated that between 6 and 10 million hybrid vehicles will be manufactured in 2020;
  - Each hybrid vehicle uses an average of 2 kg of Nd magnets in sensor and motor applications, such as electric power steerings, electric brakes, motors , speakers, etc.;
  - It is estimated that the total amount of Nd used in magnets in 2015 was 7,000 t and that this demand will rise to 17,000 t in 2020.
- **Wind turbines:**
  - Between 200 kg (hybrid) and 500-600 kg (direct drive) Nd magnets are used for each MW of output;
  - The replacement of a 500 MW coal-fired power plant with wind turbines would require about 275 t of Nd magnets;
  - The global demand for Nd for use in wind turbines in 2015 was about 8,500 t.
- **Electric bicycles:**
  - 65 to 350 g of Nd magnets are used in each electric bicycle;
  - 20 million electric bicycles were sold in China in 2009; the global market is forecast to grow to 60 million per year by 2018;
  - The annual Nd magnet demand for electric bicycles was 6,000 t in 2009 and is expected to rise to over 15,000 t by 2018.
- **Air conditioning:**
  - This industry is in a phase of rapid growth;
  - The use of Nd magnets in the motors increase the efficiency by 20% ;
  - The demand for Nd magnets in this industry in 2014 was over 4,000 t.
- **Acoustic transducers:**
  - More than 1.8 billion cell phones use speakers and vibrator motors;

- More than 280 million speakers are used in motor vehicles each year;

2.1.2.2 BATTERIES

Lanthanum is used in the manufacture of Ni-MH batteries (where M is actually lanthanum metal alloy).

Battery characteristics dictate how much energy can be stored and how quickly the energy can be delivered. The difference between these preferences can be critical for applications such as hybrid electric vehicles, which above all need power, and battery powered electric vehicles, which above all need energy to travel long distances without an internal combustion engine. These Ni-MH batteries are chosen for many hybrid vehicles like the Toyota Prius, while Tesla uses lithium-ion batteries.

Rechargeable batteries account for about 60% of the battery market and portable rechargeable batteries account for slightly more than a third of this market.

Rechargeable batteries are used in:

- Cellular phones
- Computers
- Camcorders
- Digital cameras
- MP3 Players
- Hybrid and electric vehicles
- Others (energy storage, medical applications, UPS, backup systems, etc.).

2.1.2.3 CATALYSTS

The use of rare earths in catalysts accounted for 19% of global consumption in 2010 (Anonymous, 2015).

The main uses are:

- Fluid Cracking Catalysts (FCCs) are used in the oil refining

process to convert heavy oils (gas oils and residual oils) into more valuable gasoline, distillates and lighter products. Rare earth elements are used in FCCs to control the product selectivity of the catalyst and to produce higher yields of the more valuable products such as gasoline. Lanthanum is the predominant rare earth used in FCCs, along with lesser amounts of Ce and Nd. Cerium is an important component of the FCC additives that reduce stationary source nitrogen oxide (NO_x) and sulphur oxide (SO_x) pollutants.

- Automotive catalytic converters use Ce to facilitate the oxidation of carbon monoxide (CO) and significantly reduce vehicle CO emissions. While the amount of cerium required per vehicle is small, catalytic converters are used in most passenger vehicles and accounted for approximately 9% of global rare earth demand by volume in 2015.

2.1.2.4 PHOSPHORS

The rare earths used in phosphors are necessary for the production of television sets and energy-efficient lamps. This is a small sector by volume, at about 7%, but a large sector by value, at 30-40%, as Eu and Tb command high prices.

2.1.2.5 GLASS

Cerium is used in ultra-violet light filtering and in the manufacture of glass polishing powders that take advantage of cerium's unique chemical and mechanical properties.

2.1.2.6 FUEL CELLS

Fuel cells are a promising clean energy technology for vehicle propulsion and for distributed power generation. Rare earths are used in several different fuel cell chemistries; in particular, there is no substitute for their use in solid oxide fuel cell separator stacks.

2.1.2.7 METAL ALLOYS

Rare earths are required to make many of the super alloys that are used to make components for items such as gas turbines and electric

generators. This sector accounts for about 18% of global rare earth demand. Rare earth metal alloys are also used in the manufacture of nickel metal hydride rechargeable batteries; the demand for these batteries is growing and this growth will increase the demand for La.

2.2 Market Analysis for REEs

The total market for rare earths in 1960 was about 5,000 t. By 2015, this market had grown to 145,000 t and there are forecasts that the market will grow to over 200,000 t by 2020 (Mkango Resources Ltd, 2016). The Ford Motor Corporation published a report in 2015 entitled "Rare Earths in Vehicles: Current Problems and Future Directions" which states that "A shortage in supply for neodymium, praseodymium and dysprosium is possible by the end of this decade."

2.2.1 Geographical Distribution of World Market

The countries that use the largest quantities of rare earths are China, Japan and the United States.

Over the past decade, many Japanese magnet manufacturers have relocated magnet factories to China to secure rare earth raw materials for their operations.

2.2.2 Forecast for REE Markets

As stated earlier one of the main driving forces for REEs arises from the magnet industry. The forecast for neodymium demand for use in magnets is shown in Figure 1:

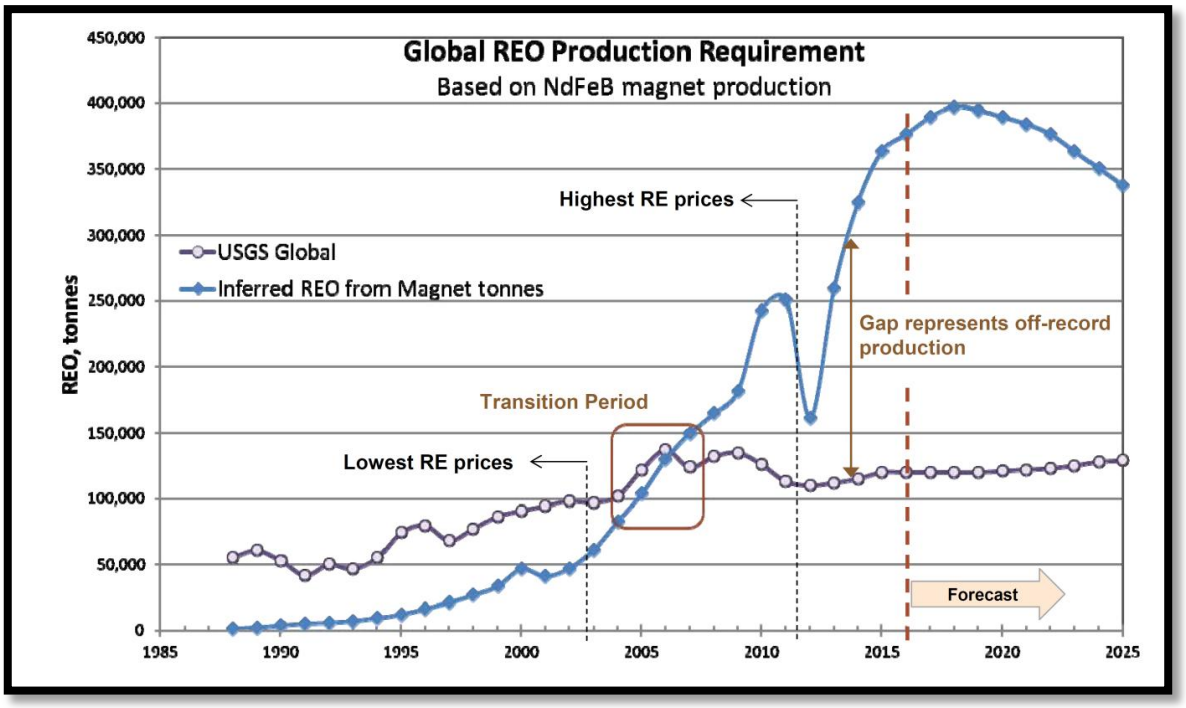

FIGURE 1: FORECAST REO CONSUMPTION IN NEODYMIUM MAGNETS (CONSTANTINIDES, 2016).

The explanation of the chart in Figure 1 is as follows:

- The purple line indicates published quantities of REO production (left scale).
- The blue line indicates the amount of REO required producing the magnet quantities shown on the chart presented in Figure 1 above.
- The sharp drop (blue line) in 2012 reflects the market contraction that was caused by high neodymium prices in 2011.
- The market has since rebounded, especially in China.
- There is a huge gap between the published rare earth production figures and the volumes of rare earths that are required to produce known magnet quantities.
- The unofficial rare earth production volumes may partly explain why rare earth prices remain relatively low.
- The volume of unofficial production is remarkable.

The normalised selling prices of the magnetic rare earths are shown in Table 2. The base year is 2002 with a value of 1; the values for 2016 are multiples of the 2002 prices indicated in the table.

TABLE 2: PRICES OF RARE EARTH METALS IN 2001

Rare Earth Metal	Value Ratio Relative to 2002 Prices ($)
Dy	32.1
Nd	7.5
Pr	6.2
Sm	5.3

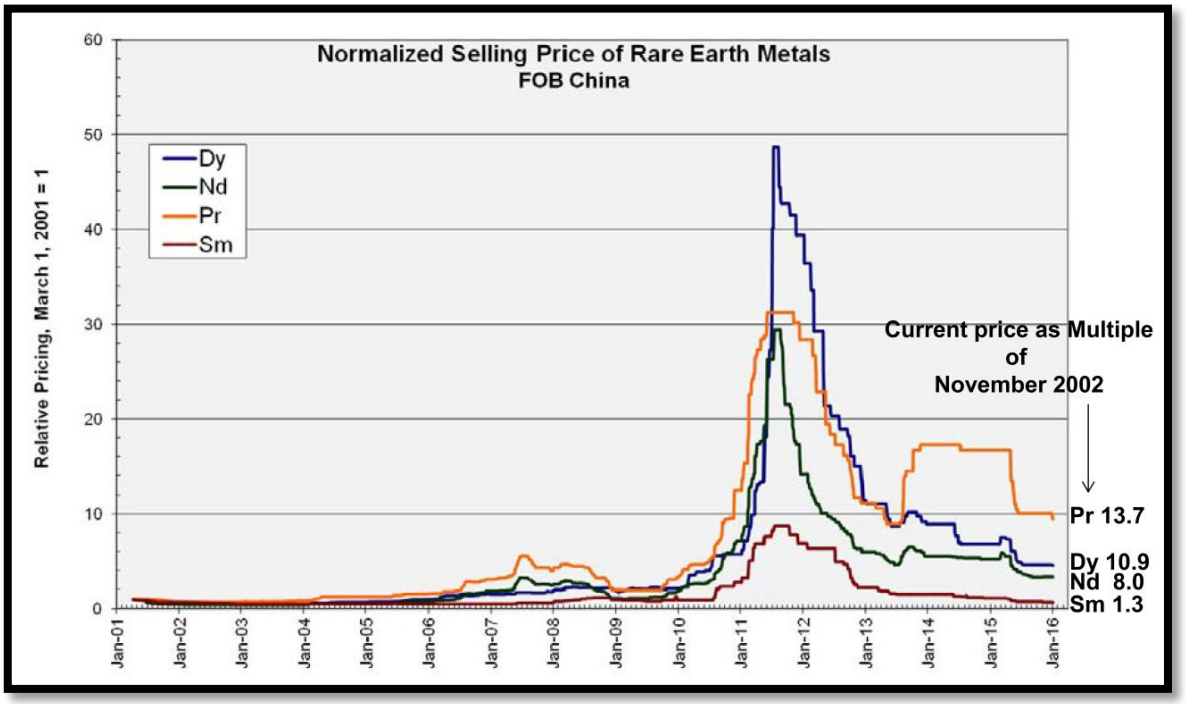

FIGURE 2: NORMALISED PRICES OF MAGNETIC RARE EARTHS (CONSTANTINIDES, 2016).

2.3 Major Mineral Sources

The major raw material for rare earths is monazite, xenotime, bastnaesite, and phosphate rock. However, ionic adsorption clays (with grades less than 0.5%) are also sources of REEs being exploited in China and are associated with extensive environmental damage, due to the poorly managed leaching methods (Papangelakis & Moldoveanu, 2014). A general overview of each will be touched on in the upcoming subsections. In addition to this, resources around the world will be

graphically depicted and a brief summary of the world's major deposits shall be tabulated together with their reserves and grades.

2.3.1 Monazite and Xenotime

Monazite is a lanthanide phosphate mineral containing some Th and small amounts of U. It occurs mainly in Brazil, Australia, India and USA. Xenotime is also a lanthanide phosphate but the individual lanthanides occur in a different proportion from that in monazite. It occurs in South East Asia associated with alluvial tin deposits. Monazite and xenotime are the main source of Th and the lanthanides; U is recovered as a by-product (Habashi, 2013).

2.3.2 Bastnaesite

Bastnaesite is a fluoro-carbonate ($Ln_2(CO_3)_3$, LnF_3, or $LnFCO_3$). The most important mined rare earth deposit is at the Mountain Pass Mine in California, where up to 40,000 tpa bastnaesite ore concentrate (70% REO) is produced by ore beneficiation (Kul *et al.*, 2008). Other important bastnaesite deposits are in Burundi, Madagascar and in Bayan Obu in Inner Mongolia in China. The bastnaesite, like monazite, is associated with magnetite-hematite-fluorspar (Habashi, 2013).

2.3.3 Phosphate Rock

Tonnage wise, phosphate rock is the most important REE source as compared with the other material; about 120,000,000 t of rock are treated annually as opposed to only 30,000 t of monazite and xenotime. However, no production of rare earths from this source is actually conducted due to the low grade (~1-2%). Phosphate rock is the main material for the production of phosphate fertilizers (Habashi, 2013).

2.3.4 Global Distribution of REE Sources and Projects

The global distribution of selected REE occurrences, deposits and mines is shown below together with the type of deposit.

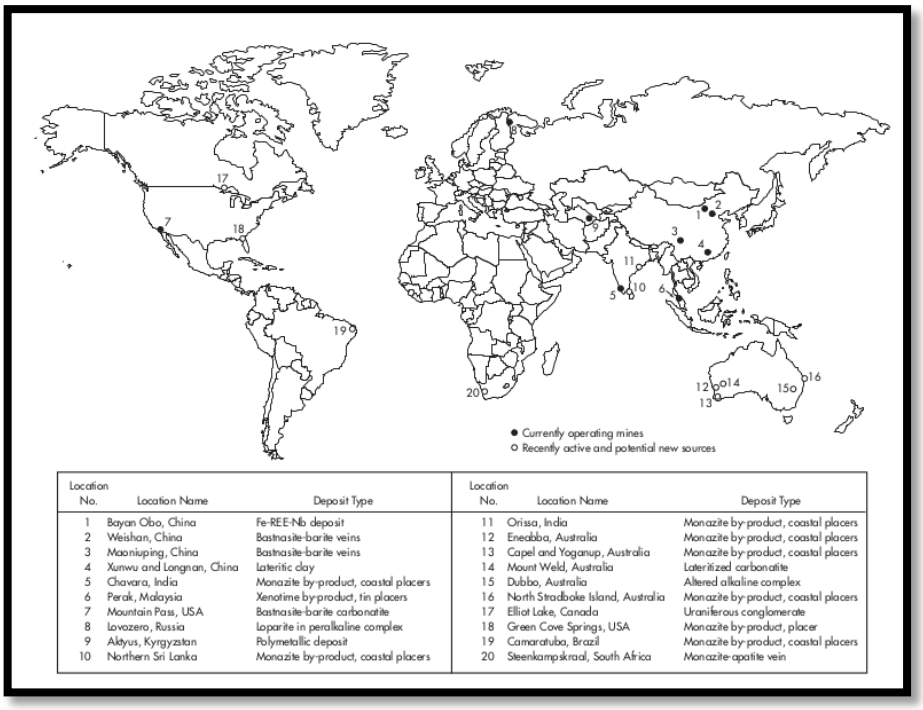

Location No.	Location Name	Deposit Type
1	Bayan Obo, China	Fe-REE-Nb deposit
2	Weishan, China	Bastnasite-barite veins
3	Maoniuping, China	Bastnasite-barite veins
4	Xunwu and Longnan, China	Lateritic clay
5	Chavara, India	Monazite by-product, coastal placers
6	Perak, Malaysia	Xenotime by-product, tin placers
7	Mountain Pass, USA	Bastnasite-barite carbonatite
8	Lovozero, Russia	Loparite in peralkaline complex
9	Aktyus, Kyrgyzstan	Polymetallic deposit
10	Northern Sri Lanka	Monazite by-product, coastal placers
11	Orissa, India	Monazite by-product, coastal placers
12	Eneabba, Australia	Monazite by-product, coastal placers
13	Capel and Yoganup, Australia	Monazite by-product, coastal placers
14	Mount Weld, Australia	Lateritized carbonatite
15	Dubbo, Australia	Altered alkaline complex
16	North Stradboke Island, Australia	Monazite by-product, coastal placers
17	Elliot Lake, Canada	Uraniferous conglomerate
18	Green Cove Springs, USA	Monazite by-product, placer
19	Camaratuba, Brazil	Monazite by-product, coastal placers
20	Steenkampskraal, South Africa	Monazite-apatite vein

FIGURE 3: MAP SHOWING THE GLOBAL DISTRIBUTION OF REE DEPOSITS (CASTOR & HENDRICK, 2006).

Table 3 indicates crucial aspects leading to the importance of the next section which addresses the question as to why the Steenkampskraal Monazite Mine is of significant interest.

TABLE 3: DEVELOPING PROJECTS AND ASSOCIATED ORE RESERVES AND GRADES (BRITISH GEOLOGICAL SURVEY, 2011).

Deposit	Company	REO reserves (million tons)	Ore reserves (million tons)	Grade (%REO)
Mountain Pass, USA	Molycorp Minerals	1.12	13.59	8.24
Mount Weld, Australia	Lynas Corp	1.42	17.49	8.1
Nolans Bore, Australia	Arafura Resources	0.85	30.3	2.8
Steenkampskraal - South Africa	Great Western Minerals Group	0.087	0.25	17
Dong Pao, Vietnam	Toyot Tsushu Corp/ Sorjitz, Vietnamese government	0.4	7.5	5.33
Zandkopsdrift, South Africa	Frontier Rare Earth	0.53	22.92	2.32
Hoidas Lake, Canada	Great Western Minerals Group	0.057	2.85	2
Strange Lake, Canada	Quest Rare Minerals	0.42	36.53	1.16
Bear Lodge, USA	Rare Element Resources	0.18	4.9	3.77
Kvanefjeld, Greenland	Greenland Minerals and Energy	4.91	457	1.07
Kutessay II, Kyrgyzstan	Stans Energy Corp	0.043	16.27	0.264
Nechalacho, Canada	Avalon Rare Metals	0.9	57.49	1.56
Zeus (Kipawa), Canada	Matamec Explorations	0.06	12.47	0.51

As can be seen from Table 3, from all the projects developing the production of rare earths, Steenkampskraal has the highest grade of rare earths in the world. This fact together with the outcome focus of this thesis (in selecting a suitable hydrometallurgical treatment for the SKK monazite) is able to render this project as the cheapest supplier of rare earth in the world. More about the mine and the processing of the monazite deposit will be discussed in the next section.

2.4 PROCESSING OF MONAZITE

This section shall deal with the overall processing of monazite. With regard to this, there seems to be a lack of literature with respect to the upgrading and cracking of monazite, with significantly more literature focused on downstream REE separation.

After mining, the ores are processed to increase their REE content. Concentration is normally undertaken at the mine or at a site close by and involves crushing the ore and separating REEs from the gangue minerals, using a range of physical and chemical processes.

2.4.1 PHYSICAL BENEFICIATION

Since placer deposits (like that of monazite) show considerable variation in mineralogy and chemical composition the beneficiation methods vary greatly. In many cases gravity separation is used as it is particularly effective for separating minerals with significant differences in densities. The sediment is fed into a suspension, and the gangue particles, having a lower density, tend to float and are removed as waste. The higher density minerals of economic value are also removed. Equipment including jigs, spiral and cone concentrators and shaking tables are used in gravity separation (Castor & Hendrick, 2006). In placer deposits the initial gravity separation is completed on the dredge during mining and unwanted tailings are discharged back into previously mined areas (Mcketta, 1994). Higher grade deposits such as the Chavra sands in India contain 70 -75 per cent heavy minerals and do not require this pre-concentration stage (Gupta & Krishnamurthy, 2005). However, monazite will normally form only 2-5% of this heavy mineral concentrate.

The concentrate produced by gravity concentration is processed in a dry mill. Concentrates of ilmenite, rutile, leucoxene, zircon and monazite are produced using a combination of gravity, magnetic and electrostatic methods. Monazite, in contrast to ilmenite, rutile and many other heavy minerals found in placer deposits, is non-conductive and is separated, with zircon, by electrostatic methods. It is then separated from the

zircon by electromagnetic or further gravity processing as it is moderately susceptible to magnetism and has a higher density. Xenotime is usually separated from monazite using precise gravity methods as they have very similar density and magnetic properties (Mcketta, 1994). For finer grained deposits (between 15 and 100 microns) gravity separation is not an efficient method as flotation is used (Gupta & Krishnamurthy, 2005).

This concentrate is then subjected to chemical treatment using either the caustic or sulphuric acid cracking routes in order to chemically extract the REEs from the lattice and then separate them. The differences between the caustic and sulphuric acid crack routes are briefly discussed in the next two subsections respectively and thereafter the separation is discussed.

2.4.2 Chemical Treatment

There are two methods of treating this concentrate i.e. the caustic cracking and sulphuric acid cracking method as indicated in Figure 4. Literature, as mentioned before is scant with details of the processes used, and overview papers mention at best block flow diagrams and brief operating conditions but no in-depth details of the actual process.

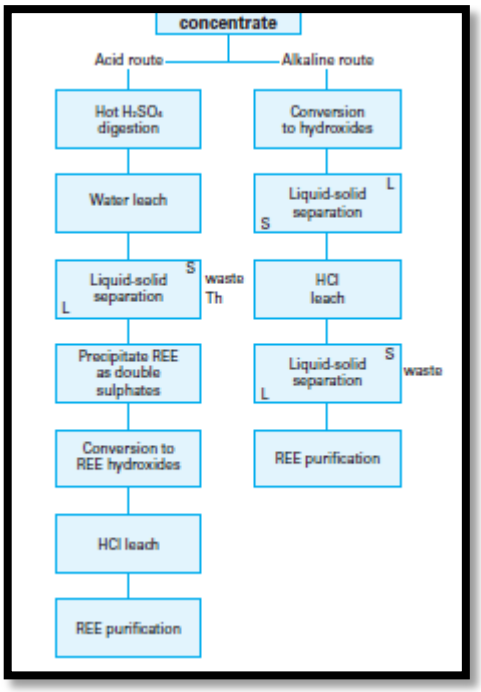

FIGURE 4: OVERVIEW OF EITHER ROUTE APPROPRIATE TO THE MONAZITE CONCENTRATE (BRITISH GEOLOGICAL SURVEY, 2011)

The decision between one and the other is an economic one; for example in Brazil, the NaOH method is used due to the shortage of sulphuric acid. However, the general tendency today is to use the NaOH process because it is possible to recover sodium phosphate as a by-product (Habashi, 2013).

2.4.2.1 THE SULPHURIC ACID CRACK

This method involves two steps i.e. digestion and dissolution of reaction mass.

Firstly, the concentrate (typically of ~30% grade) is digested in a closed reactor or baked in a rotary kiln fired either electrically or with gas together with 93% H_2SO_4 at about 200˚C for 2-4 hours at an acid to concentrate ratio of 2:1 on a mass basis. In general, the use of the kiln results in the production of SO_3 as well as radioactive dust particles resulting from the monazite undergoing cracking, which consequently requires strict emissions control. An acid to concentrate ratio lower than 2:1 results in incomplete reaction, while a higher ratio interferes with subsequent operations. Also, with temperatures lower than the

above, the reaction will be too slow, and if higher than 300 ˚C, insoluble thorium pyro-phosphate is liable to be formed (Nazari & Krysa, 2013).

The reaction of the REEs in the acid crack is exothermic and can be represented by the equation (Habashi, 2013):

$$2LnPO_4 + 3H_2SO_4 \xrightarrow{yields} Ln_2(SO_4)_3 + 2H_3PO_4$$

Thorium and Uranium present in the form of phosphates are also transformed into sulphates. Due to the high temperature used, the product is a thick paste of anhydrous sulphates or a porous solid.

The resulting mass is allowed to cool, diluted with water (to allow the insoluble material to settle) and then filtered. The clear leach solution is then subjected to further treatment to separate Th, U, and the lanthanides (Habashi, 2013).

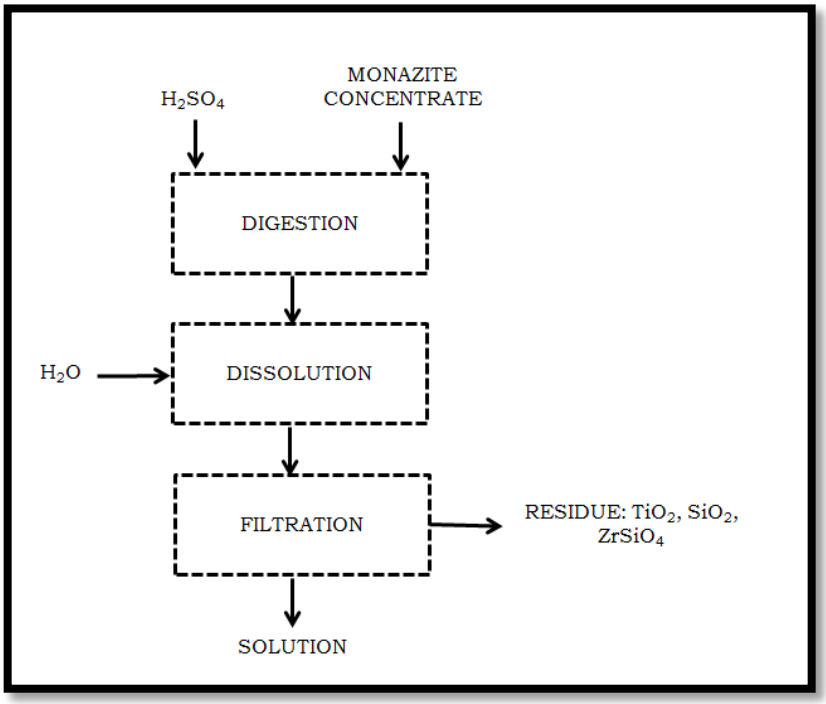

FIGURE 5: SULPHURIC ACID CRACKING OF MONAZITE.

2.4.2.2 THE CAUSTIC CRACK

The sodium hydroxide process differs from the acid process in that water soluble phosphates are formed while the lanthanides, Th, and U form insoluble hydroxides

$$LnPO_4 + 3NaOH \rightarrow Ln(OH)_3 + Na_3PO_4$$

$$Th_3(PO_4)_4 + 12NaOH \rightarrow 3Th(OH)_4 + 4Na_3PO_4$$

$$UO_2HPO_4 + 2NaOH \rightarrow UO_2(OH)_2 + Na_2HPO_4$$

Optimum conditions of digestion are 40-50% NaOH, 160˚C, NaOH to concentrate ratio of 2:1, and the time of reaction is about 3 h (Habashi, 2013). Working with NaOH concentrations such as this would require specialized materials of construction and may impact the CAPEX; additionally also OPEX is affected since NaOH itself is substantially higher in price as compared to H_2SO_4. The resultant product is a thick slurry; it is then diluted with water then filtered, washed, and dried. The cake obtained is composed of hydroxides of U, Th, and lanthanides containing small amounts of phosphates; it is dissolved in HCl for further separation. The leach solution contains unreacted NaOH as well as the phosphates originally present in the concentrate. When allowed to cool to about 60˚C tri sodium phosphate hydrate ($Na_3PO_4 \cdot 10H_2O$) crystallizes out. After separation, the solution typically analyses 47.4% NaOH, 0.5% Na_3PO_4, 1.5% Na_2SiO_3, and can be recycled.

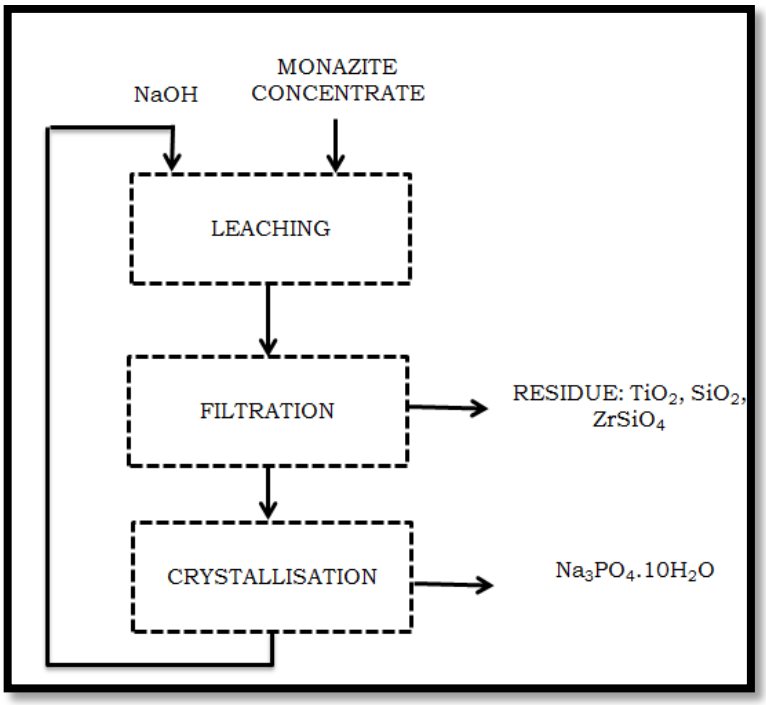

FIGURE 6: THE CAUSTIC CRACKING OF MONAZITE.

2.4.3 SEPARATION OF REES

The high value of REE depends on their effective separation into high purity compounds. Separating individual REE from concentrates is a very difficult process due to their similar chemical properties (Morais & Ciminelli, 2004). Rare earth element processing technology is most advanced in China, which can supply REE products at 99.9999% purity, whilst French companies typically produce 99.99% pure REEs and Japanese sources 99.9% REEs.

Selective oxidation or reduction of certain REEs can be useful in the separation process. In general REEs are characteristically trivalent but cerium, praseodymium and terbium can also occur in the tetravalent state, and samarium, europium and terbium display divalency. These differences in chemical behaviour can be exploited in the separation of individual elements (Gupta & Krishnamurthy, 2005). Cerium is generally separated by selective oxidation whilst other REE can be separated using fractional crystallisation, fractional precipitation, solvent extraction and ion-exchange methods. These methods are based on the small differences in basicity, resulting from decreasing size in ionic radius from lanthanum to lutetium (Morais & Ciminelli, 2004). Until the early 1950s fractional precipitation and fractional crystallisation were the only techniques available for separating REE. These processes, however, are laborious and inefficient and have consequently been superseded by more effective techniques like ion exchange and solvent extraction (Gupta & Krishnamurthy, 2005). The solvent extraction method is most appropriate for separating the LREEs, with the HREEs being more difficult to separate using this method (Moore, 2000).

Ion exchange is a process in which ions are exchanged between a solution and an insoluble (usually resinous) solid. The solution containing the REEs is passed over the ion exchange resin. The REEs displace the cations on the resin surface. This produces an aqueous waste containing the exchanged cations, with a mixture of REE deposited on the resin. Individual REEs are then separated using a

complexing agent which has different affinities for various REEs (United States Environmental Protection Agency, 2008). The ion exchange method produces highly pure REEs in small quantities. However, it is a time consuming process and only a few HREEs are purified commercially on a small scale using ion exchange.

For large scale production solvent extraction is the preferred route (Kilbourne, 1993). Solvent extraction (SX), or liquid-liquid extraction, is a method used to separate compounds on the basis of their relative solubility's in two immiscible liquids, typically water and an organic solvent. This process relies on differences in the relative solubilities of REEs in the liquid phases used.

On an industrial scale the SX process is carried out in a group of mixer settlers, called batteries. This allows repetitive fractionation during a continuously flowing process. Initially the process is relatively ineffective as the chemical properties of the REE ions in solution show only incremental variation with atomic number. However, when the process is repeated many times each REE is successfully separated from the other (Rhodia, 2009).

The end products of SX are usually solid rare earth salts or oxides. An insoluble salt is precipitated from the solution obtained from the solvent extraction process. This is separated, dried or calcined at high temperatures and then ground (Rhodia, 2009). REE compounds with a purity of more than 99.99 per cent can be produced using this method (Castor & Hendrick, 2006).

2.5 Radiological Risks

The association of Th and U with rare earths creates a health hazard problem because of its radioactivity. Monazite contains low but varying levels of primordial thorium-232 and uranium-238, along with their decay products. Uranium-235 is also present but in very low quantities. Thorium-232 and uranium-238 are rather benign by themselves, but some of their decay series products can represent a danger to the

environment due to the energetic particles and gamma rays released during radioactive decay. Therefore, uranium-238, thorium-232, and their decay products could present a threat to human health, if they are released into the environment. Radium-226 in the uranium-238 decay chain produces radon-222 gas, with $t_{1/2}$ = 3.8 days and bismuth-214, which are intensely radioactive. Due to the short half-lives of radon-222 (gas and prone to be inhaled and to decay in the lungs) and bismuth-214 ($t_{1/2}$ = 20 minutes) from the radioactive decay of radium-226, these isotopes exhibit accelerated decay rates than their parents, which have very long half-lives. This is the reason that radium-226 is often regulated as opposed to uranium-238. Nuclear radiation has the potential to dislodge electrons from important biological molecules including water, protein, and DNA (Gupta & Krishnamurthy, 2005). Thus these concerns need to be mitigated when considering the processing of the plant when treating REEs.

CHAPTER 3

3 THE STEENKAMPSKRAAL (SKK) MONAZITE MINE & PROCESSES

This chapter aims to comprehensively discuss the background and associated aspects surrounding the process at SKK, such as the fundamental background of the mine site and SKK site specific constraints etc. (leading up to the problem statement and research questions stated in chapter one); geology and mineralogy; upstream processing prior to the cracking of the resultant monazite concentrate and an outline of the two competing process options (with their respective block flow sheets); as well as scope and limitations for the trade-off analysis between the caustic and sulphuric acid cracking route to be selected.

3.1 BACKGROUND OF MINE SITE & STEENKAMPSKRAAL

3.1.1 LOCATION

The Project is located in the Knersvlakte, in the northern sector of the Western Cape Province, approximately 380 km north of Cape Town and 90km east of the Atlantic Ocean shoreline; it is therefore close to the ports of Cape Town and Saldanha Bay (approximately 286 km) and to Cape Town International Airport.

Portion 1 of the farm Steenkamps Kraal No. 70 is in the Matzikama Local Municipality, which is within the West Coast District Municipality (see Figure 7). The main town in Matzikama is Vredendal, which is both the administrative and commercial centre of the municipality. Vredendal is about 105 km south of SKK. The town of Vanrhynsdorp is about 80 km south of SKK. SKK has no link to the national electricity grid (which is ~80km away), and thus electricity at the location is entirely supplied by diesel generators since there are constraints on the CAPEX in terms of connecting to the grid. However at a later stage this may be considered.

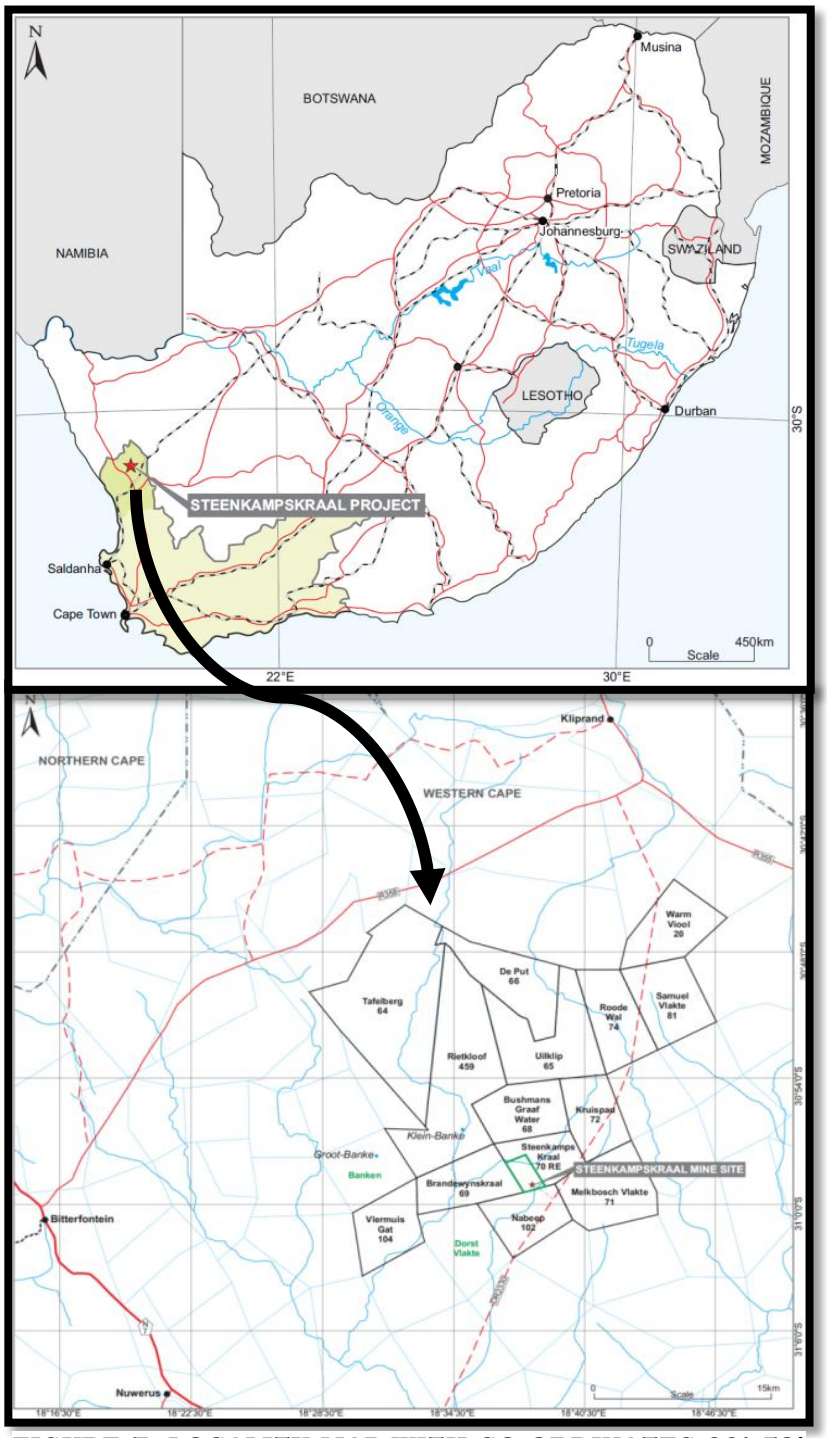

FIGURE 7: LOCALITY MAP WITH CO-ORDINATES 30° 59' 10"S AND 18° 37' 44"E

3.1.2 Recent History

The ownership of SKK and the historical exploration undertaken by the various exploration and production companies date back to 1949. For the purpose of this thesis, recent historic information is presented as it pertains to the relevant studies applicable for the re-opening of the mine.

Rareco acquired the Prospecting Right for SKK in 1989 and undertook an exploration and evaluation campaign. Highlights of this campaign included:

- A geological investigation and a quantification of the ore reserves by Dr. Felix Mendelsohn in 1991;
- The drilling and testing of three boreholes for water supplies;
- A borehole census and a groundwater sampling and analysis by the Atomic Energy Corporation;
- A survey of the blasted monazite material remaining underground in the ore passes, stopes and drives;
- A scintillometer survey of the contaminated surface area;
- Additional underground sampling focused on the host rock surrounding the monazite deposit;
- A drilling programme comprising four boreholes (RD1, RP1, RP2 and RP3) drilled on the southern limit of the known underground workings. These boreholes formed a part of the 1996 Rareco ore reserve estimate by Mendelsohn; and
- Exploration samples were submitted to the Anglovaal Research Laboratory.

Academic studies have indicated that the mineralised monazite vein showed a normal REE distribution enriched in LREE over HREE (Andreoli *et al*, 1994).

In 1994, Rareco listed on the JSE-Venture Capital Board and raised about R30 million to develop the mine. Rareco prepared a bankable feasibility study at that time. Rareco signed an off-take agreement with Rhodia in France and applied for, and received, financial support from the IDC in South Africa and from Proparco, an agency of the Agence Française de Développement. The project did not proceed at that time because Rhodia did not proceed with the off-take agreement.

During the early 2000s, rare earth prices fell to low levels and the SKK project could not proceed at that time; Rareco delisted from the JSE in 2007.

In June 2010, SMM applied for, and the Department of Mineral Resources granted a New Order Mining Right for SKK.

TABLE 4: RECENT HISTORIC OWNERSHIP AND EXPLORATION OF THE STEENKAMPSKRAAL PROJECT

	COMPANY **RIGHTS**		
1989 - 1996	Rare Earth Extraction Co. Ltd. (Rareco)		Quantification of 1991 (Mendelsohn) reserves, water borehole drilling and census, water sampling and a survey of the broken monazite rock left in the ore passes. Additional underground sampling and surface drilling (4 drill holes). Results were used in the 1996 ore reserve estimate.
1996 - 2007			Rareco listed on the JSE in 1994 to raise funds to develop the SKK Project.
2007 - 2011	Rareco	Steenkampskraal Monazite Mine (Pty) Ltd	New order (20 year) mining right issued in June 2010
2011- 2015	Great Western Minerals Group Ltd. (GWMG)		Completion of a large scale exploration campaign comprising 232 drill holes totalling 28,157m. In addition, 99 channel samples were collected totalling 122m.

			The results of this campaign were used to calculate a Mineral Resource Estimate which was used in the 2012 Snowden PEA. The Mineral Resource Estimate was updated in 2013.

On 12 July 2011, GWMG completed its acquisition of 100% of the shares of Rareco.

On 17 July 2015, Thorium Foundation completed its acquisition of 100% of Rareco's shares from GWMG.

3.1.3 Logistics

SKK is 380km north of Cape Town and access is provided by the N7, a national tarred road, for about 350 km, and then by the unsurfaced DR2230 secondary gravel road for about 30 km; this road passes the SKK access road which covers a distance of about 2 km.

The nearest tarred airport to SKK is at Vredendal, which is about 100 km south of the mine. Helicopter access from Cape Town International Airport to the SKK is the quickest and most direct access route.

SKK is 66 km from the railway station at Bitterfontein, 294km from the deep water port at Saldanha Bay and 380km from the Cape Town Harbour.

3.1.4 Property Description

3.1.4.1 Mining Infrastructure

The remaining historic infrastructure at SKK comprises:

- A single incline shaft which was the main haulage shaft located on the southern slope of the SKK "koppie" (slope);

- A single vertical shaft and a sub-vertical adit (raise) located on the surface expression of the historic workings;
- Limited open-cast excavations on the southern slope of the SKK koppie;
- Low-grade rock dumps (incorporating the contaminated historical mine ruins) and tailings;
- The historic infrastructure included the remnants of the original mine buildings which were demolished by SMM and incorporated into the historic low-grade, surface rock dump;
- The historic slimes dams were moved and consolidated (see Figure 8)

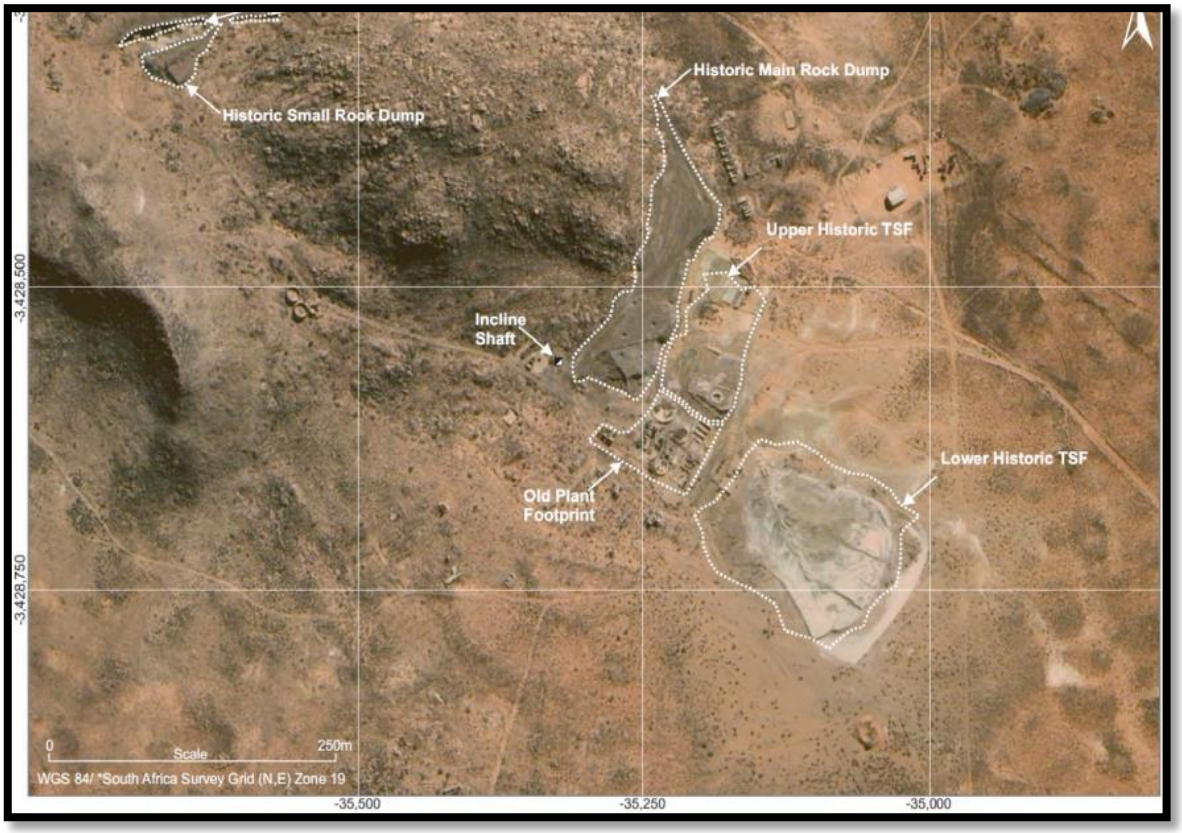

FIGURE 8: SATELLITE IMAGE OF THE HISTORIC MINE SITE

3.1.4.2 UPGRADE OF INFRASTRUCTURE AND SERVICES

SMM has embarked on a programme which incorporates the re-establishment of surface infrastructure and the underground workings for future mine production. The new infrastructure developed by GWMG between 2010 and 2015 includes:

- An upgraded historic core shed and supporting exploration infrastructure;
- Project office buildings including site administration, geology, safety and security;
- A reverse osmosis plant (since the salinity of the water is extremely high and may affect the product at the end of the process) to supply up to 30,000l/h (the source of which are numerous boreholes), which is sufficient for the mine's requirements (based on this study as well as others);
- Communications infrastructure, including four Telkom land-based telecommunication lines and a mobile telephone repeater tower that has not yet been commissioned. Electronic communication is provided by a dedicated satellite link. This infrastructure will require expansion to when construction and mining commence.
- The dispersal of naturally occurring radioactive material (NORM), occurring primarily as eroded material scattered over the slopes of the Steenkampskraal Koppie, has been partially remedied by SMM with its initial rehabilitation measures.

Figure 9 and Figure 10 show the Steenkampskraal mine site in its present state.

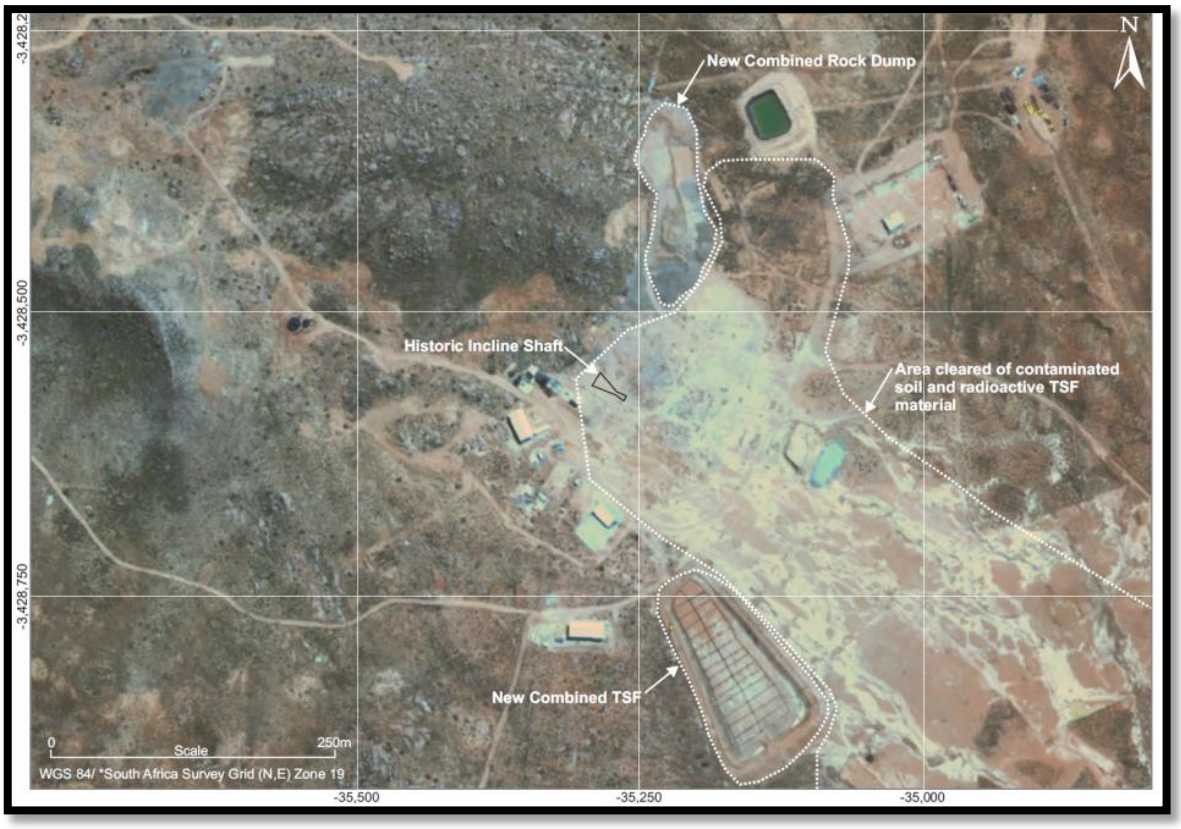

FIGURE 9: STEENKAMPSKRAAL MINE SITE IN ITS PRESENT STATE

FIGURE 10: INCLINE SHAFT HEADGEAR AND STEENKAMPSKRAAL MINE SITE

3.2 GEOLOGY & MINERALOGY OF STEENKAMPSKRAAL

3.2.1 GEOLOGY

Geological mapping of the Steenkampskraal Project area has identified numerous upper-granulite metamorphic grade gneisses belonging to the Spektakel Suite, Little Namaqualand Suite and Kamiesberg Group which include granitic gneiss, charnockitic gneiss, mafic gneiss, quartz-feldspathic paragneiss, metaquartzite, as well as minor occurrences of calc-silicate gneiss and marble.

Illustrations of the structural interpretation and geology and the geology of the Steenkampskraal project are shown Figure 11 and Figure 12, respectively.

Geochemically and mineralogically, the suite has quartz contents and feldspar ratios that span a diverse range of felsic rocks from alkali-feldspar granite through granite to quartz syenite. The Steenkampskraal Intrusive Suite also includes mafic members such as hypersthenite, anorthosite and leuconorite (Basson, 2013) as well as the associated target mineralised monazite vein. In more detail the mineralogy of the members of the intrusive suite commonly contains alkali-feldspar and quartz with variable amounts of plagioclase, biotite, garnet and orthopyroxene. Apatite, zircon and monazite are common accessory minerals; however, fluorite is rare in this regard.

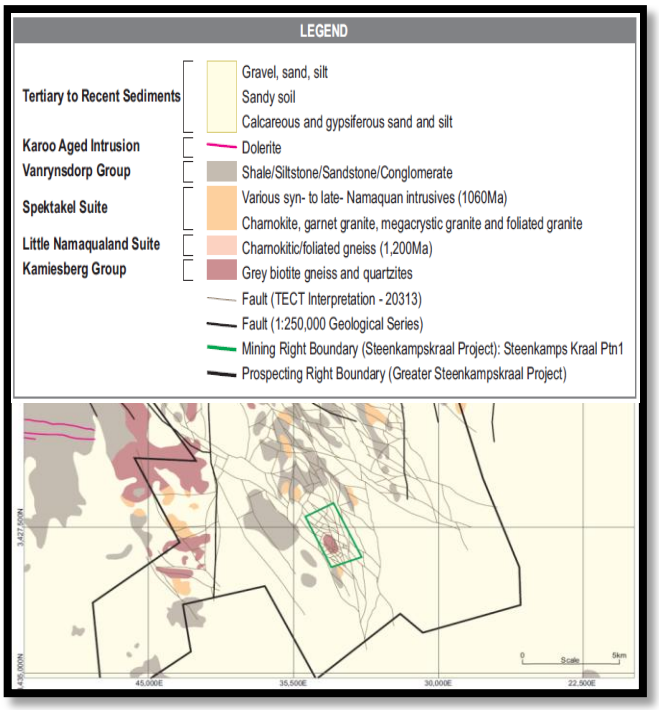

FIGURE 11: STRUCTURAL INTERPRETATION AND GEOLOGY OF THE STEENKAMPSKRAAL PROJECT AREA

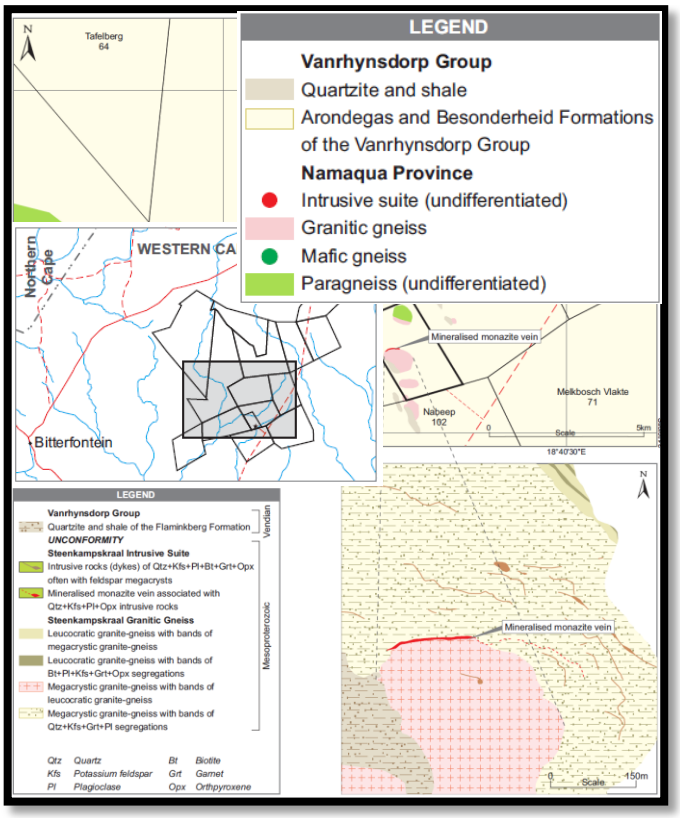

FIGURE 12: GEOLOGY OF THE STEENKAMPSKRAAL PROJECT

The mineralised monazite vein strikes east-west through the Steenkampskraal Koppie where it is spatially associated with other granitoid members of the Steenkampskraal Intrusive Suite.

The mineralised monazite vein is a narrow lenticular-shaped body, with an average thickness of 0.6 m, a strike length of approximately 400 m at surface, a total known strike length of approximately 1,200 m (Jones & Burnett, 2013) and a known dip extension to about 160m below surface.

The vein appears to be a unique intrusive body with a fundamental structural control to its dip, plunge and thickness. The thinning, pinching and swelling of the mineralised monazite vein is a primary feature associated with the development and emplacement of the vein and a later ductile shearing of the mineralised monazite vein parallel to its orientation.

The mineralised monazite vein is hosted within foliated granites, granite-gneisses and granulite-facies ortho- and paragneisses. These host rocks display uranium and thorium enrichment (Andreoli *et al*, 1994) that could have acted as a source of the radionuclides.

3.2.2 MINERALOGY

The mineralised vein consists of an unusual combination of minerals namely, monazite together with a gangue of apatite, quartz, ferruginous chlorite, iron oxide minerals, ilmenite and sulphides such as chalcopyrite, pyrite and galena (Bergmann *et al*, 2013). The modal analysis of the underground ore (the mineralized vein) is given in the table below and shows that the sample consists of 40.2 percent monazite with quartz, allanite, apatite and magnetite as the other major constituents.

TABLE 5: MODAL ANALYSIS OF THE UNDERGROUND STEENKAMPSKRAAL SAMPLE (BERGMANN *et al*, 2013).

		Relative Proportion Mass (%)
Mineral	**Density (g/cm^3)**	**Underground**
Monazite	4.6	1.8
Monazite-Th	4.6	38.4
Allanite	3.82	9.9
Xenotime-(Y)	4.75	0.1
Tritomite	3.22	0.1
Thorite	5.35	0.1
Thorianite	10	0.3
Epidote	3.45	0.1
Ilmenite	4.72	0.5
Apatite	3.2	8.5
Magnetite	5.15	8.8
Quartz	2.65	11.1
Plagioclase	2.69	4.4
Microcline	2.56	0.6
Pumpellyite (Amphibole)	3.2	0.3
Muscovite	2.9	1.2
Illite	2.75	4.7
Chalcopyrite	4.2	2.4
Covellite	4.68	0.1
Bornite	5.1	0.1
Pyrite	5.01	1.9
Almandine (garnet)	4.2	3.8
Rutile	4.25	0.5
Zircon	4.65	0.2
Titanite	3.48	0.1
Total		100

In the SKK samples, five different REE-bearing minerals were detected using the MLA. The REE-bearing minerals that were detected include: monazite, monazite-Th, allanite, xenotime and tritomite. Apatite did not contain any REEs in its crystal lattice. The monazite mineral group was divided into two different mineral groupings based on the presence and absence of thorium in the crystal lattice (termed “monazite-Th” and “monazite” respectively). Other thorium-bearing minerals present in the

samples are thorite and thorianite. In all cases, the monazite-Th displays a homogeneous and clean surface (Figure 13).

Monazite without Th in the crystal structure shows evidence of alteration and it does not have a clean surface (Figure 14). The altered monazite is also found to be hosting REE-bearing minerals such as xenotime and thorite. The presence of allanite (an epidote containing REEs) is indicated in Figure 15. Allanite shows an association with tritomite and apatite.

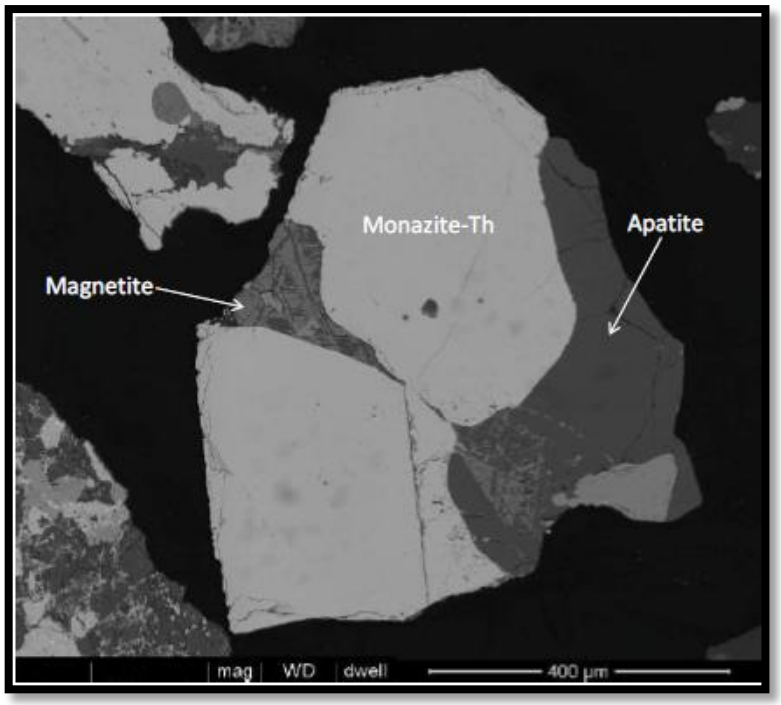

FIGURE 13: BSE IMAGE INDICATING MONAZITE CONTAINING THORIUM, MAGNETITE AND APATITE (BERGMANN *et al*, 2013).

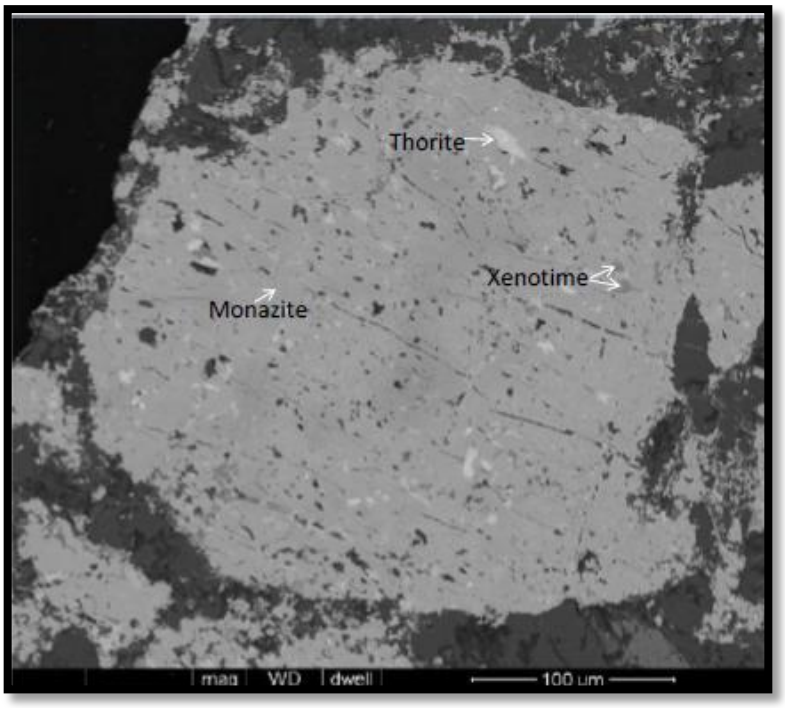

FIGURE 14: BSE IMAGE INDICATING MONAZITE, THORITE AND XENOTIME (BERGMANN *et al*, 2013).

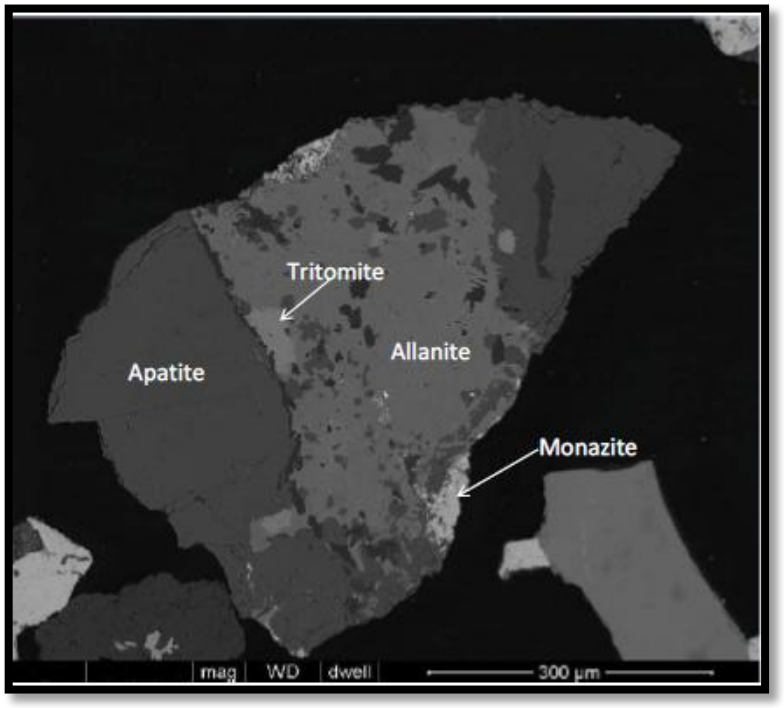

FIGURE 15: BSE IMAGE INDICATING ALLANITE, APATITE, TRITOMITE AND MONAZITE (BERGMANN *et al*, 2013).

3.3 PROCESSING AT STEENKAMPSKRAAL

The current SKK processing team are busy developing an underground mine and processing facility to produce approximately 2700 annual tons of total rare earth oxides (TREO). There are three resources that will need to be treated through the processing plant: underground ore, the historical rock dump material and the historical tails material from previous operations. Since majority of the resource is underground, the design shall be based on treating this material as a major source when considering hydrometallurgy. This section serves to provide the detailed process description for the concentrator portion of the plant. Ore mineralogy (in the previous section) has played a key part in the process route selection and understanding of metallurgical behaviour. The basis of the process route described below has been derived from historical test work conducted prior to 1995 and the modern day test work conducted at Mintek. The process route is simplified in two sections i.e. upgrading of the mined ore using beneficiation methods to concentrate monazite followed by the chemical treatment, either the sulphuric acid crack or the caustic cracking of monazite concentrate.

3.3.1 BENEFICIATION

The currently selected processing route includes the following unit operations:

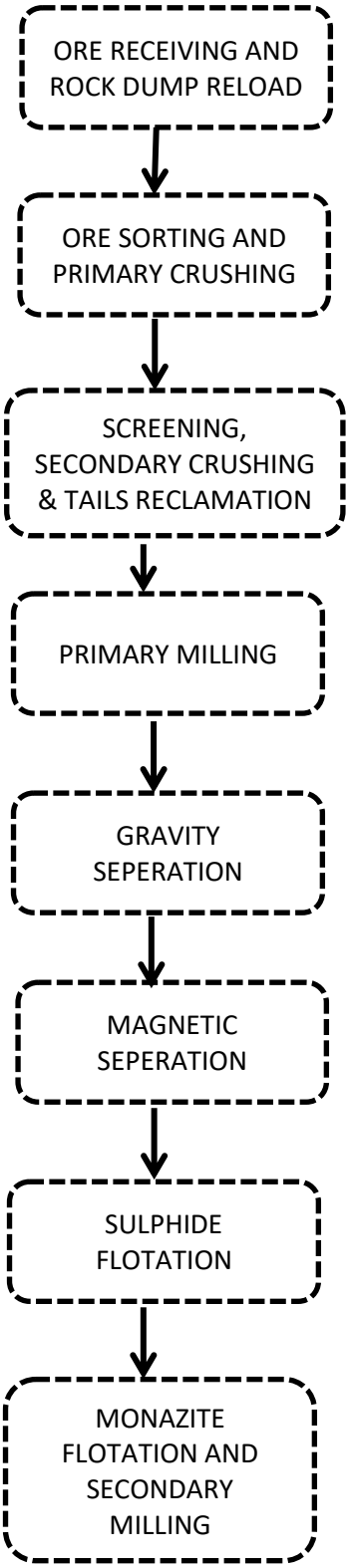

FIGURE 16: CONCENTRATOR PLANT UNIT OPERATIONS

3.3.2 HYDROMETALLURGICAL TREATMENT

The monazite concentrate can either be treated by the caustic or sulphuric acid route as depicted in Figure 4. The process in the hydrometallurgy section of the plant will be batch.

3.3.2.1 THE SULPHURIC ACID ROUTE

The acid treatment will use hot sulphuric acid digestion then leaching with water to remove the phosphate content. A dilution stage follows, whereby a process of selective precipitation deposits Th and REE as double sulphates. The sulphates are simply converted to hydroxides and leached in HCl and subsequently sent for purification.

3.3.2.2 THE CAUSTIC CRACK

At Steenkampskraal, prior to the caustic cracking of monazite, a nitric acid pre-leach is done in order to remove the apatite associated with the monazite. During this step apatite is leached together with REEs (~0.9% as indicated in unpublished test work done previously) while the refractory monazite remains as a solid. Calcium is also removed which results in an increased quality of the product since Ca moves along with the REEs downstream and typically causes complication during the SX process. The nitric pre-leach also upgrades the monazite to the desired grade suitable for caustic cracking i.e. 50% (as mentioned earlier). Thereafter the caustic method involves dissolution of the monazite in a concentrated solution of NaOH (as described in the literature review earlier) converting the REE and Th to hydroxides. The phosphate compound is separated by dissolving in water and is recovered as trisodium phosphate (TSP). The REEs are separated from Th using partial dissolution in which REEs are dissolved in concentrated HCl whilst the undissolved material is filters and forms a Th cake waste.

3.4 SCOPE AND LIMITATIONS OF TRADE OFF ANALYSIS

Now that we have defined the SKK process, it is imperative to mention the scope of this trade off analysis. The trade off will be between which process is to be used to treat the monazite concentrate. With this in

mind our scope shall include five of the most imperative factors leading to economic trade off analyses in industry i.e. the REE recoveries, CAPEX, OPEX, SHREQ aspects and finally the effects on downstream processes. Based on these 5 criteria mentioned, the objectives of the trade off study are:

- To compare the REE recovery of the two competing processes.
- To establish the CAPEX of each process based on the optimum conditions obtained in the experiments and to resultantly draw up a process flow diagram (PFD) and consequently set up a mass balance which satisfies the anticipated production i.e. 2700 tpa of TREO. Based on this, quotes are to be obtained for the respective equipment required in the PFD.
- To establish which process will result in a lower OPEX based on the optimum conditions obtained in the experiments (temperatures, reagents, and power consumptions from the above mentioned equipment).
- Taking into account both the above i.e. CAPEX and OPEX, evaluate its implication on the project NPV.
- To compare the SHREQ factors for both processes.
- In light of future expansion, to establish (long term) the effects on downstream processes.

CHAPTER 4

4 METHODOLOGY

Trade-off will be based on, as stated earlier, several factors i.e. the REE recoveries, CAPEX, OPEX, SHREQ aspects and finally the effects on downstream processes. All of these factors can only be achieved once a process flow diagram (PFD) is established for each of the process once the optimum conditions are known for each of the processes.

Important factors differ in both the caustic and sulphuric acid cracking, but it was thought that the following were the most important factors in each of the cracking step. For the caustic cracking of monazite it was decided that the optimum conditions required to be investigated were the influence of grind size and that of NaOH consumption. The reason for this was that grind size dictates cost of milling (which is generally a big contribution to OPEX) and caustic soda too is pricey and hence contributes to the OPEX. Once these were established, the optimal sample was subjected to the REE acid leach using HCl subsequent to the cracking whereby recovery was tested (since recovery dictates income). For the sulphuric acid cracking, it was decided that the optimum conditions required to be tested in order to produce a PFD would be the influence of acid dosage (since pH is directly related to the addition of acid which influences the OPEX), influence of pulp density during the water leach, the influence of feed moisture content (for if drying is required power costs are increased) and lastly that of grind size. Also, once the acid bake was optimised in terms of these, it was decided to look at the overall REE recoveries by testing the recovery /loss in the double salt precipitation and conversion since they form part of the acid route.

4.1 EXPERIMENTAL PROCEDURE

4.1.1 INPUT MATERIALS

Table 6 gives the head analysis of the sample subjected to testing. The underground ore has a rare-earth element content of approximately 24% TREO.

TABLE 6: HEAD ANALYSIS (%) OF THE STEENKAMPSKRAAL SAMPLES

Sample	TREE	TREO	Mg	Al	Ca	Fe	Cu	Th	U	Ni	Zn	P	S	Si
U/G ORE	20.32	24.37	0.21	3.28	4.25	9.6	1.05	2	0.06	0.03	0.02	5.4	1.95	9.96

Tests were carried out for both the caustic crack and sulphuric acid crack using three sets of samples as depicted in Table 7.

Some preliminary scoping studies were done at Mintek in order to identify suitable operating ranges for the cracking stages, since no "typical" operating conditions were available.

For caustic crack three different samples were used, i.e. a 24% TREO whole ore sample (milled to 95%-212 µm; 95%-75 µm; and 95%-45 µm), a Light Intensity Magnetic Separation (LIMS) product sample upgraded to 30% TREO (upgraded by rejection of magnetite and milled to 95%-212 µm; 95%-75 µm; and 95%-45 µm), and a monazite concentrate sample upgraded to 50% TREO by flotation post LIMS and leached with nitric acid at 60°C for 30 minutes (milled to 95%-212 µm; 95%-75 µm; and 95%-45 µm). As stated earlier in the literature review, the monazite requires pre-leaching to upgrade the material- since the caustic crack is best suited to high grade material (50% or greater) and, the nitric pre-leach step does just this (by increasing the grade from 41% to 50%). These samples were used because it was desired to see the response of the ore to the caustic cracking in three different upgrading scenarios i.e. in a case with no upgrading (the whole ore); with slight upgrading (by magnetite rejection); and the maximum upgrading via the use of flotation to produce a monazite concentrate which was upgraded (to 50%) by leaching it in nitric acid respectively.

For the sulphuric acid cracking test, after subjecting the LIMS product of 30% TREO to cracking, it was found that the recovery in the crack was >99% (as can be seen later in the relevant chapter). Thus, if the lowest grade produced such a recovery, it was obvious that the higher grades will perform just as well. Thus only the LIMS product was used in the sulphuric acid cracking test work.

The elemental composition for the caustic crack test samples and sulphuric acid cracking samples are given in Table 7.

TABLE 7: ELEMENTAL COMPOSITION FOR FEED MATERIAL TO THE CAUSTIC AND SULPHURIC ACID TESTS

Element, unit (g/t)	Whole ore	LIMS product	Monazite conc. (Sulphuric Acid Crack)	Monazite conc. (Caustic crack)
La	46652	53731	77232	77228
Ce	89339	108662	146347	147000
Pr	10373	12053	15628	16258
Nd	36345	42404	58311	58330
Y	7925	9167	13095	14005
Sm	6010	6914	9599	9599
Eu	83	383	203	214
Gd	8655	9706	13624	13624
Tb	541	659	940	960
Dy	2235	2580	3407	3407
Ho	322	380	550	550
Er	726	816	1309	1309
Tm	42	54	90	90
Yb	251	278	360	365
Lu	27	21	74	79
TREE, % (m/m)	21	25	34	41
TREO,% (m/m)	25	30	41	50
Na	3227	4611	2560	2573
Mg	2367	2267	1980	1980
Al	33667	31300	23437	27437
K	10233	9133	3155	3190
Ca,%	4.7	4.7	5.6	5.6
Cr	791	447	786	799
Mn	130	210	1	1
Fe,%	8.9	5.4	3.7	3.7
Co	61	63	26	26
Ni	352	417	255	221
Cu,%	1.1	1.2	0.3	0.3
Zn	201	102	95	95
As	353	378	758	758
Th	1.7	1.5	1.8	1.8
U	13.7	2.2	55	56
P,%	6.5	7.3	10	11

4.1.2 Caustic Crack tests

The caustic cracking tests followed the sequence demonstrated below:

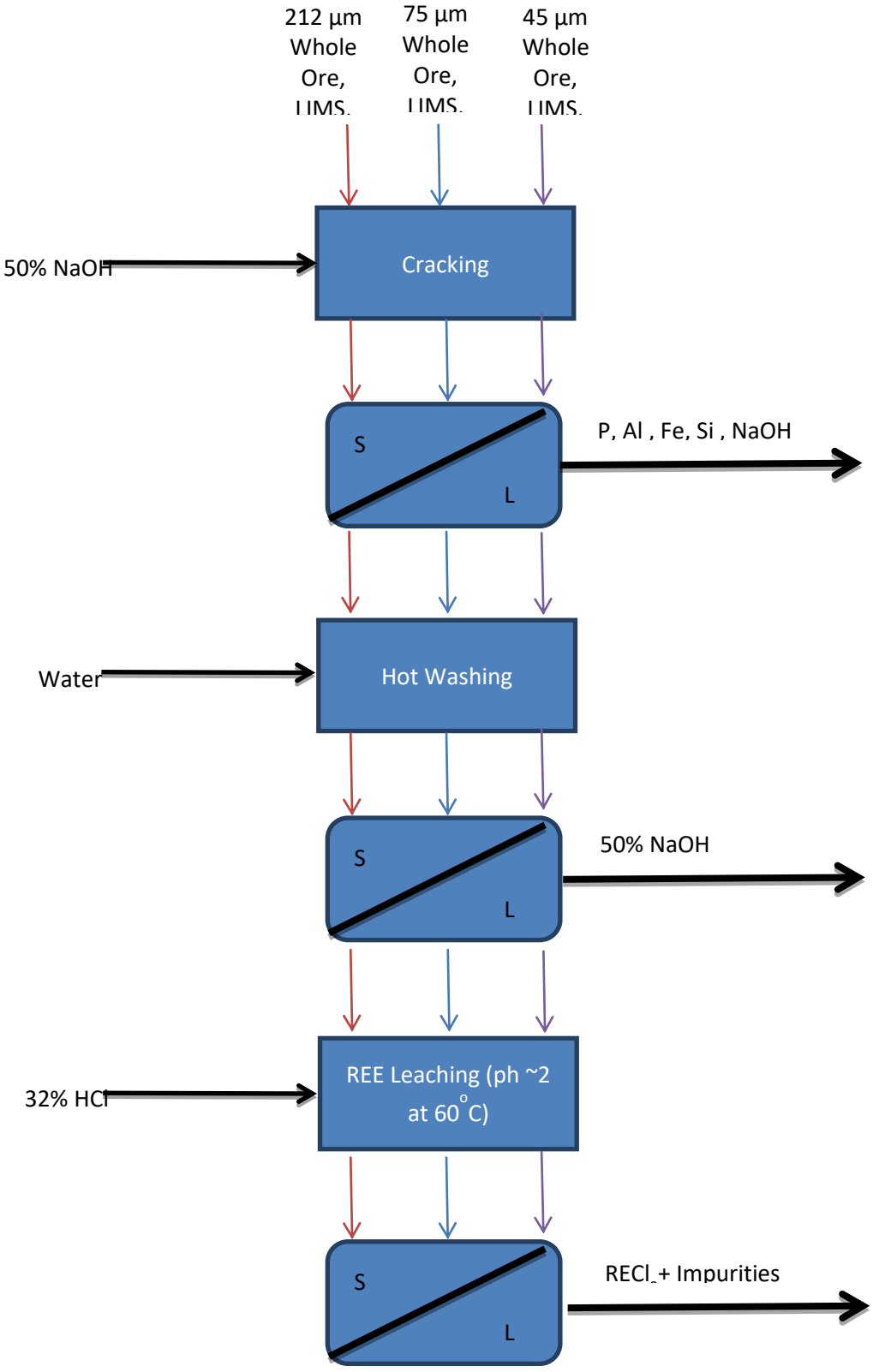

FIGURE 17: EXPERIMENTAL PROCEDURE DEPICTING THE CAUSTIC ROUTE ON THEIR SAMPLES

4.1.2.1 CRACK

For all three samples the dry feed solids were slurried in a 50% (m/m) NaOH aqueous solution. With this caustic concentration its boiling point will be greater than the chosen operating temperature of 140°C as can be seen from Figure 18.

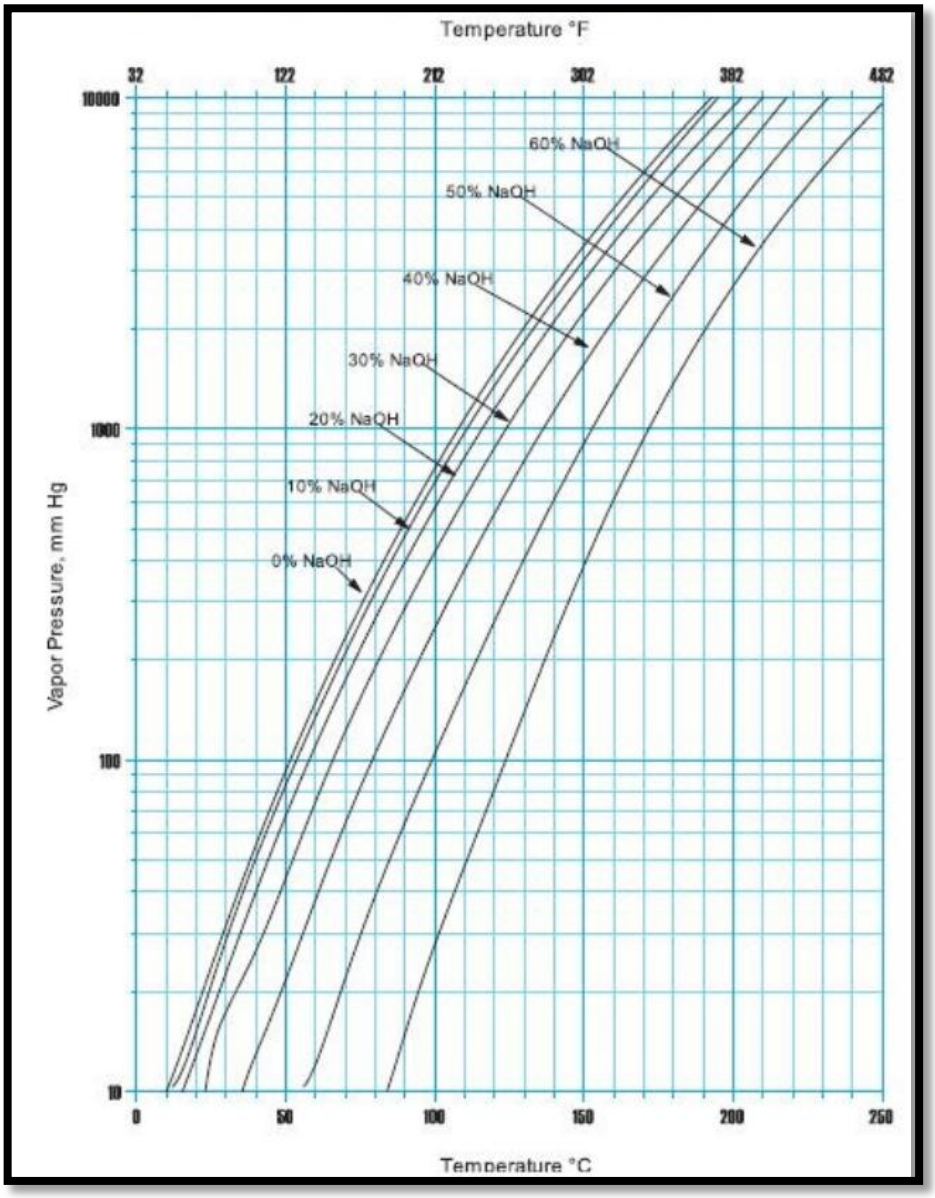

FIGURE 18: VAPOUR PRESSURE OF AQEUOUS CAUSTIC SODA SOLUTIONS (REPRODUCED FROM: CAUSTIC SODA HANDBOOK (OCCIDENTAL CHEMICAL CORPORATION, 2013))

The desired initial pulp solids concentration was 20%. Therefore 2000 kg of NaOH/ton of leach feed was added. The batch size was 2 kg. The pulp was then agitated and heated to and kept at 140°C for 4 hours

(Panda et al., 2014). This was done in a mini stainless steel reactor on a hot plate at atmospheric pressure. In order to prevent crystallisation, the pulp was vacuum filtered while hot. The material was difficult to filter. The filter cake was washed by re-pulping in a dilute caustic solution of 10 g/L NaOH at 80°C, and then with de-ionised water at 80°C at a wash ratio of 6 times the mass of wash liquor to wet cake mass. The filter cake was washed three times. This was done in order to remove any entrained NaOH and other impurities. The total volume of the combined wash liquors was recorded, and a sample of the combined wash liquors was taken for analysis. To ensure, these experiments were done in replicate.

A sample of washed leach residue was taken from the cake while in the filter pan in order to determine the moisture content and chemical composition of the filter cake. A portion of the sample was dried and assayed for the REEs, Th, U, P_2O_5, base metals and Na. The filtrates were also assayed for the REEs, Th, U, P_2O_5, base metals and Na.

4.1.2.2 HOT WATER WASH

Thus subsequent to the caustic crack, a hot water wash was done aimed at comprehensive removal of entrained NaOH and phosphates which might result in increased acid consumption in the subsequent acid leach step.

The wet caustic crack residue was slurried in de-ionised water to a 20% pulp density, after which it was agitated, heated and kept at 80°C for four hours. The pulp was then filtered and washed three times by re-pulping in de-ionised water at a wash ratio of 2.5 times the mass of wash liquor to the wet cake mass. The total volume of the combined wash liquors was recorded and a sample of the combined wash liquors was taken for analysis.

4.1.2.3 DIAGNOSTIC ACID LEACH

The washed and dried residue from the hot water wash step was used in a diagnostic REE leach test. This test aimed to dissolve the REEs

after monazite cracking and to determine the optimum pH for maximising REE recovery. An S-curve of pH vs. REE leach efficiency was plotted to show this by taking samples at different stabilised pH values. The deportment of impurities at different pH values could also be established. The results of this test were used to select the most suitable operating pH for leaching of the REEs in the subsequent test work.

The residue from the cracking experiment after the hot water wash was used as a feed to this diagnostic acid leach. The dry washed residue was slurried in de-ionised water to a 15% (m/m) pulp density. It was then heated to 40°C while being agitated. Once the operating temperature was reached, the pH of the slurry was decreased in increments to target pH values of 3.5, 3.0, 2.5, 2.0, 1.5, 1.0, 0.8, 0.5 and 0.2 by adding 6 M HCl. No reductant was added into the slurry. Once the pH of the sample was stable for 30 minutes at each new pH decrease, a slurry sample was taken. The sample was filtered and a portion of the filtrate was analysed for base metals, Th, Sr, Ba, U, P_2O_5 and REEs. The rest of the filtrate was used to backwash the solids into the reactor. The parameters such as pH, temperature, redox potential, volume of sample taken and volume of acid added were recorded.

After the test, the slurry was filtered and the filter cake was weighed. It was then washed three times by re-pulping in acidified (pH 1.5 with HCl) de-ionised water at a ratio of 2.5 times the wash liquor mass to wet cake mass. The washes were combined and the total volume recorded. A sample of the combined wash waters was analysed.

The washed cake was weighed and a representative sample taken to determine the moisture content. After the wet solids were air dried, a representative sample was assayed for the rare earths, Th, Sr, Na, Ba, residual HCl and base metals.

4.1.2.4 REE ACID LEACH

Eleven laboratory batches were conducted using the residues of the hot water wash step. The tests were done at a pH of 2.0, a temperature of

60°C and a solution redox potential controlled at 600 mV (vs. Ag/AgCl). The tests were done for 2.5 hours as mentioned in appropriate literature (Mackowski *et al*, 2011). Sodium meta-bisulfite (SMBS) was used as reductant in order to control the redox potential to reduce the possibility of oxidation of Ce. The pH of 2.0 was chosen as the diagnostic acid leach tests showed that it was the optimum pH for leaching the REEs.

The dry washed residue was slurried in de-ionised water to a pulp density of 20% (m/m) solids. It was then heated to 60°C while being agitated. The pH of the slurry was decreased to 2.0 by adding 6 M HCl once the operating temperature was reached. Sodium meta-bisulfite was added so that the redox potential was controlled at between 500 mV and 600 mV (vs. Ag/AgCl). The parameters such as temperature, redox potential and volume of acid added were also recorded.

The slurry was filtered after the test and the filter cake was weighed. It was then washed three times by re-pulping in acidified (pH 1.5 HCl) de-ionised water at a ratio of 2.5 times the wash liquor mass to wet cake mass. The washes were combined and the total volume was recorded. A sample of the combined wash waters was analysed.

The washed cake was weighed and samples were taken in order to determine the moisture content. A representative sample (using the cone and quarter method) of the air dried solids was assayed for individual rare earths, Th, Na, K, Ba, residual HCl and base metals.

4.1.3 Acid Bake and Water Leach

4.1.3.1 Acid contact and bake

The amount of sulphuric acid needed, based on the required acid dosage of 1000, 1200, 1400, 1600, 2000 and 2500 kg/t feed, was calculated. Although literature has identified the need to operate at a 2:1 acids to solids ratio (Habashi, 2013), four different dosages below this ratio were tested because the ratio in literature is dependent on a specific ore and obviously differs from ore to ore. Since no tests were

done on SKK ore, a variation of acid to solids ratio was required to be tested. The required amount of sulphuric acid was then weighed and transferred into a container fitted with an overhead impeller. The acid was then agitated. The feed solids were then added in 2 kg batches into the reactor slowly, after which the slurry was agitated for another 20 minutes.

The acid pulp was then placed evenly into ceramic trays. This was done to attain an even bed thickness. The mass of the tray plus the slurry was weighed before the mixture was placed into a preheated muffle furnace. The material was baked at 280°C for 3 hours, which is the required residence time as discussed in the literature section. The baked solids were then removed from the oven and allowed to cool in ambient conditions for about an hour. The mass of the tray and its contents was recorded after cooling.

The baked material was removed from the tray and stored in a sealed container. The solids were homogenized by breaking the lumps with a hammer and blending the baked solids using a pestle and mortar. A representative sample was taken using the cone and quartering method for chemical assaying and determination of bulk densities. The remainder of the sample was used as feed for the subsequent test work.

4.1.3.2 WATER LEACH

The solids were slurried in de-ionised water so that the pulp density was between 20% and 40% (m/m). The reactor content was agitated with a thermal plastic coated impeller. The temperature of the slurry was carefully monitored and ice was added (and the addition recorded) to the slurry in order to cool the slurry when the temperature went above 35°C- since $RESO_4$ solubility decreases with increasing temperature. The increase in temperature was caused by the exothermic heat of dilution that took place when the unreacted acid was mixed with water in the baked material.

After 2 hours the test was completed and the mixture was filtered. The mass of the wet residue, as well as the volume and mass of the filtrate was recorded. The filter cake was weighed, re-slurried and washed three times. The first wash was done using acidified de-ionised water, where the water had the same pH as the slurry. Thereafter the slurry was washed with de-ionised water. A wash ratio of 5 times the mass of wash liquor to the wet cake mass was used. The wash liquors were combined and the total volume was recorded.

A sample of the filtrate and combined wash liquors were taken for chemical analysis. The washed solids were dried in an oven that was kept at 50°C. A representative sample of the washed and dried cake was taken by using the cone and quartering method for chemical assaying. The rest of the cake was stored in a sealed plastic bag. The remaining filtrate was stored and used as feed in subsequent test work.

4.1.3.3 DOUBLE SALT PRECIPITATION

An excess sodium sulphate addition of 3 times the stoichiometric requirement was selected as an optimum reagent addition based on preliminary laboratory optimisation test work. The selected precipitation temperature was 90°C for 2 hours also based on preliminary test work.

The REEs were precipitated from the water leach PLS as REE double sulphates by means of the addition of dry anhydrous sodium sulphate (Na_2SO_4). The following procedure was followed:

The stoichiometric amount of sodium (Na) required to precipitate the REEs was calculated according to the following reaction:

$$Ln^{3+} + Na^{+} + 2SO_4^{2-} + x\,H2O \rightarrow NaREE(SO_4)_2 \cdot xH_2O$$

The PLS was transferred into a reactor which was fitted with an overhead stirrer and baffles. The solution was heated to 90°C while agitating. At this temperature, the precipitating agent was slowly added within the first 10 minutes of the test. The temperature of the mixture was controlled at a set-point of 90°C for the remainder of the test duration. Upon completion of the test (after 2 hours), the slurry was

filtered and the mass of the wet precipitate recorded. The volume and the mass of filtrate were also recorded.

The filtered cake was weighed, subsequently re-slurried and washed three times, with hot (90°C) Na_2SO_4 (5% (m/m)) solution at a wash ratio of 5 times the mass of wash liquor to the mass of wet cake. The wash liquors were combined and the total volume recorded. A sample of the combined wash liquors and filtrate was taken for chemical analysis. A representative sample of the washed cake was taken for determination of the moisture content, bulk density and for chemical analysis. The remainder of the sample was stored in a sealed plastic bag for subsequent test work.

4.1.3.4 DOUBLE SALT CONVERSION

The aim of this step was to convert the rare earth sulphates into rare earth hydroxides. Sodium sulphate would be formed as a by-product in this process. The efficiency of conversion was determined by measuring the leach efficiency of sulphates in the conversion step.

The $NaREE(SO_4)_2$ was converted into REE hydroxides by using NaOH. This was done by reacting $NaREE(SO_4)_2$ with a stoichiometric excess (20% excess) of NaOH (4 M concentration) at 90°C. The required amount of NaOH was calculated by using the following reaction:

$$NaREE(SO_4)_2 \cdot xH_2O + 3NaOH \rightarrow REE(OH)_3 + 2Na_2SO_4 + xH_2O$$

The calculated amount of reagent was prepared by dissolving NaOH flakes into a known volume of deionised water, targeting a NaOH concentration of 4 M (160 g/L) in solution. The NaOH addition was 1 kg/kg of TREEs in the feed. The REE double salt was re-pulped into the NaOH solution and transferred into a stainless steel reactor whilst agitating. The temperature of the slurry was increased and maintained at 90 °C for 2 hours (Abreu & Morais, 2010). After 2 hours of reaction, the mixture was filtered and the mass of the wet unwashed precipitate recorded. The volume and the mass of filtrate were also recorded.

The filtered cake was weighed, subsequently re-slurried and washed three times, initially with alkaline deionised water (deionised water adjusted to the pH of slurry with NaOH and thereafter with deionised water, at a wash ratio of 5 times the mass of wash liquor to the wet cake mass. The wash liquors were combined and the total volume recorded.

A sample of the filtrate and combined wash liquors were taken for chemical analysis.

4.1.3.5 REE ACID LEACH

The aim of this step was to selectively leach REEs in the REE hydroxide precipitate. The test work was conducted using the following selected conditions: pH 2.8, ambient temperature and 3 hours residence time. An optimum pH of 2.8 was selected for leaching the REEs based on the diagnostic pH vs. extraction S-curve leach test conducted in prior test work.

The REE hydroxide from the conversion step was slurried in deionised water, targeting a REE concentration of about 100 g/L in the final solution when assuming about 99% REE dissolution (excluding Ce). The feed slurry was transferred into a reactor fitted with an overhead stirrer and baffles. The pH of the slurry was decreased slowly to a value of 2.8 by the addition of 32% HCl, while agitating. The pH of the slurry was controlled at the target pH throughout the duration of the test. Test parameters such as pH, redox potential (Eh), temperature as well as the amount of acid added were recorded on a half-hourly basis.

After 3 hours of reaction, the mixture was filtered and the mass of the wet unwashed residues recorded. The volume and the mass of filtrate were also recorded.

The filtered cake was weighed, subsequently re-slurried and washed three times, initially with acidified deionised water (deionised water acidified to the pH of slurry) and thereafter with deionised water. The cake was initially washed at a ratio of 1 times the mass of wash liquor

to the wet cake mass and the second and third washes at a ratio of 5 times the mass of the of wash liquor to the wet cake mass. The volume and the mass of the first wash were recorded and stored for subsequent test work. The second and third wash waters were combined and the total volume recorded.

A sample of the filtrate, first wash and combined second and third wash liquors were submitted for chemical analysis. A representative sample of the washed cake was taken for determination of the moisture content, bulk density and for chemical assaying. The remainder of the sample was stored in a sealed plastic bag for subsequent test work.

4.1.4 ANALYTICAL TECHNIQUES FOR ASSAYING

All chemical analyses were outsourced to De Bruyn Spectroscopic Solutions. Their method of analysis is based on ICP-OES and utilises three sample preparation steps for solid samples to ensure total dissolution of all REE. The certified reference material (CRM) used was OKA-2 Rare Earth- Thorium ore. Every tenth sample was repeated as an internal standard check. All MBH London CRM's are certified on a monthly basis. The laboratory is ISO 17025 / 34 (calibration CRM) accredited and is the first calibration laboratory in Africa.

Due to the limited budget associated with the project together with the high prices of the analytical analyses which resulted in limited amount of samples being tested. This indeed limits the reliability of analyses undertaken and it is recommended that when funds do become available that more analyses are done in order to obtain reproducibility of results.

All REO assays presented in this report are on the basis of the oxidation states given in Table 8. Note that Ce, Pr and Tb are not in the 3+ oxidation state.

TABLE 8: RARE EARTH OXIDATION STATES

La_2O_3	CeO_2	Pr_6O_{11}	Nd_2O_3	Sm_2O_3	Eu_2O_3	Gd_2O_3	Y_2O_3
Dy_2O_3	Ho_2O_3	Er_2O_3	Tm_2O_3	Yb_2O_3	Lu_2O_3	Tb_4O_7	

4.2 Subsequent methodology of interpreting results

4.2.1 Recovery

The recovery for each process was obtained from the measurements recorded in the experiments. Recovery refers to the recovery of REEs obtained in the HCl leach of the $RE(OH)_3$ (subsequently being fed to the purification step (which is beyond the scope of this study)) relative to what enters with the feed to the crack stage. All REEs lost to other streams will not be considered beyond this study as recovering these is not likely to be economic given the current price of REEs.

4.2.2 Flow sheet development

4.2.2.1 Capex

The components of the flow sheet were sized in order to produce 2700 tpa of TREO for each of the processes. Since production values are extremely low (2700 tpa), it is uneconomic to run a plant of such small magnitude in a continuous manner (since the CAPEX in a continuous process is high due to the elaborate control and instrumentation; piping; as well as size of equipment needed for long residence times), thus designing for a batch operation was decided upon. Obviously, the OPEX in a batch process is significantly higher than in a continuous process (Seider, Seader and Lewin, 1999), however, its overall impact is still lower than the impact from the CAPEX. The sizing of the vessels was based on the capacities obtained from a mass balance drawn up for both processes and shown in Appendix B: Mass Balances. In order to produce this 2700 tpa of TREO it was deduced that 1861 batches (~3 tons each) per annum to the respective hydrometallurgy section would be required to fulfil this TREO production. This was obtained based on the assumptions in Table 9. The size of the vessels was indicated to suppliers and a quote was obtained. For some cases such as that of the FRP tanks, the sizing was done and it was found that the tanks were smaller than 25 m^3 (in the caustic cracking e.g. 10 m^3 or 8 m^3). In these cases a 25 m^3 was selected as the supplier only manufactures tanks of 25 m^3 and above (increasing 5 m^3 at a time). These prices were then

tabulated and the total for each process indicated the CAPEX respectively. An example of the calculations on sizing appears on page 130.

TABLE 9: ASSUMPTIONS MADE IN ORDER TO SIZE EQUIPMENT

Factor	Amount assumed
Operating days per annum	365 days
Operating days per month	26 days
Operating hours per day	24 hours
Availability	85%
Utilization	100%
Available run days per annum	310 days
Hours per year	7446
Rate determining step for Caustic/Sulphuric Acid Crack	4 hours (based on the consideration of two vessels at the rate determining step- thus accounting for fill and discharge times)
Number of batches	1861 batches per annum
Annual throughput to hydrometallurgy	6121 tpa
Tonnage per batch of monazite concentrate	~3.28 tons

4.2.2.2 OPEX

For comparison purposes the OPEX was calculated based on only two factors i.e. power and reagents. Labour and other factors usually contributing to OPEX was considered as constant because the material being handled is radioactive and thus all process steps should be automated and the cost of automation will be included in the CAPEX.

Resultantly, the conditions at which the experiments were conducted at were now applied to the specified equipment used for processing and the relevant power was noted in order to calculate the power consumption for both processes on plant scale. The cost of electric power produced by generators was R8/kW.h of which R3.50 was for diesel (from previous work done).

The reagents and their respective consumption were also tabulated from the mass balance for each of the processes.

4.2.2.3 NPV

The NPV was calculated using the following formula:

$$NPV = \sum_{t=1}^{T} \frac{C_t}{(1+r)^t} - C_o$$

Where;

C_t = net cash inflow during the period t

C_o = total initial investment costs

r = discount rate, and

t = number of time periods

The net cash flow i.e. C_t was calculated for each year based on a \$10/kg (R140/kg) selling price minus the cost price of what will be obtained from the results in this study. Exchange rates used were R14 to the US\$. It was assumed that the beneficiation plant would remain the same with its associated cost and only the OPEX and CAPEX costs for each of the cracking processes would change. The CAPEX and OPEX for both processes was calculated as described above and were then used to calculate the NPV over a period of 20 years as per the life of mine. A discount rate of 14% was used since this was what was decided by the financial team designing the model. The initial investment costs (C_o) was taken as R292,000,000 and this included the cost of the mining and processing plants (excluding the hydrometallurgy sections) as well

as the associated infrastructure. The values calculated for each of the processes i.e. the caustic and sulphuric acid cracking were added to the R292,000,000 and the NPV was then compared for both processes and thereafter the results were discussed with regard to those factors that influenced this difference.

4.2.3 SHREQ

During the experiments, all aspects influencing safety and radiation risks were taken note of and analyzed according to the flow sheet drawn up (as per the above methodology) and thereafter scrutinized and reported upon in terms of the health and safety regulations covered in OHSA (Occupational Health and Safety Act) Act No. 85 of 1993; the South African nuclear and radioactivity authority -National Nuclear Regulator (NNR) requirements, as well as local and international environmental, radiological, ventilation, storage and transport of radioactive material.

4.2.4 Effect on Downstream Processes

A brief overview of the flow sheet drawn up also led to the discussion of these aspects.

CHAPTER 5

5 Results and Discussion: The Caustic Crack

5.1 Experimental Results

5.1.1 Influence of Grind Size

The effect of grind size on REE recovery was investigated using a pulp density of 20% at a NaOH concentration of 50% (m/m). All tests were done for 4 hours.

Figure 19 shows the effect of grind size on phosphorous extraction in the whole ore sample (24% TREO). The starting material for the experiment was all the same sample but ground to different degrees of fineness. Data for this graph can be found in Table 20 in Appendix A. The highest P extraction was 79% and was measured when the 95%-45 µm whole ore sample was cracked. The whole ore 95%-212 µm sample gave P extraction of 31%. The effect of grind size when changing from 212 µm to 75 µm has quite a significant effect on leaching being improved, however beyond 75 µm the effect is minor. The P extraction increases dramatically from 212 µm to 75 µm but only marginally going from 75 µm to 45 µm, indicating that the reaction time is insufficient beyond the 75 µm points. Due to the high shear agitation during the experiments, no product layer inhibition could have resulted which could have hindered the recovery. However, it should be made clear that P extraction does not fully represent monazite cracking efficiency as the samples do have apatite which contains P and is essentially inert under the caustic crack.

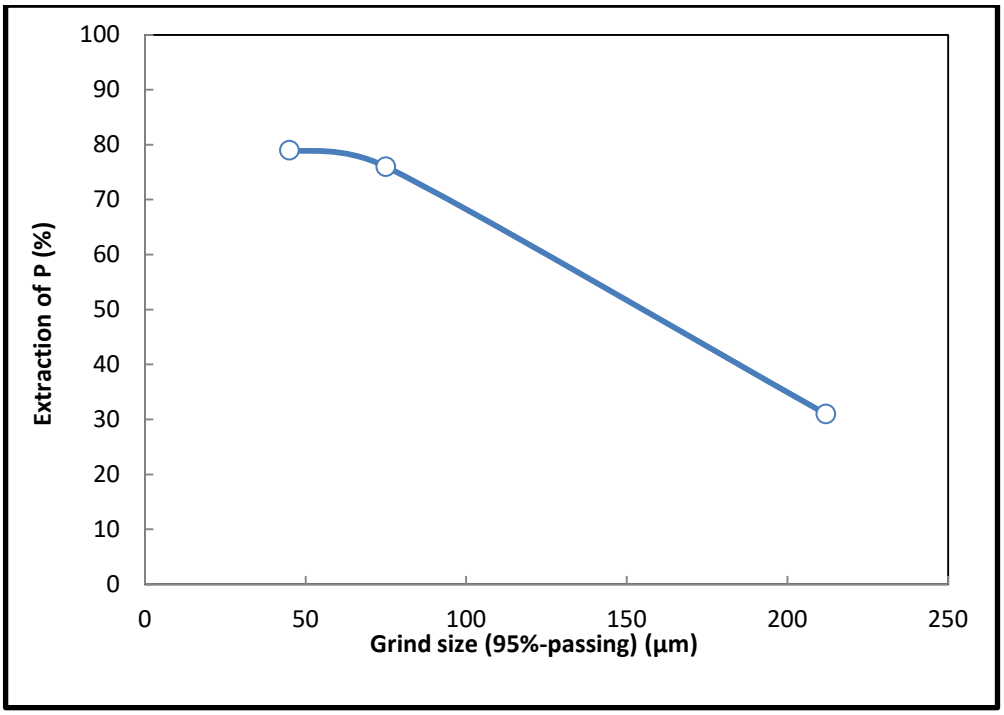

FIGURE 19: P EXTRACTION VS GRIND SIZE IN THE 4 HOUR CAUSTIC WHOLE ORE CRACK.

5.1.2 Influence of pH during the HCl Leach

In order to evaluate the leachability of the individual REEs after the caustic crack, a scoping leaching test was done on the whole ore sample with a grade of 25% TREO that was cracked under standard conditions. This test was done simply to diagnose at around which pH optimal REE leaching of the cracked material would be achieved.

Figure 20 shows the solution based REE extraction and HCl consumption as a function of pH. The data for this graph was taken from Table 21 in appendix A. Figure 21, with data taken from Table 22 in Appendix A, shows the impurity extraction as function of pH, while Figure 22 shows the REE dissolution as it changes with a change in pH. Data for Figure 20 is shown in Table 23 in Appendix A. At a pH of 3.5, 70% of the REEs can be leached. When leaching at a pH of 2.0, the leaching efficiency increased to 77%. There was a correlation observed between the increase in phosphorous concentration in solution and the decrease in REE recovery at pH below 2.0.

The highest extraction of REEs occurred at a pH of 2.0, where the HCl consumption was 661 kg of 32% HCl/ton of cracked residue. This equates to 211 kg of 100% HCl/ton of cracked residue. This consumption is quite high because there was a lot of Cu, Fe and Ca which consume acid at this 25% grade. But at a pH=3 consumption was 383 kg of 32% HCl/ton of cracked residue and recovery was 74%. Thus a pH of 3 was aimed for in the experiments in the next section, since the consumption of acid is relatively lower than at pH of 2 while the recovery is not much less (74% as opposed to 77%).

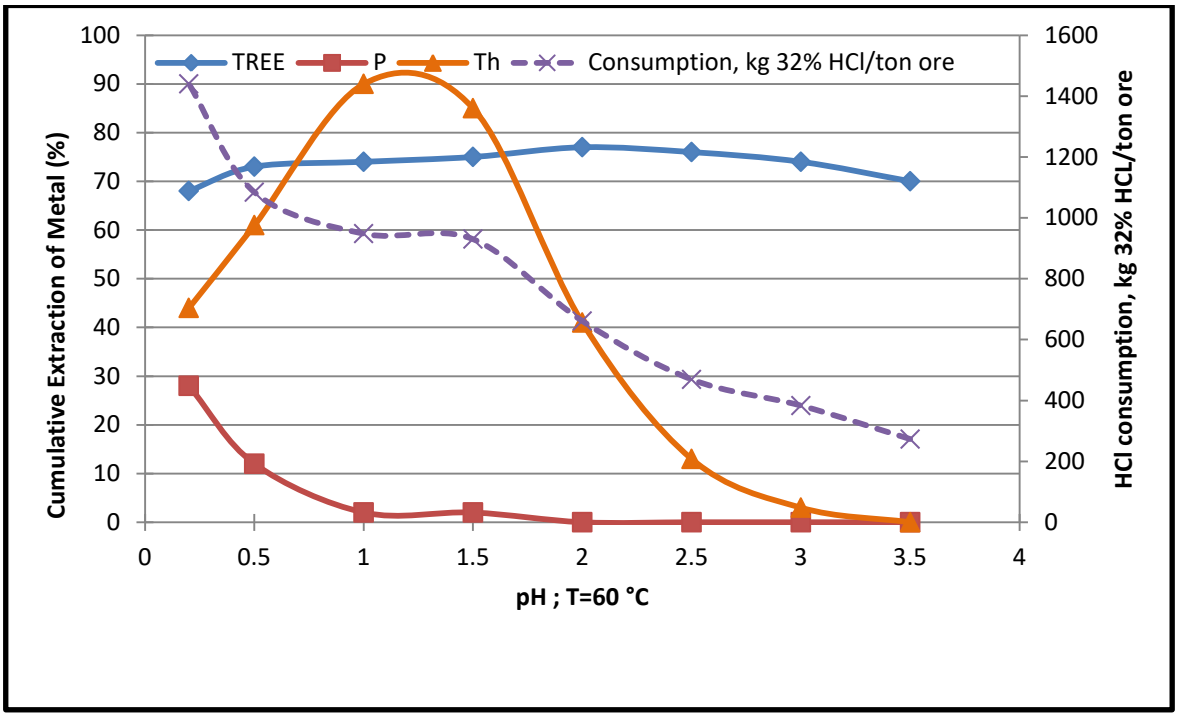

FIGURE 20: THE EFFECT OF PH ON EXTRACTION AND HCL ADDITION.

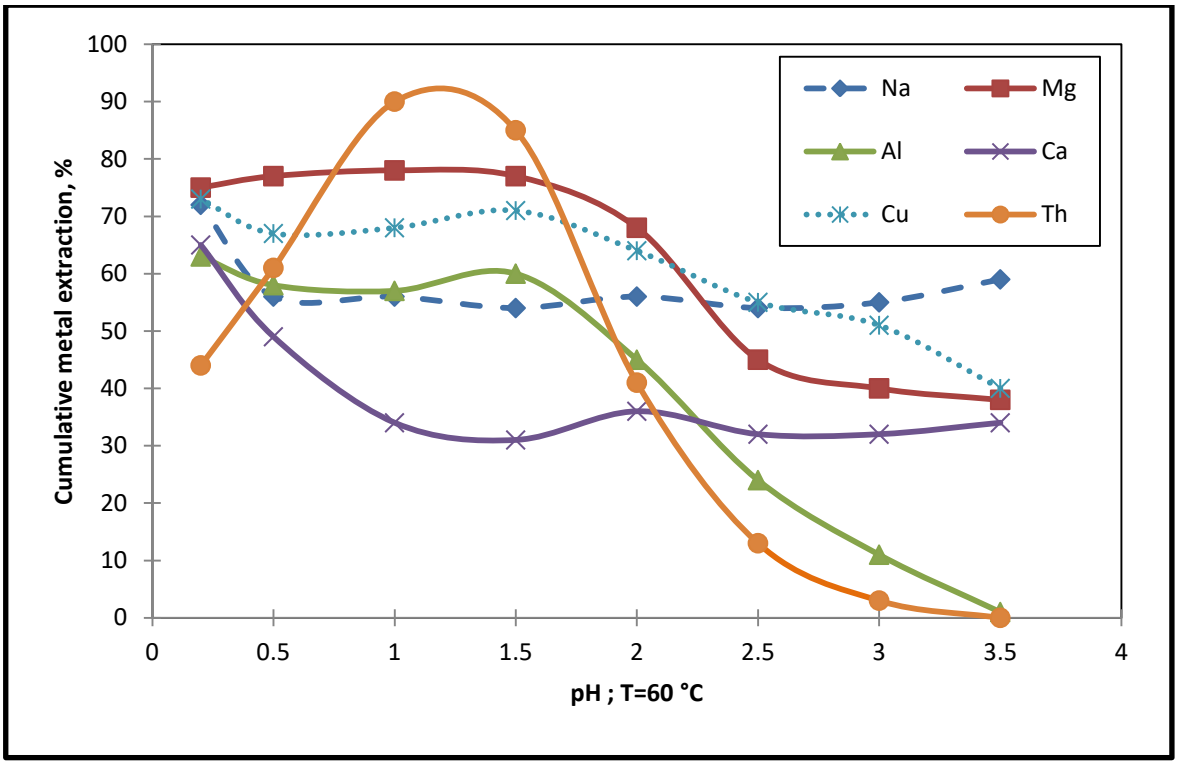

FIGURE 21: IMPURITY DISSOLUTION PLOTTED AGAINST PH.

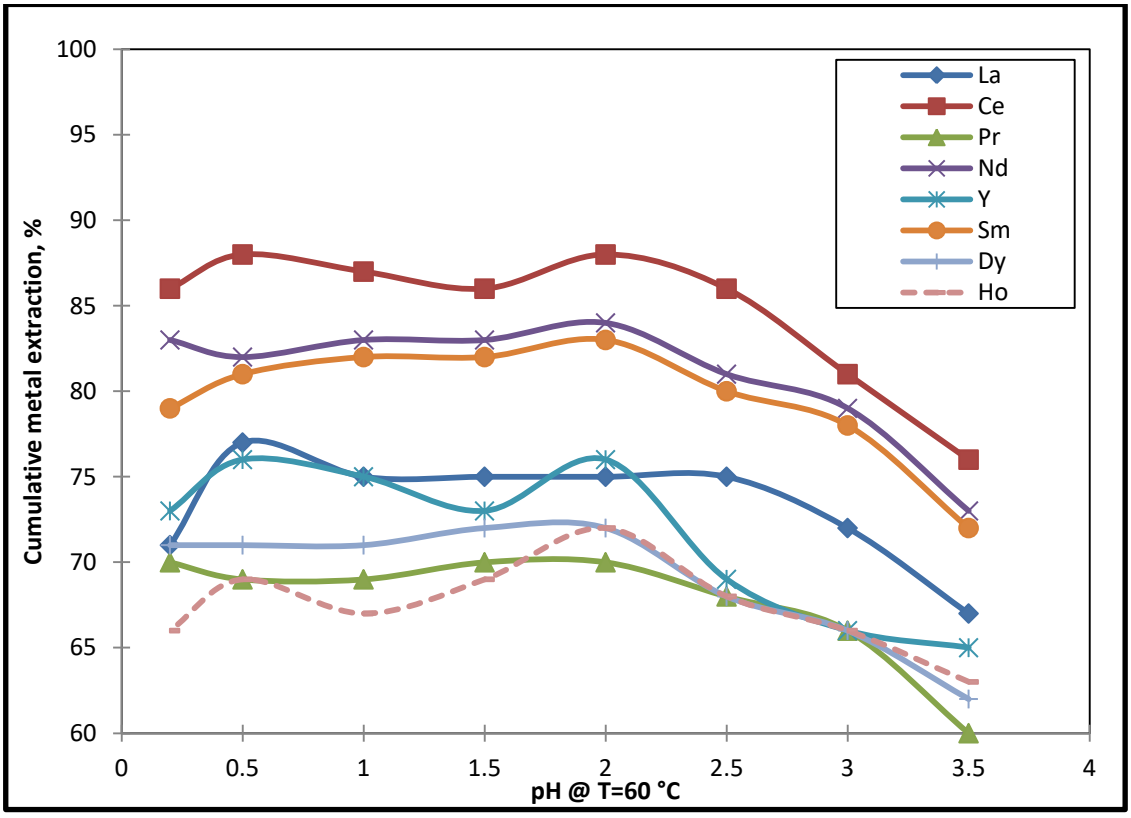

FIGURE 22: REE DISSOLUTION WITH CHANGE IN PH

5.1.3 Influence of feed material and size on REE recovery

Various feed materials and sizes were subjected to the standard caustic crack and subsequently leached in HCl at pH 3. The grind sizes tested were 95%-45 µm and 95%-75 µm of the whole ore, LIMS product and monazite concentrate which was pre-leached in nitric acid as stated in 4.1.1. Due to the findings in 5.1.1 the 212 µm size was not considered further.

The 95%-45 µm and 95%-75 µm had similar leach efficiencies when treating the whole ore and pre-leached monazite concentrate. The whole ore sample that was milled to 95%-45 µm had a REE leach efficiency of 76%, which is similar to the 95%-75 µm leach efficiency of 75%.

The whole ore leach tests (75 and 45 µm) achieved REE recoveries between 75% and 79%. This variance in leach efficiency might be due to experimental variation in final solution pH. The whole ore underground material yielded a maximum of 79% recovery at the conditions applied. The best results were obtained when treating the 95%-45 µm monazite concentrate which achieved an overall recovery of 89% at a pH of 3.

Figure 23, the data for which is in Table 24 in appendix A, shows the comparison between the two grind sizes for each sample.

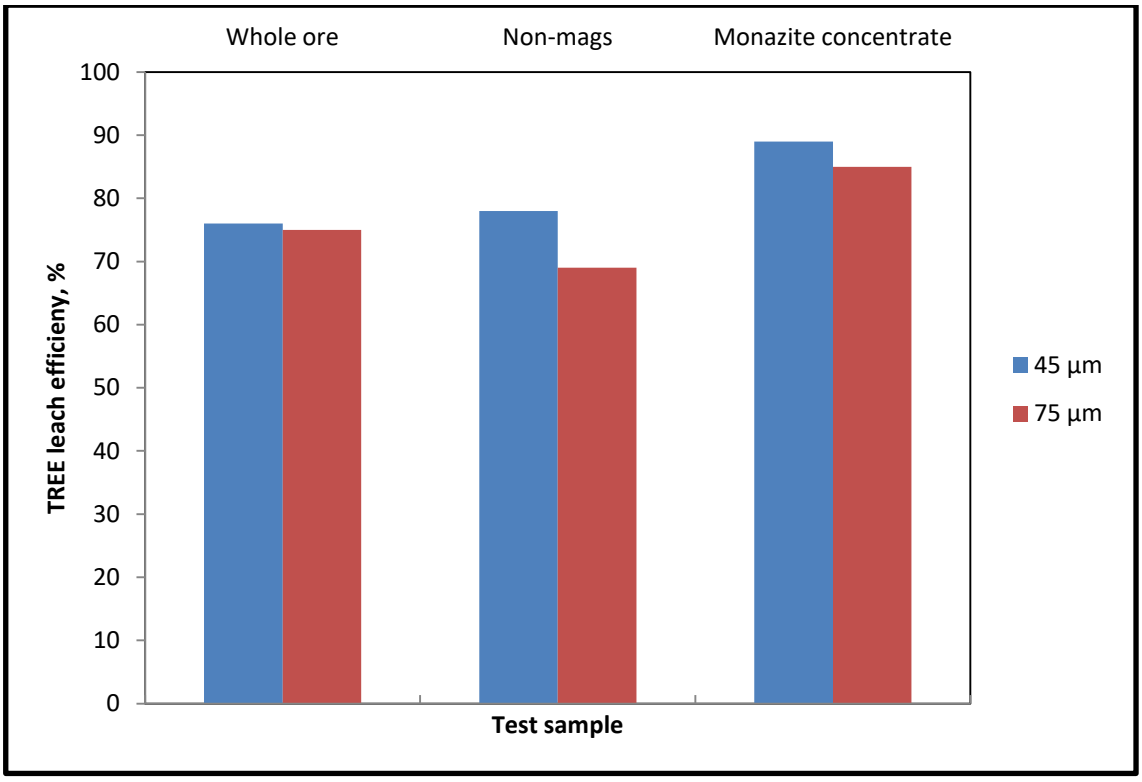

FIGURE 23: TREE LEACH EFFICIENCY OF DIFFERENT GRIND SIZES.

After the caustic crack, the main impurity elements in the solids were Al, Si, Th, Mg, Fe, Na and Cu. In most of the tests, the leach efficiency of Al, Na, Ca, Cu and Mg was over 50%. By leaching at a pH greater than 2.0 the co-leaching of Al, Th and Cu can be minimised, but at the same time this could decrease the REE leach efficiency slightly. Choosing the optimum pH for REE leaching is therefore a compromise between REE recovery and solution purity. Although the leaching of the impurities occurred, they may be rejected easily from the circuit by selective precipitation. The influence of pH, temperature and residence time on REE recovery may have to be optimised.

Figure 24 shows the leach efficiency for individual elements of the whole ore sample. The data depicted in this graph can be found in Table 25 in Appendix A.

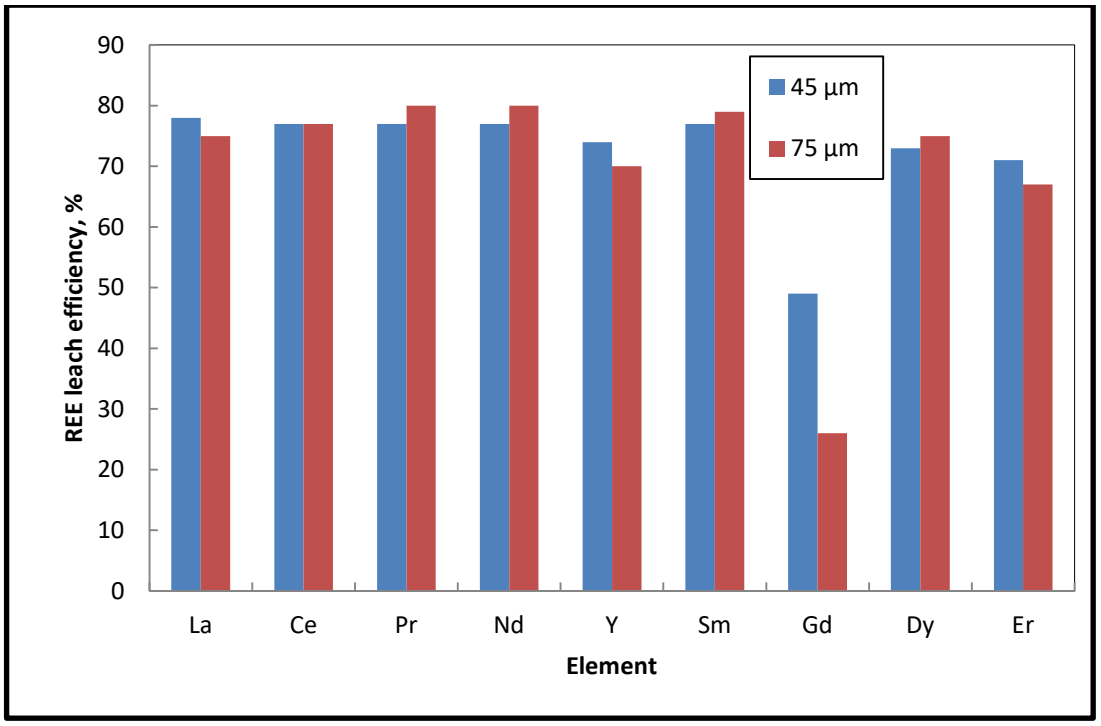

FIGURE 24: WHOLE ORE SAMPLE LEACH EFFICIENCY OF INDIVIDUAL ELEMENTS.

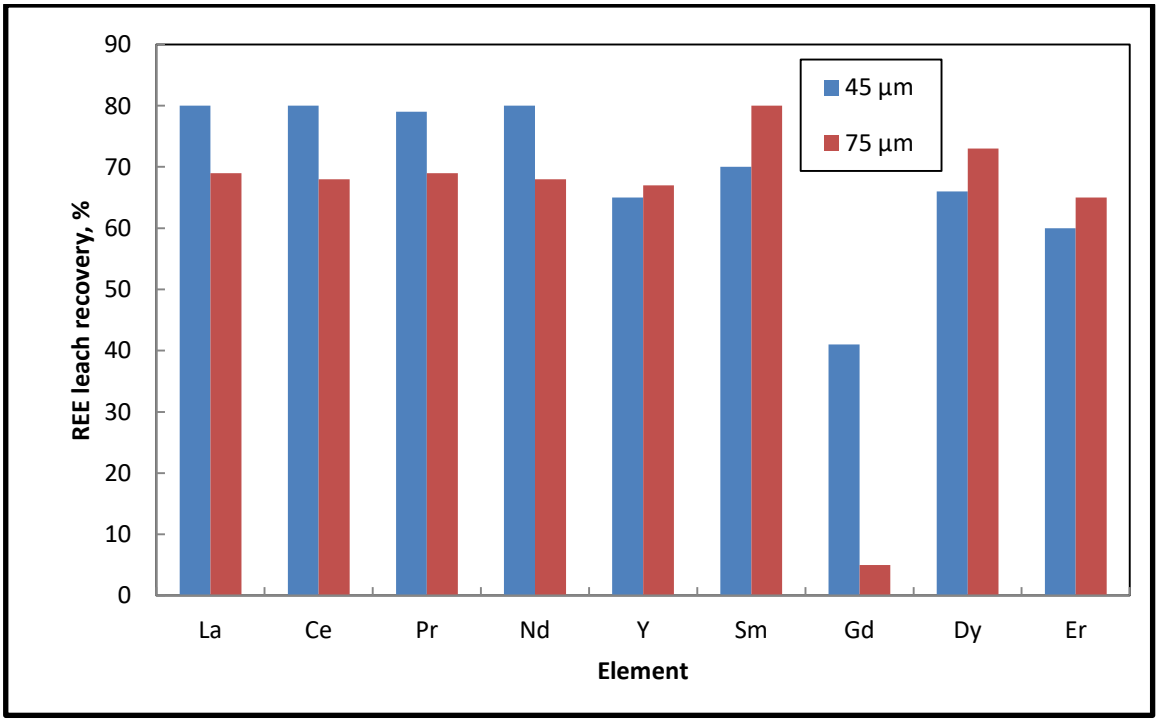

FIGURE 25: NON MAGS SAMPLE LEACH EFFICIENCY OF INDIVIDUAL ELEMENTS.

Figure 25 shows the leach recovery of the non mags sample at different grind sizes. Data can be found in Table 26 in Appendix A.

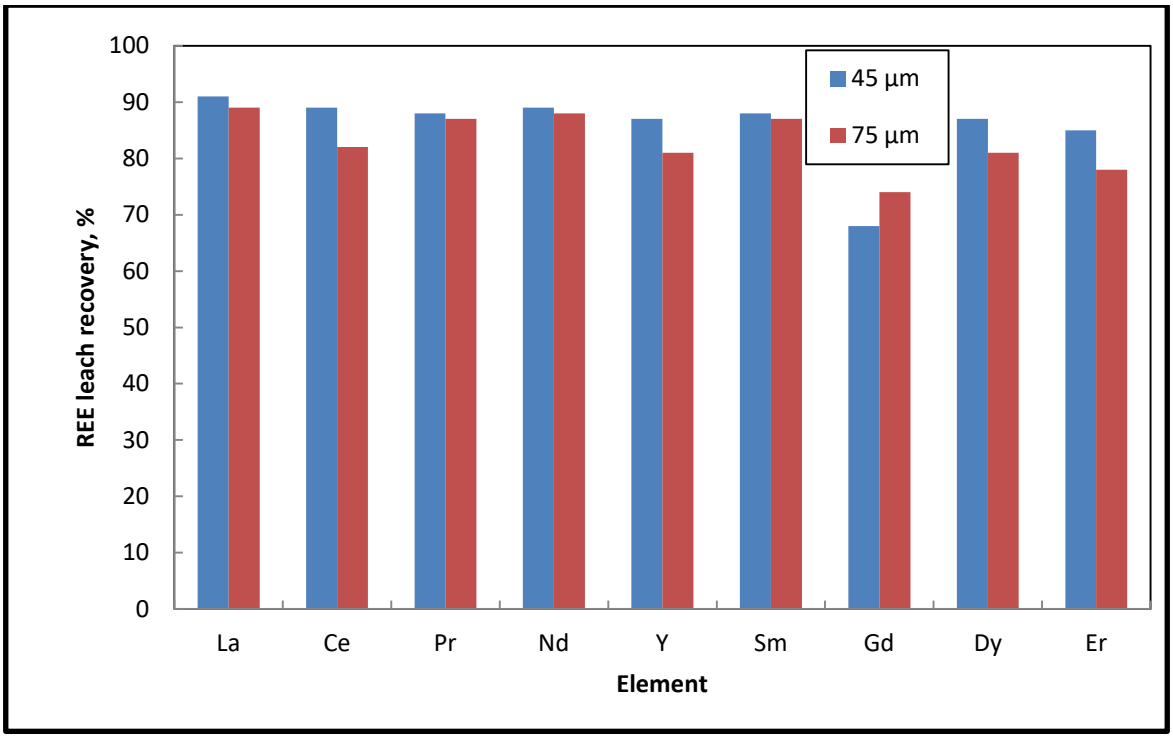

FIGURE 26: MONAZITE CONCENTRATE SAMPLE LEACH EFFICIENCY OF INDIVIDUAL ELEMENTS.

5.1.4 NaOH Consumption for the cracking step

The chemical NaOH consumption was approximated based on the stoichiometric amount of NaOH that reacted with Al, Si, P and Fe in the ore according to the following reactions:

$$Al_2O_3 + 2NaOH \rightarrow 2NaAlO_2 + H_2O$$

$$SiO_2 + 2NaOH \rightarrow Na_2SiO_3 + H_2O$$

$$2FeS_2 + 8NaOH + 7O_2 \rightarrow 2Fe(OH)_2 + 4Na_2SO_4 + 2H_2O$$

$$REPO_4 + 3NaOH \rightarrow RE(OH)_3 + Na_3PO_4$$

The whole ore (25% TREO) and LIMS product (30% TREO) samples had NaOH consumptions between 264 and 388 kg 100% NaOH/ton ore. The monazite concentrate (50% TREO) had a consumption of only 162 kg 100% NaOH/ton ore based on actual extractions.

5.2 FLOW SHEET DEVELOPMENT

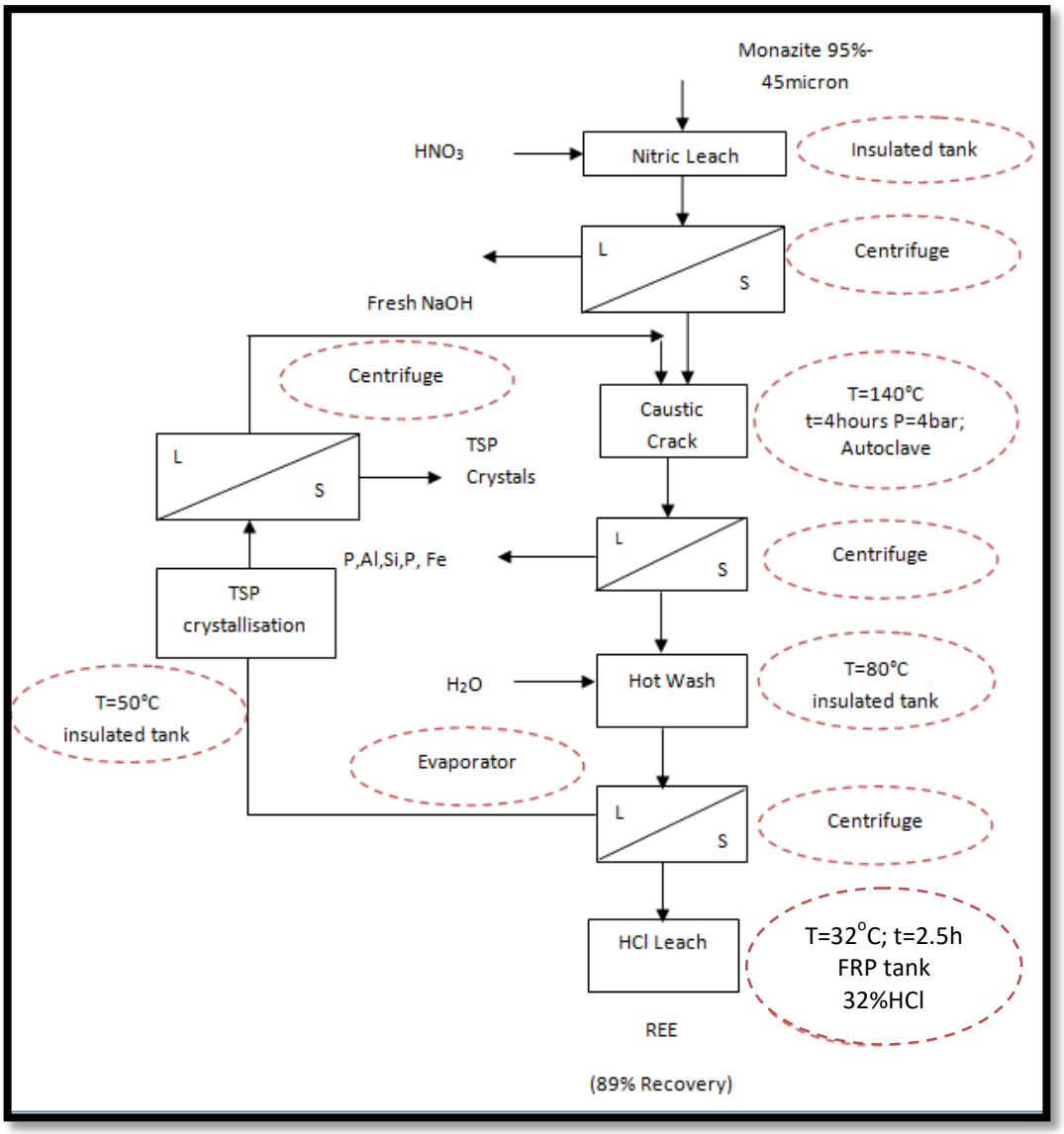

FIGURE 27: FLOW SHEET DEVELOPED FOR THE CAUSTIC CRACKING OF MONAZITE.

It can be seen from the above that the monazite concentrate at 95%-45 µm was chosen since this feed produced the greatest recovery after the cracking stage (89 %) and consumed the least amount of NaOH (162 kg of 100% NaOH equivalent i.e. 324 kg of 50% NaOH). With the conditions established in the experiments, on an industrial scale this will need to be done in an autoclave (probably made out of Ni-lined mild steel) at 140°C at 4 bar pressure for 4 hours. It is to be noted that the entire hydrometallurgy operation is to be operated in a batch manner. It is also important to note that the batch operation (in this case) uses two

autoclaves (although only one is required), which implies that filling and discharging times do not need to be accounted for in the 4 hour reaction time required. It should also be mentioned that all the reactors are connected to a central scrubbing system to clean the gases and vapour before they are released.

The resulting product from the autoclave will need to be transferred to holding tanks directly under them in which cold water has been added and thereafter solid-liquid separation through a centrifuge (since it was seen in the test work that this material doesn't filter easily and was recommended by the supplier after in-depth scrutiny of test results) in which in the liquid overflow contains the dissolved impurities such as Al, P, Si and Fe and the solids moving forward into an insulated tank for a hot water wash at 80°C for four hours. The insulation is critical since a drop in temperature below 80°C will result in crystallization of Na_3PO_4 and thus the tank ought to be jacketed in order to ensure that the solution does not cool too far.

The product of the hot water wash undergoes S/L separation through a further centrifuge. The solids from the hot wash stage then move forward as RE hydroxides and are leached at pH 3, maintained with 32% HCl, at 60°C for 2.5 hours. The liquid part moves to an evaporator to drive off excess water and then, once concentrated enough to crystallize TSP, the solution temperature is allowed to cool to below 50°C to crystallize out TSP. Cooling occurs easily since it is batch and can be left to cool overnight. It is then filtered through a centrifuge the liquid portion of NaOH is regenerated to the feed. No regeneration test work was done as it is a standard process.

It has been mentioned earlier that REE recovery from the monazite concentrate subjected to such treatment (as described above and in the flow sheet) will obtain a value of 89% reporting to the PLS.

5.3 EQUIPMENT SIZING

Based on the above flow sheet and experiments conducted, a detailed mass balance was calculated based on ~3 ton batches (refer to 4.2.2.1) of pre-leached monazite concentrate to the caustic cracking circuit and is shown in Table 42 in the appendix. The volumes in each of the vessels calculated were then sent to the respective equipment suppliers and quotes obtained to fulfil the required duty. These prices are discussed in the next section 5.4.2.

5.4 FINANCIAL CONSIDERATIONS

The purpose of this part of the chapter is to interpret the flow sheet established from the results in the previous chapter with the objective to determine which flow sheet will best suit the SKK monazite concentrate. As said earlier, this analysis will be done in terms of the REE recovery to the final step (which is the HCl leach of which the product is subsequently sent to purification), CAPEX, OPEX, SHREQ and lastly the effects on downstream processes. A summary of this study will be presented in tabular form as a conclusion in the final chapter.

5.4.1 RECOVERY

The recovery achieved in the experiments using the caustic route is to be discussed in the relative section in comparison to the sulphuric acid route. For now it is sufficient to say that using the 95%-45 µm pre-leached monazite concentrate achieved 89% overall recovery after the selective leach with HCl.

5.4.2 CAPEX

The dotted circles adjacent to each of the blocks in the flow sheet depicted in Figure 27 contain the equipment wherein the associated steps are carried out. Each of these pieces of equipment was sized based on the amounts obtained in the mass balances, and these amounts then forwarded to manufacturers of the equipment in South Africa. Each significant step shall be discussed with regard to its impact

on CAPEX. In brief, this circuit comprises of an autoclave, four centrifuges, four insulated FRP tanks, a normal reaction tank and an evaporator.

The material experimented upon was leached with nitric acid to upgrade it to 50% grade of TREO.

As one can see, the caustic cracking occurs in an autoclave at a temperature of 140°C and a pressure of 4 bar. At these conditions optimum cracking occurs as per the experiments carried out. The most common material to handle caustic environments is carbon steel if the contamination by iron can be tolerated (International Nickel Company, 1963). If temperatures were lower than 80°C at concentrations lower than 20% NaOH stress relieved carbon steel may have been an option, however, at a concentration of 50% NaOH (as in our case) and at a temperature of 140°C only nickel alloys are recommended. Thus the CAPEX will be severely impacted upon since a mild steel Ni-lined autoclave shall be used on industrial scale (although the experiments were not done in an autoclave).

A centrifuge for solid liquid separation then follows the autoclave and the materials of construction typically are selected as 316 L stainless steel together with some 316Ti parts. However, the difference between the CAPEX between a centrifuge in the caustic crack and in the acid bake flow sheets is not much since they experience similar duty as per the comparisons between their respective mass balances in the appendix.

After the first stage of S/L separation, the solids are washed with hot water in a fibre reinforced plastic (FRP) tank which is insulated and is able to withstand temperatures up to 110°C. Insulation is key since a drop in temperature below 80°C will cause crystallization of TSP. After the second stage of S/L separation the solids are leached in an FRP tank with 32% HCl and the liquid forwarded to the evaporator to drive off excess water (hence increasing the concentration) and then

resultantly to another FRP tank for recrystallization at 50°C. This tank is not insulated.

TABLE 10: CAPEX FOR CAUSTIC CRACK.

Caustic Crack			
Equipment	**Number Required**	**Price per unit**	**Total Price**
		R	**R**
Scrubbing system	1	1,000,000	1,000,000
PVDF/FRP 25 m³	4	320,000	1,820,000
Autoclaves (mild steel Ni-lined)	2	1,000,000	2,000,000
Pumps	10	33,000	330,000
Tanks (25 m³) SS jacketed	1	200,000	200,000
Steel tank (25 m³) with jacket	2	200,000	400,000
Centrifuge	4	320,000	1,280,000
Evaporator	1	3,000,000	3,000,000
TOTAL			10,030,000

5.4.3 OPEX

In a hydrometallurgical plant, the OPEX associated with processes usually implicate costs stemming from mainly three factors i.e. the reagents, power and labour. However, the labour shall be ignored since the plant has highly sophisticated control systems independent of human interaction since the radioactivity of the plant restricts this (thus limited labour shall not impact the NPV that much and will be taken as constant). Thus only power and reagents shall be considered. These two factors will be discussed in depth as well as other factors contributing to these two circuits in their respective chapters.

5.4.3.1 REAGENTS

Prior to cracking the ore needs to be leached with nitric acid. Since the cost of nitric acid was not included in the OPEX and from other test work it was established that the consumption was 717 kg HNO_3/ton of feed. Thus it requires 9124.4 tpa of nitric acid.

The first step of the caustic crack is fed with caustic soda, which is almost four times the price of sulphuric acid. However, an important highlighted benefit of the caustic crack should be brought up at this juncture. The caustic crack has been preferred in industry because of its ability to recover tri-sodium phosphate as a by-product according to Habashi (2013) as mentioned in 2.4.2. This point holds little value in the current economic market, since TSP is not really marketable as it used to be used as a common degreasing detergent, until it was superseded by more modern formulations that don't contain phosphates and hence are more environmentally acceptable.

Since this, as mentioned earlier, is a batch process, control is much easier. The mother liquor of the TSP is simply NaOH which is recycled to the caustic crack. Hence the overall OPEX discussion leads to the conclusion that NaOH can be recycled and ultimately reduces the key contributor to the OPEX in this process. Previously the market for TSP was huge; however it has dwindled over time. Since the value is currently low, currently no value has been attributed to the TSP product.

The remainder of the reagents in this circuit is water as indicated in the mass balance in Appendix B: Mass Balances (which is not a problem at SKK as discussed in the chapter regarding SKK since there is numerous boreholes) and HCl of 32% concentration which is the same concentration and similar quantity ~6000 tpa (depicted in the respective mass balances) as that used in the acid bake to leach the REOH at the end.

5.4.3.2 POWER

It is imperative to highlight OPEX in terms of operating temperatures, more so in this study. When one compares this section to the related section in the acid bake we can see the effect of metallurgical chemistry coming into play. As indicated in our test work, we see that the caustic crack is carried out at 140°C for 4 hours. The autoclave is decompressed manually in a slow manner into large holding tanks filled

with water at the bottom of the autoclaves. The product is then subjected to a hot water wash at any temperature above 80°C- and the water (at room temperature) does not require heating since the residual heat from the product is sufficient to maintain a temperature above 80°C. It goes through a centrifuge (which can operate at a maximum 120°C) as opposed to a filter press (which cools as a result of the air blown through).

The solids are forwarded to the leaching stage. The liquid, as mentioned earlier is aimed at recovering caustic and producing TSP. The TSP can only begin to crystallise if the liquid is of a certain concentration at a specific temperature. Thus, an evaporator is required to concentrate this solution. An evaporator as can be seen from Table 11 is quite demanding on power. However, this is essential. Table 11 and Table 12 summarise the OPEX for the caustic crack and are comprised of the power requirements and associated costs for each piece of equipment. The cost of power was based on a value of R8/kw.h as calculated from previous work. Indicated in Table 12 is the caustic crack reagent inventories which were obtained from the mass balance based on the experimental results presented earlier.

TABLE 11: POWER REQUIREMENTS FOR THE CAUSTIC CRACK.

Equipment	Power Rating	Total Power	Cost (R8/kWh) (R3.50/kWh for diesel stipulated)	Cost per annum (operating for 7446 hours)
	kW	kW	R	R
Scrubbing system	2	2	16	119,136
Autoclaves INCONEL	10	20	160	1,191,360
Pumps (diesel motor)	3	81	283.5	2,110,941
Centrifuge	7.5	22.5	180	1,340,280
Evaporator	15	15	120	893,520
TOTAL		140.5	1,124	5,655,237

TABLE 12: ASSOCIATED REAGENTS OF THE CAUSTIC CRACK.

Reagent	Requirement (tpa)	Price per ton (R)	Cost per year (R)
Nitric Acid (60%)	9,125	3,683	33,607,375
Caustic	3,253	9,881	32,142,893
HCl (32%)	6,512	2,300	14,977,600
Total Reagents for Plant	9,765		80,727,868

5.4.4 NPV

Based on the above CAPEX and OPEX values, the NPV values were calculated over the period of 20 years and are indicated in Table 13.

As mentioned earlier in 4.2.2.3 the NPV was calculated using the following formula:

$$NPV = \sum_{t=1}^{T} \frac{C_t}{(1+r)^t} - C_o$$

Where;

C_t = net cash inflow during the period t

C_o = total initial investment costs

r = discount rate, and

t = number of time periods

As can be seen in Table 13, the basic net cash flow was calculated by subtracting the expenses i.e. the total amount for reagents and power from the total income i.e. total amount of REEs produced (2700 tons) by the selling price per kg (R140/kg). This was then used to calculate the Ct value for each year. The Ct for all the years over the life of mine was then added up. The initial total investment which comprised of the amount of the entire project (excluding hydrometallurgy) calculated in previous work i.e. R292M was added together with the cost of the hydrometallurgy circuit based on the CAPEX calculated (R10,030,000).

The total of this was subtracted from the total Ct over the life of mine which resulted in a net NPV of ~R1.6B.

TABLE 13: NPV CALCULATED FOR THE CAUSTIC CRACK OVER THE 20 YEAR PERIOD

	Ct (Basic Net Cash Flow)	(2700*1,000*140)-(80,727,868+5,655,237)	R291,616,895
	Co	(292,000,000+10,030,000)	R302,030,000
	R		0.14
Net Cash Flow (Ct)	YEAR (t)		
Ct at year 1	1	(291,616,895/(1+14%)^1	R255,804,294
Ct at year 2	2	(291,616,895/(1+14%)^2	R224,389,731
Ct at year 3	3	(291,616,895/(1+14%)^3	R196,833,098
Ct at year 4	4	(291,616,895/(1+14%)^4	R172,660,612
Ct at year 5	5	(291,616,895/(1+14%)^5	R151,456,677
Ct at year 6	6	(291,616,895/(1+14%)^6	R132,856,734
Ct at year 7	7	(291,616,895/(1+14%)^7	R116,540,995
Ct at year 8	8	(291,616,895/(1+14%)^8	R102,228,943
Ct at year 9	9	(291,616,895/(1+14%)^9	R89,674,511
Ct at year 10	10	(291,616,895/(1+14%)^10	R78,661,852
Ct at year 11	11	(291,616,895/(1+14%)^11	R69,001,625
Ct at year 12	12	(291,616,895/(1+14%)^12	R60,527,741
Ct at year 13	13	(291,616,895/(1+14%)^13	R53,094,510
Ct at year 14	14	(291,616,895/(1+14%)^14	R46,574,131
Ct at year 15	15	(291,616,895/(1+14%)^15	R40,854,501
Ct at year 16	16	(291,616,895/(1+14%)^16	R35,837,282
Ct at year 17	17	(291,616,895/(1+14%)^17	R31,436,212
Ct at year 18	18	(291,616,895/(1+14%)^18	R27,575,625
Ct at year 19	19	(291,616,895/(1+14%)^19	R24,189,144
Ct at year 20	20	(291,616,895/(1+14%)^20	R21,218,548
		Ct over 20 years Life of Mine	R1,931,416,767
NET NPV		Ct over 20 years Life of Mine-C	R1,629,386,767

The net NPV over the project period is R1,81B using the caustic cracking method.

5.5 SHREQ Analysis

The analysis for the caustic crack shall be discussed comparatively in the next chapter under this heading in comparison with the sulphuric acid cracking process.

5.6 EFFECTS ON DOWNSTREAM PROCESSES

The effects on downstream processes for the caustic crack shall be discussed comparatively in the next chapter under this heading in comparison with the sulphuric acid cracking process.

CHAPTER 6

6 Results and Discussion: The Sulphuric Acid Crack

6.1 Experimental Results

6.1.1 Influence of acid addition

The LIMS samples (depicted in Table 7) were used for these tests.

In order to test the influence of sulphuric acid addition on REE recovery, seven acid addition optimisation tests were done. The acid dosage that was tested ranged from 1000 kg/t to 2500 kg/t feed. All other parameters were kept constant. The feed solids used for these tests were dried prior to acid baking and the acid baking was conducted at 280°C for 3 hours. The water leach was conducted at ambient temperatures and at a pulp density of 20% (m/m) for 2 hours.

The baked solids at an acid addition of 2000 kg/t feed and 2500 kg/t feed were not submitted for chemical assaying since the acid dosage was too high (as can be seen from Figure 28).

FIGURE 28: IMAGE OF A BAKED SAMPLE THAT ABSORBED MOISTURE FROM SURROUNDINGS.

Figure 29, the data for which is in Table 30 in Appendix A, shows that as the acid dosage is increased, the recovery of TREE was increased as well. The TREE recovery was increased from 88% to 99.7% by increasing the sulphuric acid dosage. The graph also shows that the HREEs are more sensitive to acid dosage than the LREEs because the acid dosage causes a greater change in the recovery percentage for HREE than for LREE. When the dosage was increased from 1200 to 1400 kg/t, the HREE recovery improved from 86% to 90%, whereas the LREE recovery improved from 94% to 96% for the same dosage change. MREE was also more sensitive than LREE.

At an acid of addition of 1600 kg/t, a 99% recovery was achieved and this was selected as the optimum dosage.

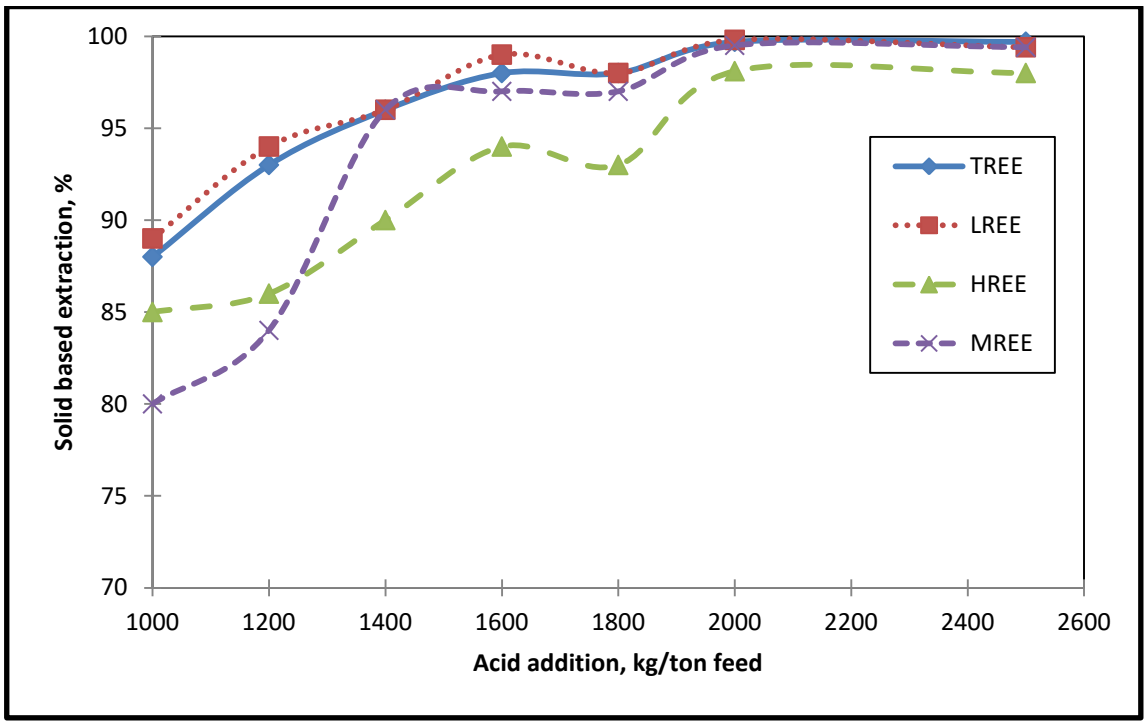

FIGURE 29: RELATIONSHIP BETWEEN ACID ADDITION AND REE RECOVERY.

6.1.2 Influence of Initial Pulp Density

The influence of pulp density on REE recovery was tested by using different pulp densities. The feed used for these tests was a blended portion of solids baked at an acid addition of 1600 kg/t and 1800 kg/t feed. The grade of REEs in the baked feed was 12.4% (m/m). The pulp densities tested were 20%, 25%, 30%, 35% and 40% (m/m).

The water leach was done at ambient temperature and the slurry temperature remained below 30°C. The slurry temperature, however, is expected to increase significantly due to the exothermic dilution of residual acid with water that will compromise the dissolution of $RE_2(SO_4)_3$ because the $RE(SO)_4$ solubility decreases with increasing temperature.

Figure 30 shows the relationship between an increase in pulp density and the recovery of REEs. Data was taken from Table 31 in Appendix A. From the figure it can be seen that increasing the pulp density from 20% to 40% has no significant influence on REE recovery relative to the feed. The TREE recovery increased from 98% to 99%. The decrease in recovery when increasing pulp density from 20% to 25% might have been due to an analytical error.

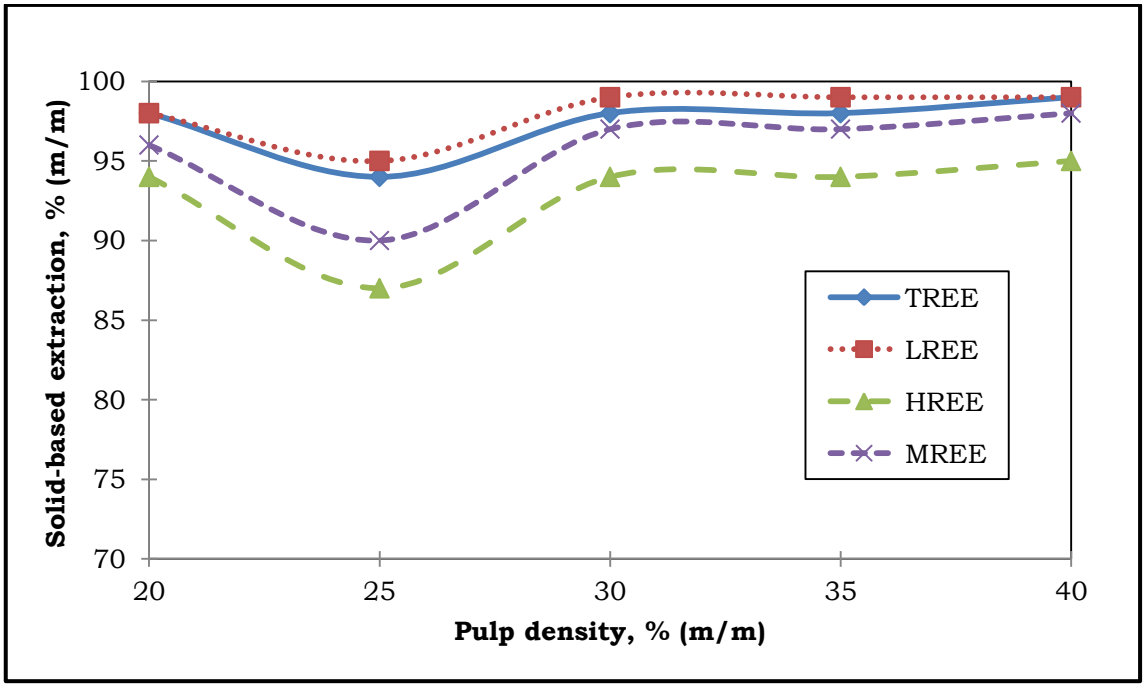

FIGURE 30: RELATIONSHIP BETWEEN PULP DENSITY AND REE RECOVERY.

Figure 31 shows the relationship between pulp density and the impurity leach efficiency. Data for this graph is in Table 32 in Appendix A. When pulp density is increased, it can be seen that the dissolution of Al, Si and Fe decreases. The Si leach efficiency at 20% pulp density was 9% whereas the efficiency at 40% pulp density was 6%. The change in pulp density did not affect the leach efficiency of Th or Cu significantly.

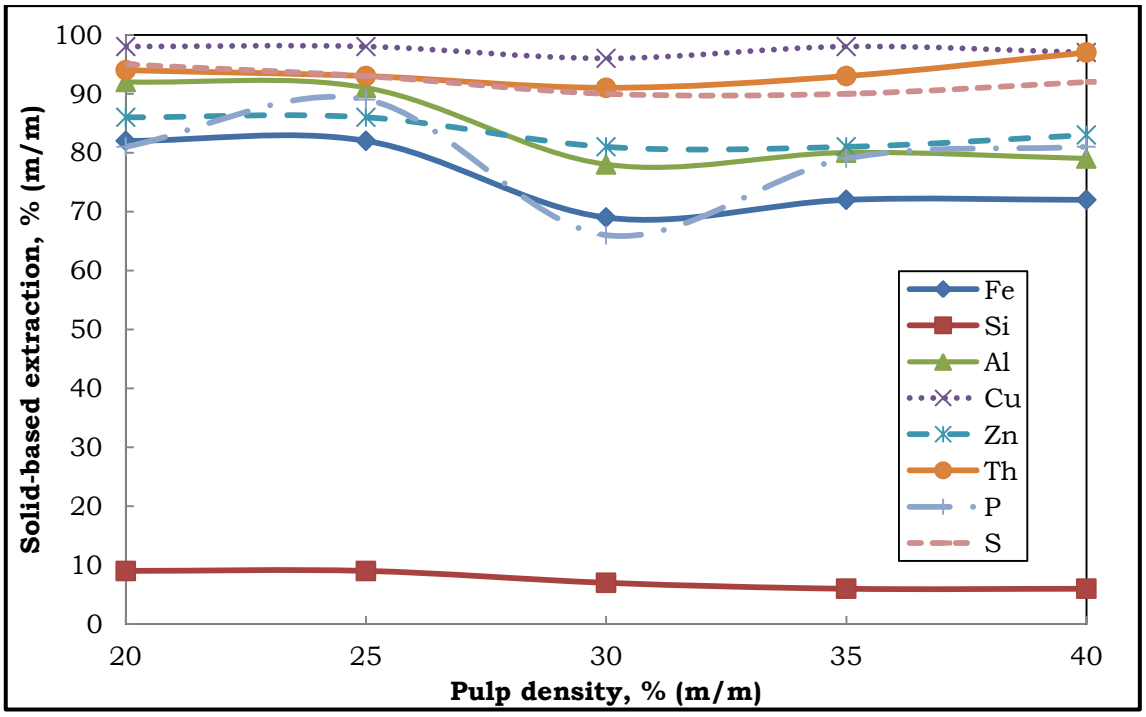

FIGURE 31: RELATIONSHIP BETWEEN PULP DENSITY AND IMPURITY LEACH EFFICIENCY.

The TREE tenor in the leach liquor was 73 g/L at a pulp density of 40% while it was 33 g/L at 20% pulp density. The P tenor in the leach liquor at 40% pulp density was 21.6 g/L while it was only 11 g/L at 20% pulp density. High impurity tenors in solution may result in high impurity entrainment during the REE recovery step. There are some elements that might precipitate earlier due to the formation of complex compounds such as thorium pyro phosphate. Figure 32 shows the influence of pulp density on the metal tenors in the leach filtrate. The data depicted in this graph can be found in Table 33 in Appendix A.

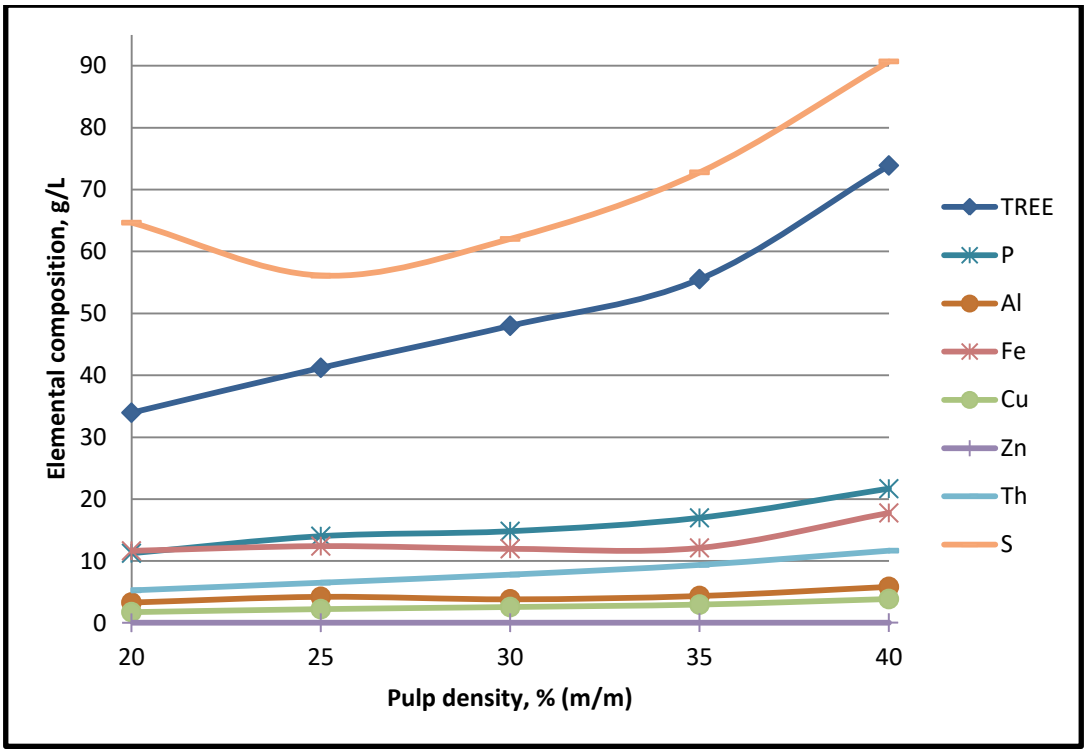

FIGURE 32: INFLUENCE OF PULP DENSITY ON WATER LEACH FILTRATE COMPOSITION.

6.1.3 Influence of Feed Moisture Content

The tests showed that a moisture content of 15% did not influence the recovery of REEs significantly at an acid addition of 1800 kg/t feed. The REE recovery at 1800 kg/t feed was 99% when feeding dry feed and 98% when feeding wet feed. When the acid dosage was 1600 kg/t feed, however, the moisture content had a significant influence on the REE recovery. When feeding wet feed at a dosage of 1600 kg/t feed the recovery was 80% while the recovery was 99% when dry feed was fed at the same acid dosage.

The residues were submitted for mineralogical investigation by XRD (X-Ray diffraction). Some minerals diffract better than others, and this can create an inflated mass abundance. Because of this, mineral mass per cent results are reported in a descriptive range of relative abundance, i.e. predominant, major, intermediate, minor, trace or not detected. Amorphous phases are not detectable.

The mineralogy given in Table 14 indicated that the wet feed after a 1600 kg/t acid addition contains minor amounts of aluminium phosphate and minor amounts of unreacted monazite.

TABLE 14: XRD ANALYSIS ON 1600 kg/t SAMPLE

Mineral name	**Formula**	**Compound proportion**		
Alunogen	$Al_2(SO_4)_3 \cdot 17H_2O$	minor	minor	minor
Monazite-(Ce)	$(Ce,La,Nd)PO_4$	minor	minor	trace
Anhydrite	$CaSO_4$	major	major	major
Aluminium phosphate	$AlPO_4$	minor	nd	nd
Quartz	SiO_2	major	major	major
Gonnardite	$Na_2Ca(Al_2Si_3O_{10})_2(H_2O)_6$	trace	nd	nd
Aluminium iron sulphate hydrate	$Fe(Fe, Al)\ (SO_4)_3\ (H_2O)_9$	nd	nd	intermediate
Albite	$NaAlSi_3O_8$	minor	minor	minor
nd –not detected, trace < 5mass %, minor 5-15mass%, intermediate 15-25mass%, major 25-50mass%, predominant >50mass%				

The samples that achieved good recovery did not contain aluminium phosphate. The REE recovery at an acid addition of 1800 kg/t feed was not affected by adding feed with a moisture content of 15%, but it is expected that the REE recovery will be affected by adding feed with high moisture content. It is therefore a challenge to control the plant when feeding wet solids.

Figure 33 shows the relationship between moisture content and REE recovery at the two different acid dosages and the data can be found in Table 34 in Appendix A.

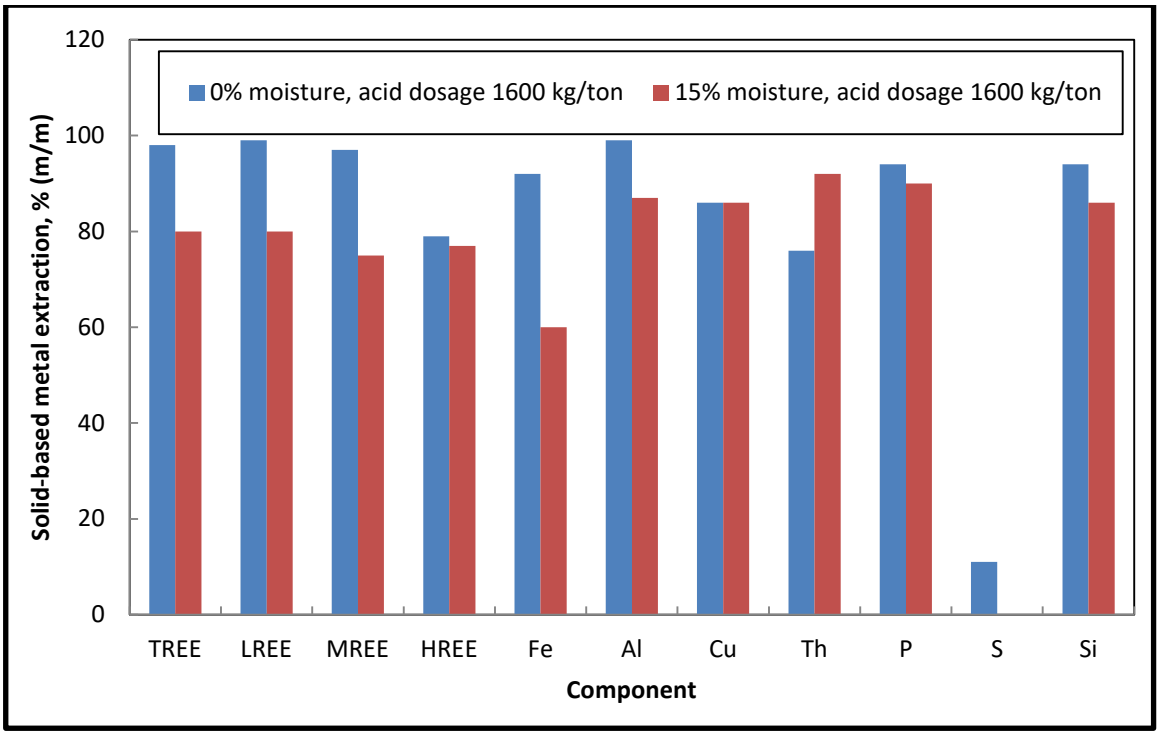

FIGURE 33: EFFECT OF MOISTURE CONTENT ON REE RECOVERY.

6.1.4 Influence of Grind Size

Two grind sizes, 45 µm and 75 µm, were tested in order to investigate the influence of milling finer on the recovery of REEs. The feed solids were dried prior to acid baking. The acid baking was conducted at 280°C for 3 hours with an acid dosage of 1600 kg/t feed. The water leach was done at ambient temperature at a pulp density of 20% (m/m) for 2 hours.

The different grind sizes did not have a significant influence on the recovery of REEs, as shown in Figure 34. The data for this graph is listed in Table 35 in Appendix A. Both grind sizes resulted in a REE recovery of about 98%. It is recommended to investigate the effect of coarser grind on REE recovery. A coarser grind will be beneficial to the plant because the cost of milling will be decreased and the solid-liquid separation efficiencies will be improved.

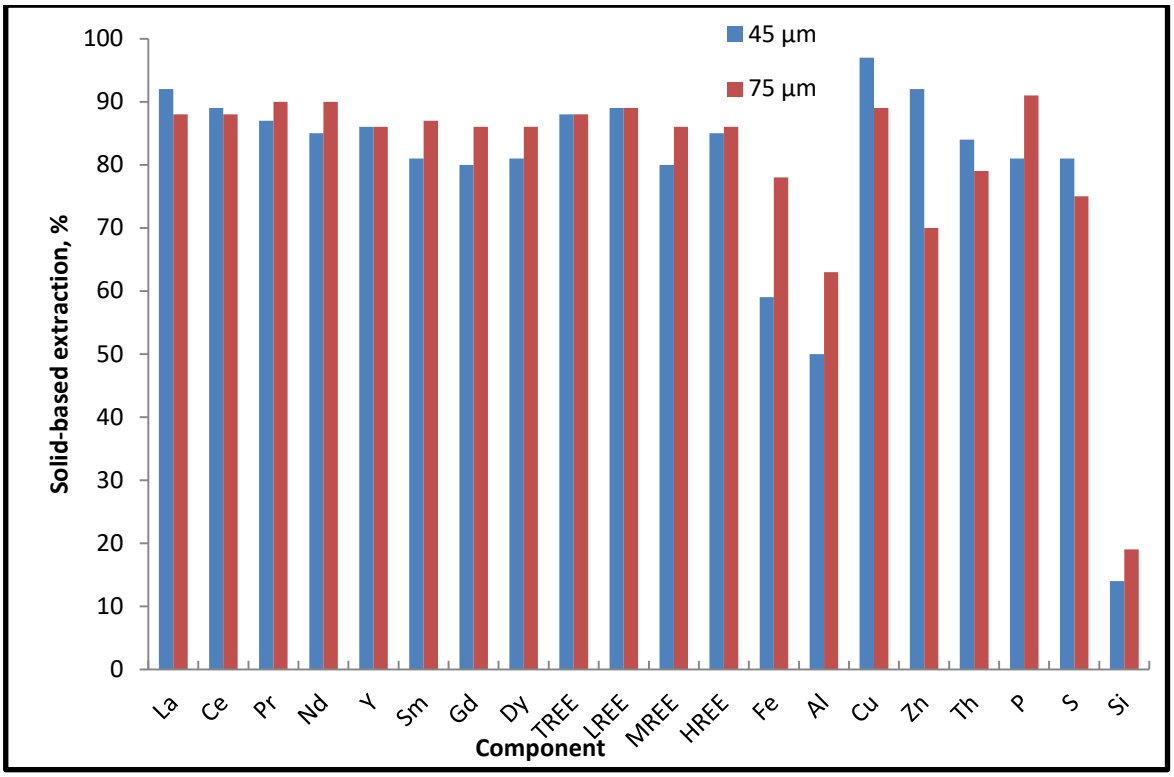

FIGURE 34: EFFECT OF GRIND SIZE ON REE RECOVERY.

6.1.5 REE Double Salt Precipitation

Table 38 presents the elemental composition of the feed and residual liquor in this process step. The TREE concentration in the feed solution to the first and second pilot plant run was 30.8 g/L and 44.9 g/L, respectively. These were quite different because the water leach was done with different initial % solids. The major elements in the feed samples were, in the order of increasing concentration, P, Fe, Th and Al. The TREE in the filtrate and the combined washes were 1.5 g/L and 0.29 g/L respectively. The precipitate was washed with hot Na_2SO_4 solution (2% (m/m)) to prevent the re-dissolution of REEs. Some of the REEs were dissolved during the washing step as the composition of some of the REEs in the wash water was higher than in the filtrate solution.

Table 39 presents the REE double salt test conditions and the summary of results obtained. The density of the final solutions, as well as the slurry pulp density were 1.2 t/m^3 and 8.2% (m/m), respectively.

Sodium sulphate was added as dry solids, and the addition was 6 kg/kg of TREE (5.8 times the stoichiometric requirements).

Table 36 in Appendix A presents the precipitation efficiencies of the major elements from solution. The recovery of REEs into the precipitate for the first and second pilot plant run was 95.2% and 96.5% (approximately 4% loss), respectively. The recovery of HREE into the precipitate improved from 32.6% in the first run to 44.5% in the second run. This improvement in the HREE recovery in the second run might have been due to slightly higher REE tenor in the feed solution. The balance of the REEs deported into the barren solution of which about 95% were heavy REEs in run 1 and 86% in run 2. About 45% of the Th in the feed reported to the REE precipitate in pilot run 1 and 56% in run 2.

The elemental composition of the REE precipitate is presented in Table 40 in Appendix A, the grade of REEs in the precipitate was 30% (m/m) of which Ce contributed about 45%. The major impurities in the REE precipitate were Th (3.1% (m/m)), Fe (1.1% (m/m)), Al (0.6% (m/m)) and Ca (0.6% (m/m)). The uranium grade in the precipitate was less than 1.3 mg/kg.

6.1.6 REE Double Salt Conversion

Table 41 in Appendix A presents the REE double salt conversion test conditions and the summary of results obtained. The REE content was upgraded from 30% (m/m) to 59% (m/m) TREE and the corresponding mass loss was 48%. The REEs did not dissolve but converted from one precipitate to another precipitate (DSP) under a highly alkaline environment with excess sodium hydroxide. The mass balance indicated TREE losses of about 0.2% but it would likely be due to suspended solids. The conversion efficiency of sulphate was 99.5% and the grade of S in the REE hydroxide was 0.2% (m/m). The concentration of sulphate and sodium in the leach liquor were respectively 129 g/L and 35 g/L. A portion of Na in the cake might have being present as NaOH, while the

balance would have been Na_2SO_4. The grade of Na in the cake was 0.1% (m/m).

Based on the amount of sulphate dissolved and the grade of Na and S in residues, more than 99% of the REEs in the cake were present as hydroxides. It was anticipated that most of the Al will dissolve during this step; however only 16% of the Al did dissolve. The grade of Th and P in the cake was 6% (m/m) and 0.9% (m/m) respectively. A portion of the Th in the cake might have existed as thorium phosphate.

The concentration of S in the filtrate was used to calculate the concentration of sodium sulphate present in this solution. Based on the calculation, the concentration of sodium sulphate was estimated to be about 52% (m/m). The Na_2SO_4 will be recycled as a reagent into the double salt precipitation stage. Depending on the water balance across the plant, it might be necessary to evaporate the solution.

6.1.7 REE Acid Leach

The solid-based REE and impurity leach efficiencies obtained in the leach tests, as well as HCl consumption, are presented in Table 37. The grade of REEs in the feed was 59%.

The total REE leach efficiency, at the test pH value of 2.8, was 94%. Copper and calcium were highly soluble at pH 2.8 and their respective leach efficiencies were 88% and 79%.

The HCl consumption at the test pH value of 2.8 was 1.7 kg of 32% HCl/kg TREE in feed.

6.2 Flow sheet Development

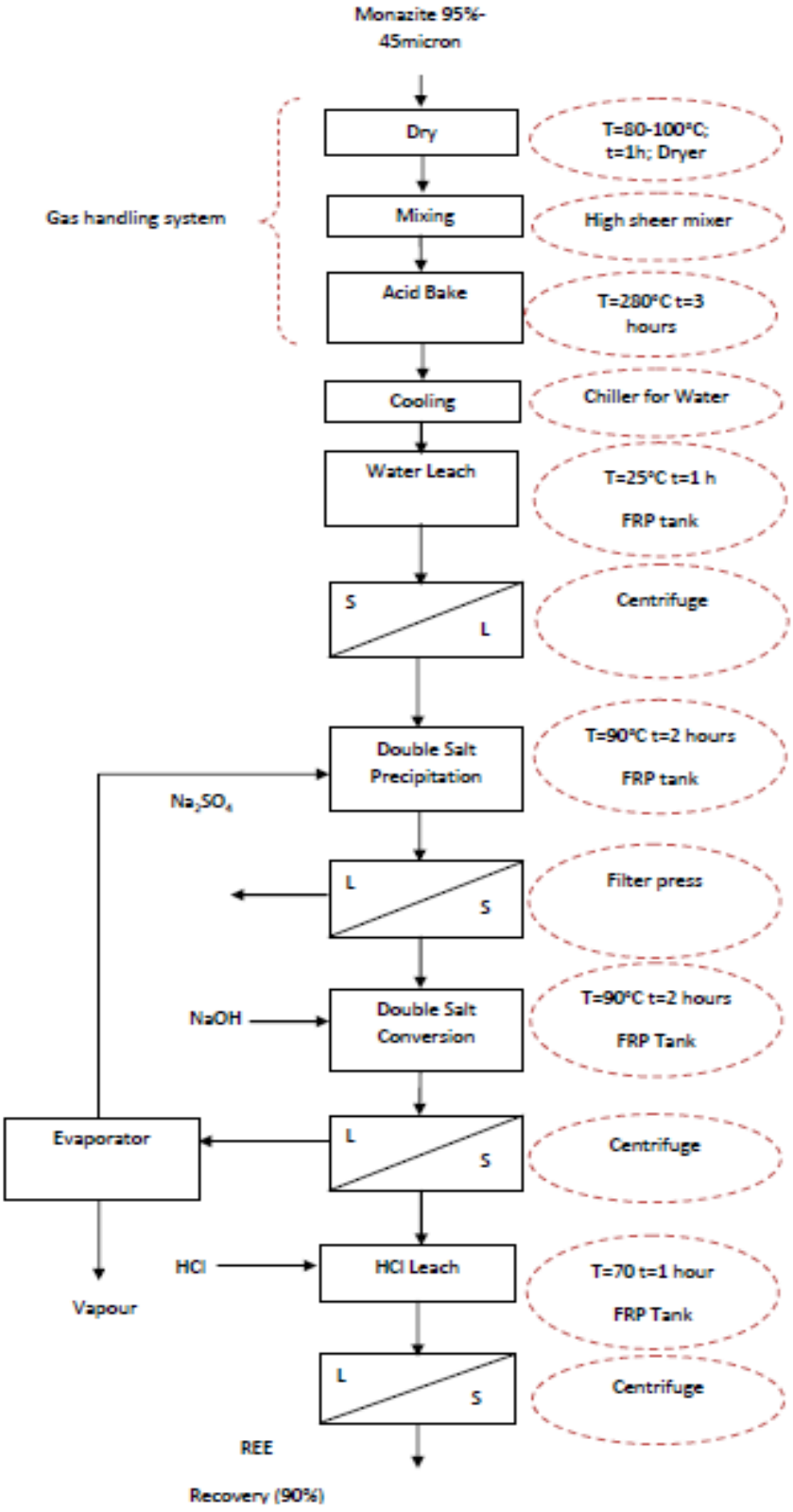

FIGURE 35: FLOW SHEET DEVELOPED FOR THE H_2SO_4 ACID BAKE PROCESS.

Based on the results from the acid baking route in the previous section, one can see (from the flow sheet developed on the previous page) that, firstly due to the influence of feed moisture content of the 95% passing-45 micron feed, a drying stage is required since at an acid dosage of 1600 kg/t (the required dosage) the recovery drops by approximately 20% in the presence of moisture. Therefore drying was done in an oven to reduce the moisture content which typically would be implemented in a dryer on a plant at a temperature around 100°C for approximately an hour. It is to be noted again that this is a batch type of process.

The dry material is then forwarded to mixing with sulphuric acid (which is usually achieved within 30 minutes to an hour) such that it may thicken in order not to simply pass through the subsequent rotary kiln.

Subsequently, the dried feed is then baked at 280°C for 3 hours in a batch wise manner in a rotary kiln with the acid dosage of 1600 kg/t. The solids are allowed to cool to room temperature naturally. The cooled solids are now transferred to an FRP tank whereby it is leached with water cooled by a chiller. This is indeed another crucial step, since (and beyond the scope of this thesis) it is indicated from test work that in order to leach the REE, the solubility needs to be maximised; different from the norm, REE sulphates have higher solubility at lower temperatures. The water leach is conducted for 2 hours and then passed through a centrifuge. This concludes the actual "cracking of monazite" with a recovery of 99%.

However the flow sheet is expanded beyond this point up until the leaching of $RE(OH)_3$ with HCl, since the point of this study is to provide an "apples for apples" study with regard to choosing between the caustic and sulphuric acid bake. The reason to expand this flow sheet after the water leach is because the product is a solution of $RE_2(SO_4)_3$ which cannot be separated into individual REEs (since all the elements are in solution with the impurities) and in real circumstances needs to be converted to a $RE(OH)_3$ which can then be leached with HCl in the same manner as it was done in the caustic cracking flow sheet.

The conversion after the water leach step is done by using double salt precipitation with Na_2SO_4 at 90°C in an FRP tank. The consumption is 3 kg/kg TREE. The recovery of REE from this stage is approximately 95.2%. The product, i.e. $RENa(SO_4)_2$, is then passed through a centrifuge and the resulting liquid undergoes double salt conversion by addition of NaOH. This converts the double salt to $RE(OH)_3$ which is easier to leach. The liquid portion from this process is evaporated since the Na_2SO_4 required for recycling to the double salt precipitation steps is required in high concentration.

The solids move forward as a $RE(OH)_3$ and is leached with HCl at room temperature. Ultimately after this step, the overall REE recovery is 90%. Majority of the remaining residue is Th.

6.3 Equipment sizing

Based on the above flow sheet and experiments conducted, a detailed mass balance was drawn up based on 1862 batches and is shown in appendix B on page 125. As mentioned earlier, 1862 batches (approximately 3 tons each) to the hydrometallurgy process per annum will fulfil the requirement of production i.e. 2700 tpa. The volumes in each of the vessels calculated were then sent to the respective equipment suppliers and quotes obtained to fulfil its duty. Considering Table 9 and the assumptions made therein, a sample calculation appears in the appendix on page 125 to demonstrate how the sizing of equipment was carried out. The corresponding prices are discussed in section 6.4.2 .

6.4 Financial Considerations

6.4.1 Recovery

Firstly, in every industry the major focus is always on recovery; for the obvious reason that what is being recovered is of economic value. However, what is less obvious is that achieving high recovery of something with high economic value doesn't necessarily mean that it may be economically exploitable and comes with consequences such as

that of CAPEX and OPEX (discussed in the next point). The optimum results achieved from testing the combination of the stages represented in the respective flow sheets is that by using the caustic cracking route one obtains an overall REE recovery of 89%, whereas for the sulphuric acid crack it is 90%. It should be mentioned that from the results of the sulphuric acid crack we can see that a 99% REE recovery can be achieved after the actual cracking stage but from the subsequent steps carried out, we see from other test work done that approximately 4% during the double salt precipitation step and further an additional 5% during the HCl leach on the converted REOH are lost. This results in the 99% being reduced to an overall REE recovery of 90% from the sulphuric acid cracking route. The question attained from the latter statement now arises, is whether the 1% percent difference in recovery from 89% (in the caustic crack) to 90% (in the sulphuric acid crack) is worth selecting the superior route based on recovery? This will be answered by further scrutiny of the upcoming criteria discussed below.

6.4.2 CAPEX

The dotted circles adjacent to each of the blocks in the flow sheet depicted in Figure 35 contain the equipment wherein the associated step is carried out. Each significant step shall be discussed with regard to its impact on CAPEX. In brief, this circuit comprises of a dryer, a rotary kiln, an elaborate gas handling system, a chiller, three centrifuges, four FRP tanks, and an evaporator.

The first four stages of this acid bake process (the flash dryer, mixer, rotary kiln and chiller) entail a significant portion of the CAPEX; a higher CAPEX to offset the high cost incurred by the most elaborate piece of equipment in the caustic crack i.e. the mild steel autoclave lined with nickel autoclave. This is owed specifically to the cost implicated by the chiller as well as the high shear mixer with special materials of construction.

Coupled with this first part of the sulphuric acid crack is an elaborate gas handling system which is crucially required, as explained in section

6.5. After these first four stages, what follow are seven stages (an equivalent to the entire caustic cracking process) of which an evaporator forms a significant part of the CAPEX. The remainder of the equipment is similar and has already been mentioned earlier in section 5.4.2.

In actual fact when one interprets the CAPEX between the caustic and acid bake, it can be seen that CAPEX in the sulphuric acid crack is approximately twice as much than that of the caustic crack.

TABLE 15: CAPEX FOR ACID BAKE.

Equipment	Number Required	Price per unit	Total Price
		R	R
Scrubbing System	1	2,000,000	2,000,000
Dryer	1	1,000,000	1,000,000
High shear mixer	1	160,000	160,000
Rotary Kiln	1	1,980,000	1,980,000
Chillers for cooling water	1	960,000	960,000
Tanks (30 m^3) PVDF/FRP	4	455,000	1,820,000
Centrifuge	3	320,000	960,000
Evaporator	1	4,000,000	4,000,000
Pumps (including standby)	20	33,000	660,000
TOTAL			13,540,000

6.4.3 OPEX

6.4.3.1 POWER

Unlike the caustic crack which required intermediate temperatures for which it was desired to use heat exchangers to recover the heat of generators (since there is no national grid linkage onsite), the acid bake itself is an energy intensive process which runs at temperatures approximately 280°C for a period of three hours. Thus, such heat exchange is not possible. Thus with the lack of onsite power, energy is a major contributor to the OPEX.

But, even prior to the actual bake the test work discussed earlier emphasizes the effect of initial pulp density on recovery. If the feed

material is not dry, it can be seen that recovery may decrease by as much as 20%. Thus the flash dryer is essential, but it adds additional energy costs to the OPEX. Subsequently, thorough mixing of the acid and monazite concentrate (as mentioned) is crucial, and due the thickness of the pulp formed by prolonged mixing time the energy requirements of a high shear mixer is another contributor to the OPEX of this process. The gas handling system associated with the flash dryer to capture the fine, potentially radioactive active dust particles further contributes to the power segment of the OPEX.

Furthermore, the material produced by the acid bake is at a very high temperature at 280°C - from here it is impossible to leach with water since the solubility of REEs is decreased with higher temperatures. Thus, it is necessary to allow the bake to cool to room temperature batch-wise. But, the water added to this is required to be cooled by a chiller because when the water leach begins, the heat of solution arising from the H_2SO_4 pushes up the solution temperature high enough to impair the solubility of the RE sulphates.

6.4.3.2 REAGENTS

The sulphuric acid for the acid bake needs to be bought in since having an acid plant on site is not justified economically when the production is less than 3000 tpa of TREO, as was established by previous work. For the required acid consumption of 12,000 tpa (as indicated in the mass balance in Appendix B: Mass Balances) it is thus established that purchasing and transporting the acid to the mine is the only option.

The double salt precipitation takes place at a temperature of 90°C together with the reagent Na_2SO_4 which is equivalent to the price of NaOH used in the caustic crack. However, the Na_2SO_4 may be regenerated since the $RENaSO_4$ is converted with excess NaOH (which impacts significantly on the OPEX). But, it is crucial in terms of OPEX to mention that this regeneration involves evaporating the liquid which is certainly an energy intensive process. If the Na_2SO_4 is not dry, double salt precipitation can't occur efficiently, because the recovery was even

impaired due to slight dilution. As can be seen from the mass balance, the Na_2SO_4 recycle is 78%.

The HCl leach takes place at room temperature as opposed to that of 60°C in the caustic crack, which doesn't have any major implications on OPEX in this regard.

This leads to the conclusion that the caustic crack is lower in OPEX associated with heat management and that the reagents are also minimized in this process due to a low energy regeneration, as opposed to a high energy regeneration, of a salt used only for part of the process.

Based on 6121 tpa feed of monazite concentrate of 41% TREO to the hydrometallurgy circuit (required annual throughput to produce the 2700 tpa of TREO production), one may see from the tables below that the reagent costs for the caustic crack is approximately 30% lower than the sulphuric acid cracking. Also, the latter has a power requirement which is almost double.

TABLE 16: POWER REQUIREMENTS FOR THE ACID BAKE.

Equipment	Power Rating (kW)	Total Power (kW)	Cost (R8/kWh) (R3.50/kWh for diesel stipulated)	Cost per annum (operating for 7446 hours)
Scrubbing system	2	2	16	119,136
Flash Dryer (diesel)	4	8	28	208,488
High shear mixer	12	24	192	1,429,632
Rotary Kiln (diesel engine)	30	30	105	781,830
Chiller	40	40	320	2,382,280
Centrifuge	7.5	22.5	180	1,340,280
Evaporator	15	15	120	893,520
Pumps (diesel motor)	3	60	480	3,574,080
TOTAL		**309.5**	**1921**	**9,388,966**

TABLE 17: ASSOCIATED REAGENTS OF THE ACID BAKE.

Reagent	Requirement (tpa)	Price per ton (R)	Cost per year
Sulphuric Acid	12,000	2,138	25,656,000
Sodium Sulphate (first year)	7,573	2,916	22,082,868
Sodium Sulphate (year 2 -20)	1,220	2,916	3,557,520
Caustic	6,057	9,881	59,849,217
HCl	6,113	2,300	14,059,900
Total (year 1)			125,205,505
Total (year 2 up to 20)			103,122,637

6.4.4 NPV

Based on the above CAPEX and OPEX values, the NPV values were calculated over the period of 20 years. The same method mentioned in 5.4.4 was used to calculate the NPV for the sulphuric acid cracking route. As can be seen in Table 18, the basic Ct (net cash flow) was calculated by subtracting the expenses i.e. the total amount for reagents and power from the total income i.e. total amount of REEs produced (2700 tons) by the selling price per kg (R140/kg). This was then used to calculate the Ct value for each year. However, the Ct for the first year was lower due to the sodium sulphate in the first year being different from years 2-20. Thus the Ct for years 2-20 are depicted separately. The Ct for all the years over the life of mine was then added up. The initial total investment which comprised of the amount of the entire project (excluding hydrometallurgy) calculated in previous work i.e. R292M was added together with the cost of the hydrometallurgy circuit based on the CAPEX calculated (R13,540,000). The total of this was subtracted from the total Ct over the life of mine which resulted in a net NPV of ~R1.4B.

TABLE 18: NPV FOR THE ACID CRACK OVER THE 20 YEAR PERIOD

	Ct (Basic Net Cash Flow) year 2-20	(2700*1,000*140)-(103,122,637+9,388,966)	265,488,397
	Ct (Basic Net Cash Flow)	(2700*1,000*140)-(125,205,505+9,388,966)	R243,405,529
	Co	(292,000,000+13,540,000)	R306,640,000
	R		0.14
Net Cash Flow (Ct)	YEAR		
Ct at year 1	1	(243,405,529/(1+14%)^1	R213,513,622
Ct at year 2	2	(265,488,397/(1+14%)^2	R204,284,701
Ct at year 3	3	(265,488,397/(1+14%)^3	R179,197,106
Ct at year 4	4	(265,488,397/(1+14%)^4	R157,190,444
Ct at year 5	5	(265,488,397/(1+14%)^5	R137,886,354
Ct at year 6	6	(265,488,397/(1+14%)^6	R120,952,942
Ct at year 7	7	(265,488,397/(1+14%)^7	R106,099,072
Ct at year 8	8	(265,488,397/(1+14%)^8	R93,069,362
Ct at year 9	9	(265,488,397/(1+14%)^9	R81,639,791
Ct at year 10	10	(265,488,397/(1+14%)^10	R71,613,852
Ct at year 11	11	(265,488,397/(1+14%)^11	R62,819,168
Ct at year 12	12	(265,488,397/(1+14%)^12	R55,104,533
Ct at year 13	13	(265,488,397/(1+14%)^13	R48,337,310
Ct at year 14	14	(265,488,397/(1+14%)^14	R42,401,149
Ct at year 15	15	(265,488,397/(1+14%)^15	R37,193,990
Ct at year 16	16	(265,488,397/(1+14%)^16	R32,626,307
Ct at year 17	17	(265,488,397/(1+14%)^17	R28,619,568
Ct at year 18	18	(265,488,397/(1+14%)^18	R25,104,884
Ct at year 19	19	(265,488,397/(1+14%)^19	R22,021,828
Ct at year 20	20	(265,488,397/(1+14%)^20	R19,317,393
		Ct over 20 years Life of Mine	R1,738,993,376
NET NPV		Ct over 20 years Life of Mine-C	R1,432,353,376

6.5 SHREQ ANALYSIS

The association of thorium with rare earths creates a health hazard problem because of its radioactivity. Thorium disintegrates to radium 224 which in turn disintegrates to radon 220 (thoron) which is a gas that decays to polonium 216 which is a solid. Hence, there is a possibility of respiration of the gas and the deposition of the radioactive decay product in the lungs. In avoiding this problem the caustic crack

poses advantages as opposed to the sulphuric acid crack due to the fact that in the caustic cracking there is no stage whereby the drying of the fine monazite is present, hence any inhalation of radioactive dust is minimised.

During the sulphuric acid cracking experiments, a white vapour was observed. The composition was unknown but the optimization baking test work in other testwork indicated a sulphur loss of 28%, which suggest that the smoke might have been some form of decomposed acid i.e. SO_3 gas. The formation of SO_3 gas is sufficient enough to influence the decision to change to the caustic route due to the severity of SO_3 gas and its implications. This needs scrubbing and neutralization before it can be released into the environment. Again this not only contributes to the SHREQ but also to the CAPEX and OPEX to treat the scrubber blown-down with lime. Thus, one of the major shifts from the sulphuric to caustic is motivated by SHREQ factors hereby mentioned

Further consideration needs to be given to the waste stream of the DSP step (the mother liquor), which contains large amounts of acid, Fe and 50% of the Th content. This stream ultimately poses a high risk and requires intense neutralization before being disposed of. The U (only approximately 600 g/t) also remains in this stream. Thus the radioactive risk is not simply in dust form but in this case in the form of the liquid which can severely impact on the environment. Recovering the Th and U from this stream using ion-exchange is possible, but was not attempted.

In terms of quality, the sulphuric acid crack produces a product similar in quality to that produced when using the caustic cracking method. However, in the latter case this is only achieved when used together with a nitric leach of the apatite prior to cracking. In considering the SHREQ of this pre-treatment step, all that can be said is that the product is $Ca(NO_3)_2$ which can report to the residue containment ponds.

6.6 Effects on Downstream Processes

6.6.1 The Yttrium Problem

During the sulphuric acid cracking route, the product of the water leach tends to be converted from the sulphate form to a hydroxide. As can be seen from the test results (discussed in 6.1.5 and 6.1.6 depicted earlier and in the flow sheet shown in Figure 35) that this was achieved by using double salt precipitation and conversion. However, from the results it is clear that during the double salt precipitation the recovery of the REEs was approximately 95%, thus a 5% loss was experienced. Of this 5% present in this stream, 75% is Y. Although the price of Y has dropped over the years, recovery of this stream at a later stage (if needed) could increase CAPEX and OPEX to the flow sheet, as preliminary test work showed that recovery would be very difficult.

6.6.2 The Thorium Problem

The rare earth ores and commodities, as well as by-products and waste from REEs, are naturally radioactive, mostly because of contained Th and U. As thorium has experienced recent interest to be used as an alternative nuclear fuel, REE recovery is aiming to co-recover Th. This requires evaluating downstream processes in the two process routes. With regard to the acid bake process, during the DSP step, 50% Th goes with the RE stream going forward and 50% Th goes with the 5% RE that are lost. This Th split is highly unattractive, and if Th is to be recovered it needs to be recovered from both paths. This is likely to complicate the process and can be costly.

Looking at the above scenarios, it can be seen that in the caustic cracking route no such complications on downstream processes are encountered, since all the Th and U remain in the solid residue after the HCl leach.

CHAPTER 7

7 CONCLUSIONS AND RECOMMENDATIONS

This chapter will briefly summarise the components which have been investigated and directly affect the ultimate aim of this study i.e. to draw up a trade-off study between the caustic and sulphuric acid bake in terms of the recovery, CAPEX, OPEX, SHREQ and influence on downstream processes.

7.1 CAUSTIC CRACK

- The caustic crack produced optimum results at a NaOH to feed ratio of 2:1 (2000 kg/ton TREE in feed)
- A grind size greater than 75 microns has an effect on caustic cracking (i.e. less recovery), and a 45 micron grind yielded a higher recovery. Hence 45 microns were chosen for process applications.
- The final HCl leach produced a 89% overall TREE recovery and was carried out at a pH = 2 at an acid consumption of 432 kg of 32% HCl/ton of TREE in feed.

7.2 SULPHURIC ACID CRACK

- The recovery of REE improved from 88% to 99.5% when the acid to feed ratio was changed form 1:1 to 2:1, however at a 1.6:1 ratio 99% was achieved and subsequently the latter was chosen as the ratio to be used in process application (1600 kg/t TREE in feed) for dry feed per ton of ore.
- The grind sizes between 45 and 75 microns did not have any significant impact on recovery, hence 45 microns were chosen for process application since the caustic crack was done at this grind size and hence an unprejudiced comparison could be done.
- Other factors investigated included pulp density and feed moisture, however the former had no effect while the latter

indicated that at the process choice of reagent consumption of 1600 kg/t the recovery decreased by approximately 20% at 15% moisture. This indicated that before the bake the feed should be dried, even though this would pose a risk to SHREQ factors and contribute to the CAPEX and OPEX.

- It was decided that since the rare earth sulphates obtained from the bake cannot be recovered directly from solutions, additional steps will be required, including double salt precipitation and caustic conversion. These were tested and indicated that >5% of REE were lost in these steps. These steps also impacted on the CAPEX and OPEX, resulting in a significant increase in both. The losses of REE in these steps were due especially to significant Y losses, and as Y of some interest it would require further downstream recovery processes. Also, a split of Th resulted, with 50% exiting the double salt precipitation in the solids and 50% moving with the liquid. This requires a complex recovery route for Th if it is of interest.
- The resultant HCl leach produced a 90% overall recovery and was carried out at a pH = 2.8 at an acid consumption of 1700 kg of 32% HCl/ ton of TREE in feed.

7.3 TRADE OFF STUDY

TABLE 19: TRADE OFF STUDY.

Factor	Implication	
	Caustic Crack	**Sulphuric Acid Bake**
Recovery	89%	90%
CAPEX	R10,030,000	R13,540,000
OPEX	Power = 140.5 kW	Power = 309.5 kW
	Reagents = R80,727,868	Reagents = R103,122,637
NPV	R1,81B	R1,63B
SHREQ	Minimal	Extreme: SO_3 emissions and excessive dust
Effects downstream	None	Th split and Y loss

As can be seen from Table 19 the caustic cracking is similar to the sulphuric acid cracking route in terms of recovery. However, the former has a CAPEX which is ~26% less than that of the sulphuric acid cracking route. Additionally, the caustic cracking route offers further superiority in terms of OPEX since the power requirement is almost half that of the sulphuric acid route and the reagents almost 22% less. The NPV which encompassed the CAPEX and OPEX for each of the routes respectively shows that the caustic crack produces ~R200M more over the life of mine.

The effect on downstream processes was also more negative in the sulphuric acid crack since there was a 5% loss during the double salt precipitation (DSP), 70% of which was Y. Were Y to be recovered at a later stage, its recovery, necessitating further process steps, would have further implications in the plant's CAPEX and OPEX. In addition to this, Th splits at an almost 1:1 ratio after the DSP step and would require an introduction of two new processing legs.

The SHREQ aspects that were considered identified minimal impact in the caustic crack route. These, however, were quite extreme in the acid crack route, due to the latter containing high volumes of chemically altered effluents as well as the handling of fine dust particles resulting from its numerous drying stages. In addition to this, the main motivation to favour the caustic cracking route was to avoid the SO_3 gas emissions that occurred when using the sulphuric acid cracking route.

Hence, it was concluded that the caustic cracking was superior to the sulphuric acid cracking route when treating SKK monazite.

7.4 RECOMMENDATIONS

- To investigate the effect of having a grind size of less than 45 micron on recovery and its associated OPEX during the caustic cracking of monazite as this may increase recovery further.
- To investigate the complete leaching of material during the HCl leach and find ways of purifying Th and other impurities from the solution without significant implications on CAPEX and OPEX.
- It is recommended to investigate the effect of coarser grind on REE recovery. A coarser grind will be beneficial to the plant because the cost of milling will be decreased and the solid-liquid separation efficiencies will be improved.
- In order to establish more accurate analyses specifically with regards to recovery, it is recommended that when sufficient funding is obtained more assays should be sent for testing so that more appreciation can be given to concepts of statistical significance and experimental error.

8 REFERENCES

Abreu, RD, Morais, CA (2010) "Purification of rare earth elements from monazite sulphuric acid leach liquor and the production of high-purity ceric oxide" *Minerals Engineering*, 23, 536 - 540.

Andreoli, MAG, Smith, CB, Watkeys, M, Moore, JM, Ashwal, RD, and Hart, RJ, (1994) "The Geology of the Steenkampskraal Monazite Deposit, South Africa: Implications for REE-Th-Cu Mineralization in Charnockite-Granulite Terranes." *Econ. Geol.* 89.

Anonymous (2015) "Rare earth elements: Enablers of high tech applications and green energy technologies", http://www.amrmineralmetal.com/download/corporate/REE [2016, 2 June].

Basson, IJ, Muntingh, A, Jellicoe, BC and Anthonissen, CJ (2013) "Structural interpretation of the Steenkampskraal Monazite Mine, Western Cape, South Africa" *Journal of African Earth Sciences.*

Bergmann, C, Khosa, G, Pawlik, C, Sehlotho, N, (2013) "Flowsheet Development for the Steenkampskraal REE deposit", MINTEK, Johannesburg.

British Geological Survey (2011) "Rare Earth Elements", Minerals, UK.

Carlsen, BW, Dixon, BW, Eggert, RG, Jordan, BW, (2015) "Thorium: Crustal abundance, Joint Production and Economic Availability" *Resources Policy*, 44(1), 81-93.

Castor, SB, Hendrick, JB (2016) *Rare Earth Elements,* SME, Michigan.

Constantinides, S (2016) "Market Outlook for Ferrite, Rare Earth and other Permanent Magnets", presented at *The International Forum for Magnetic Applications, Technologies and Materials,* 21 – 22 January, 2016, Jacksonville, Florida.

Gupta, CK, Krishnamurthy, N (2005) *Extractive Metallurgy of Rare Earths,* CRC Press, Florida.

Habashi, F, (2013) “Extractive Metallurgy of Rare Earths, *From Mine to Materials,* 52(3).

Internasional Nickel Company (1963) “Corrosion Resistance of the Austenitic Chromium-Nickel Stainless Steels in Chemical Environments”, International Nickel Company, New York.

Jackson, W, Christiansen, G (1993) “International Strategic Minerals Inventory Summary”, Map Distributor, Denver.

Jones, I, Burnett, M (2013) “Technical Report and Mineral Resource Estimate October 2013, Snowden Group, Perth.

Kilbourne, BT (1993) *A Lanthanide Lanthology*, Molycorp Inc, Mountain Pass California.

Kul, M., Y. Topkaya, and I. Karakaya, *Rare earth double sulfates from pre-concentrated bastnasite.* Hydrometallurgy, 2008. 93(3): p. 129-135.

Mackowski, SJ, Raiter, R, Soldenhoff, KH, Ho, EM (2011) “Recovery of Rare Earth Elements”, US Patent 7,993,612 B2.

Mcketta, JJ (1994) *Encyclopedia of Chemical Processing and Design*, Marcel Dekker INC, New York.

Mkango Resources Ltd (2016) “Background and Trends in the REE market”, http://www.mkango.ca/s/rareearths.asp [2016, January 7].

Moore, BW (2000) “Selective Separation of Rare Earth Elements using Ion Exchange in Aminodiacetic Resin”, US Patent 6,093,376.

Morais, CA, Ciminelli, VST (2004) “Process Development for the Recovery of high-grade Lanthanum using Solvent Extraction”, *Hydrometallurgy*, 73(1), 237 – 244.

Nazari, G. and B. Krysa. Assessment of various processes for rare earth elements recovery (I): A review. *Proceedings of the 52nd conference of metallurgsts (COM)*, hosting by Materials Science Technology Conference (MS&T), October 27 to 31, 2013, Montreal, Quebec, Canada, pp. 325-333

Occidental Chemical Corporation (2013) *Caustic Soda Handbook,* Occidental Chemical Corporation, Texas.

Panda, R., Kumari, A., Jha, M., Hait, J., Kumar, V., Rajesh Kumar, J. and Lee, J. (2014). Leaching of rare earth metals (REMs) from Korean monazite concentrate. *Journal of Industrial and Engineering Chemistry*, 20(4), pp.2035-2042.

Papangelakis, VG, Moldoveanu, G (2014) "Recovery of Rare Earth Elements from Clay Minerals", paper presented at *European Rare Earth Resource Conference*, 4 – 7 September, 2014, Milos.

Rhodia (2009) "Rhodia Products", www.rhodia.com [2017, 8 January].

Seider, W., Seader, J. and Lewin, D. (1999). *Process design principles*. New York: Wiley, pp.39-41.

United States Environmental Protection Agency (2008) "Identification and Description of Mineral Processing Sectors and Waste Streams", https://archive.epa.gov/epawaste/nonhaz/industrial/special/web/html/index-8.html [2017, 8 January].

Van Gosen, BS, Verplanck, PL, Long, KR, Gambogi, J, Seal, RR (2014) "The Rare-Earth Elements — Vital to modern technologies and lifestyles", https://pubs.usgs.gov/fs/2014/3078/ [2017, June 20].

Voncken, JHL (2015) *The Rare-Earth Elements: An Introduction,* Springer International Publishing, Switzerland.

Zepf, V (2013) *A New Approach to the Nexus of Supply, Demand and Use: Exemplified along the use of Neodymium in Permanent Magnets,* Springer, Berlin.

APPENDIX A

CAUSTIC CRACK

TABLE 20: LEACH EFFICIENCY OF PHOSPHOROUS AT DIFFERENT GRIND SIZES FOR THE WHOLE ORE SAMPLE.

Grind size, µm	Leach efficiency, %
45	79
75	76
212	31

TABLE 21: CUMULATIVE METAL EXTRACTION AND HCL CONSUMPTION AT DIFFERENT PH LEVELS AT 60°C.

pH	TREE	P	Th	Consumption, kg 32% HCl/ton ore
3.5	70	0	0	273
3.0	74	0	3	383
2.5	76	0	13	469
2.0	77	0	41	661
1.5	75	2	85	930
1.0	74	2	90	948
0.5	73	12	61	1084
0.2	68	28	44	1440

TABLE 22: IMPURITY DISSOLUTION AT DIFFERENT PH LEVELS AT 60°C.

pH	Na	Mg	Al	Ca	Cu	Th
3.5	59	38	1	34	40	0
3.0	55	40	11	32	51	3
2.5	54	45	24	32	55	13
2.0	56	68	45	36	64	41
1.5	54	77	60	31	71	85
1.0	56	78	57	34	68	90
0.5	56	77	58	49	67	61
0.2	72	75	63	65	73	44

TABLE 23: CUMULATIVE EXTRACTION OF REES AT DIFFERENT PH LEVELS AT 60°C.

pH	La	Ce	Pr	Nd	Y	Sm	Dy	Ho
3.5	67	76	60	73	65	72	62	63
3.0	72	81	66	79	66	78	66	66
2.5	75	86	68	81	69	80	68	68
2.0	75	88	70	84	76	83	72	72
1.5	75	86	70	83	73	82	72	69
1.0	75	87	69	83	75	82	71	67
0.5	77	88	69	82	76	81	71	69
0.2	71	86	70	83	73	79	71	66

TABLE 24: TOTAL REE RECOVERYOF THE SAMPLES AT DIFFERENT GRIND SIZES.

	Whole ore TREE efficiency %	Non-mags TREE efficiency %	Monazite concentrate TREE efficiency %
95%-45µm	76	78	89
95%-75 µm	75	69	85

TABLE 25: LEACH EFFICIENCY OF THE INDIVIDUAL REES IN THE WHOLE ORE SAMPLE AT DIFFERENT GRIND SIZES.

	La, %	Ce, %	Pr, %	Nd, %	Y, %	Sm, %	Gd, %	Dy, %	Er, %
95%-45µm	78	77	77	77	74	77	49	73	71
95%-75µm	75	77	80	80	70	79	26	75	67

TABLE 26: RECOVERY FOR INDIVIDUAL REES IN THE NON MAGS SAMPLE AT DIFFERENT GRIND SIZES.

	La, %	Ce, %	Pr, %	Nd, %	Y, %	Sm, %	Gd, %	Dy, %	Er, %
95%-45µm	80	80	79	80	65	70	41	66	60
95%-75 µm	69	68	69	68	67	80	5	73	65

TABLE 27: FILTRATE ELEMENTAL COMPOSITION OF THE DIFFERENT SAMPLES.

	Whole ore 45 µm	Whole ore 75 µm	Non mags 45 µm	Non mags 75 µm	Monazite conc. 75 µm	Monazite conc. (HNO_3) 45 µm
TREE, %	0.043	0.045	0.044	0.043	0.118	0.084
Mg, %	0.263	0.265	0.373	0.035	2.624	0.157
Al, %	0.923	2.846	2.277	0.06	4.01	0.182
Ca, %	4.225	3.654	5.358	0.485	17.662	2.352
Mn, %	0.052	0.084	0.112	0.0028	0.087	0.007
Fe, %	1.339	0.854	0.85	0.08	10.456	0.365
Ni, %	0.063	0.0415	0.068	0.0014	0.252	0.07
Cu, %	2.672	1.358	3.319	0.074	1.458	0.03
Zn, %	0.021	0.027	0.0098	0.001	0.007	0.005
Th, %	0.356	2.082	0.889	0.201	4.572	7.853
U, %	0.045	0.09	0.00033	0.0015	0.0014	0.00033

TABLE 28: OVERALL RECOVERY OF THE THREE SAMPLES TESTED.

	Whole ore	LIMS product	Monazite conc.
Final REE % recovery to PLS,	79	75	77
REE leach efficiency, %	79	78	89
Total HCl addition, kg 32% HCl/ton feed	733	716	292
SMBS addition, kg/ ton leach feed	0	0	9.1

TABLE 29: TOTAL REE LEACH EFFICIENCY OF THE SAMPLES AT DIFFERENT GRIND SIZES.

	Whole ore	Non mags	Monazite concentrate
95%-45 µm	76	78	85
95%-75 µm	75	69	89

SULPHURIC ACID CRACK

TABLE 30: LEACH EFFICIENCY OF THE ACID BAKE AT DIFFERENT SULPHURIC ACID DOSAGES.

	Leach efficiency, %			
Acid, kg/ ton feed	**TREE**	**LREE**	**HREE**	**MREE**
1000	88	89	85	80
1200	93	94	86	84
1400	96	96	90	96
1600	98	99	94	97
1800	98	98	93	97
2000	99.7	99.8	98.1	99.5
2500	99.7	99.4	98	99.4

TABLE 31: SOLID-BASED REE LEACH EFFICIENCIES AT DIFFERENT PULP DENSITIES.

	Element, % (m/m)			
pulp density, % (m/m)	**TREE**	**LREE**	**HREE**	**MREE**
20	98	98	94	96
25	94	95	87	90
30	98	99	94	97
35	98	99	94	97
40	99	99	95	98

TABLE 32: SOLID-BASED METAL LEACH EFFICIENCIES AT DIFFERENT PULP DENSITIES.

	Element, % (m/m)							
Pulp Density	Fe	Si	Al	Cu	Zn	Th	P	S
20	82	9	92	98	86	94	81	95
25	82	9	91	98	86	93	89	93
30	69	7	78	96	81	91	66	90
35	72	6	80	98	81	93	79	90
40	72	6	79	97	83	97	81	92

TABLE 33: ELEMENTAL COMPOSITION OF THE WATER LEACH FILTRATE AT DIFFERENT PULP DENSITIES.

	Pulp Density, %				
Element, g/L	20	25	30	35	40
TREE	33.96	41.216	48	55.54	73.894
HREE	1.64	1.904	2.145	2.415	2.995
LREE	30.782	37.471	43.748	50.681	67.867
MREE	1.511	1.805	2.07	2.402	2.976
P	11.252	14.006	14.808	16.978	21.687
Al	3.301	4.219	3.814	4.352	5.824
La	7.326	9.017	10.747	12.094	14.557
Pr	1.603	1.934	2.3	2.671	3.322
Nd	6.059	7.298	8.536	10.004	12.386
Y	1.152	1.344	1.513	1.697	2.137
Sm	0.946	1.134	1.304	1.52	1.892
Gd	0.545	0.648	0.738	0.85	1.045
Dy	0.285	0.326	0.37	0.419	0.5
Fe	11.652	12.411	11.979	12.125	17.77
Cu	1.745	2.232	2.571	2.97	3.865
Zn	0.027	0.033	0.039	0.044	0.053
Th	5.268	6.504	7.808	9.377	11.672
S	64.65	56.093	62.021	72.78	90.697

TABLE 34: SOLID-BASED METAL EXTRACTION AT DIFFERENT MOISTURE CONTENTS.

	0 % moisture content		15% moisture content	
	extraction at 1600 kg/ton acid dosage, %	extraction at 1800 kg/ton acid dosage, %	extraction at 1600 kg/ton acid dosage, %	extraction at 1800 kg/ton acid dosage, %
TREE	98	98	80	99
LREE	99	98	80	99
HREE	97	97	75	99
MREE	79	79	77	30
Fe	92	90	60	38
Al	99	97	87	98
Cu	86	83	86	91
Th	76	73	92	93
P	94	92	90	92
S	11	8	0	0
Si	94	93	86	96

TABLE 35: SOLID-BASED EXTRACTION AT DIFFERENT GRIND SIZES.

	Grind Sizes	
	Solid-based extraction at 95%-45 µm, %	**Solid-based extraction at 95%-75 µm, %**
La	92	88
Ce	89	88
Pr	87	90
Nd	85	90
Y	86	86
Sm	81	87
Gd	80	86
Dy	81	86
TREE	95	95
LREE	94	94
MREE	94	94
HREE	85	86
Fe	59	78
Al	50	63
Cu	97	89
Zn	92	70
Th	84	79
P	81	91
S	81	75
Si	14	19

TABLE 36 : METAL PRECIPITATION EFFICIENCIES.

Element, unit	Pilot DS 1	Pilot DS 2
TREE **	95.2%	96.5
TREE excl. Ce **	91.5%	94.2
L+MREE **	99.8%	99.5
MREE **	99.5%	99.8
HREE **	32.6%	44.6
Al	17%	15
Ca	69%	74
Fe	13%	22
Ni	2%	1
Cu	1%	1
Zn	2%	2
Th	45%	15
U	0%	0
P	3%	7
S	12%	20
Si	12%	84
Pb	55%	58

TABLE 37: SUMMARY OF RESULTS: REE LEACH CONDITIONS, FEED AND RESIDUE COMPOSITIONS, REAGENT CONSUMPTIONS AND LEACH RECOVERIES.

Conditions and test outcome	
Feed source	Dried REE hydroxide
Initial pulp density, % (m/m)	33
Reagent	32% (m/m) HCl
Reagent consumption, kg 32% (m/m) HCl /kg TREE	1.7
Residence time, hours	3
Test temperature, °C	Ambient
Final temperature, °C	60
Final pH	~2.9

Final redox potential (Eh), mV		438
Final pulp density,%		3.9
Density of filtrate solution, t/m³		1.2
Density of residues, t/m³		-
Mass loss,%		43
Elemental composition of feed and residues		
Element, unit	**Feed**	**Residues**
TREE, % (m/m)	59	50
LMREE, % (m/m)	54	49
MREE, % (m/m)	2.8	0.4
HREE, % (m/m)	1.7	0.5
Al, % (m/m)	1	1.5
Ca, % (m/m)	1.2	0.5
Fe, % (m/m)	1.7	2.5
Cu, mg/kg	206	45
P, % (m/m)	0.9	1.4
S, % (m/m)	0.2	0.3
Solid-based metal leach efficiency		
Y		93%
TREE		52%
TREE		94%
LREE		48%
MREE		91%
HREE		85%
Al		9%
Ca		79%
Fe		16%
Cu		88%
P		15%

TABLE 38: ELEMENTAL COMPOSITION: FEED, FILTRATE SOLUTION AND WASH LIQUOR.

Element, unit	Pilot DS 1			Pilot DS 2		
	Feed	Filtrate	Combined washes	Feed	Filtrate	Combined washes
La, mg/L	6819	0.14	54	10024	41	138
Ce, mg/L	13906	26	82	20355	158	220
Pr, mg/L	1412	15	12	2127	7	22
Nd, mg/L	5227	12	30	7924	10	76
Sc, mg/L	27	19	0	29	19	1
Y, mg/L	1491	1134	61	1683	1149	18
Sm, mg/L	813	2	8	1219	4	14
Eu, mg/L	18	0	0	27	0	0
Gd, mg/L	532	5	10	744	0	7
Tb, mg/L	34	21	2	43	20	0
Dy, mg/L	323	135	15	462	133	11
Ho, mg/L	52	29	1	61	28	0
Er, mg/L	97	79	7	145	74	4
Tm, mg/L	9	6	1	0	4	0.1
Yb, mg/L	50	44	2	48	40	0.2
Lu, mg/L	6	6	0	6	5	0
TREE, mg/L	30815	1533	285	44898	1691	512
TREE excl Ce, mg/L	16909	1507	204	24543	1533	291
LREE, mg/L	27364	53	178	40430	215	457
MREE, mg/L	1362	7	18	1990	4	21
HREE, mg/L	2062	1454	89	2449	1452	33
Al, g/L	3.6	3.8	0.16	4	4	0.04
Ca, g/L	0.9	0.94	0.06	1	1	0.02
Fe, g/L	8.5	8.61	0.36	7	7	0.04
Co, mg/L	6	6.5	0.26	10	10	0.3

Ni, mg/L	25	41	3	42	74	1
Cu, mg/L	1.9	2.00	0.09	2	2	0.03
Zn, mg/L	37	41	2.9	36	46	3
Th, g/L	7.2	4	0.1	8	4	0.01
U, mg/kg	197	159	7.7	267	176	4
P, g/L	19	18.7	0.6	23	22	0.13
S, g/L	101	139	12.3	95	115	3
Si, mg/L	5.3	23.8	0.2	383	68	0.49
Pb, mg/L	6.1	1.5	1.5	7	6	6

TABLE 39: REE DOUBLE SALT PRECIPITATION CONDITIONS AND REAGENT CONSUMPTIONS.

Feed source	**Pilot WL-1**	**Pilot WL-2**
Density of feed solution, t/m³	1.2	1.25
Reagent	Na_2SO_4	Dry Na_2SO_4
Reagent addition, kg/kg TREE	6.0	3
Reagent stoichiometric excess, %	580	341
Residence time, hours	2	2
Final temperature, ˚C	90	85
Final pulp density, %	8.2	8.7
Density of filtrate solution, t/m³	1.2	1.25
Density of residues/precipitate solids, t/m³	0.56	0.57

TABLE 40 : ELEMENTAL COMPOSITION OF THE REE DOUBLE SALT PRECIPITATE.

Element, unit	Pilot DS 1	Pilot DS 2
TREE, % (m/m)	30.4	31.6
TREE excl. Ce, % (m/m)	16.6	17.4
LREE, % (m/m)	28	28.8
MREE, % (m/m)	1.4	1.6
HREE, % (m/m)	0.9	1.1
Al, % (m/m)	0.6	0.5
Ca, % (m/m)	0.6	0.6
Fe, % (m/m)	1.1	1.5
Co, µg/g	8.5	24.7
Ni, µg/g	4.4	4.2
Cu, µg/g	172	0.0
Zn, µg/g	6.0	7.1
Th, % (m/m)	3.1	1.1
U, µg/g	1.3	2.2
P, % (m/m)	0.6	1.4
S, µg/g	16.5	17.1
Si, %	6	0.6
Pb, µg/g	32.4	37.4

TABLE 41: REE DOUBLE SALT CONVERSION TEST CONDITIONS AND SUMMARY OF RESULTS.

Test conditions	
Feed source	REE double salt
Density of feed solids, t/m³	
Feed moisture content, % (m/m)	35
Initial pulp density,% (m/m)	30.9
Reagent	4M NaOH
Reagent addition, kg (100% NaOH)/kg TREE	1
Reagent stoichiometric excess, %	15
Residence time, hours	2
Final temperature, ºC	92
Final pH	9.1
Final redox potential (Eh), mV	-100
Final pulp density,%	19.4
Density of filtrate solution, t/m³	1.2
Density of residues, t/m³	
Mass loss,%	48
By-product	Na_2SO_4
Concentration of Na_2SO_4 solution, % (m/m)	52
Elemental composition of the REE hydroxide precipitate	
Ce, % (m/m)	26.5
TREE, % (m/m)	58.8
TREE excl. Ce, % (m/m)	32.2
LREE, % (m/m)	54.2
MREE, % (m/m)	2.8
HREE, % (m/m)	1.7
Al, % (m/m)	1.0
Ca, % (m/m)	1.2
Fe, % (m/m)	1.7
Th, % (m/m)	6.0

P, % (m/m)	0.9
Na, % (m/m)	0.1
S, % (m/m)	0.2
Solids based metal efficiency	
TREE**	0.2%
Al	16%
Fe	16%
Th	1%
P	25%
S	99.5%
Elemental composition of filtrate solution	
TREE, mg/L	25
S, g/L	129
Na, g/L	35
Al, mg/L	24
Zn, mg/L	0.3
Th, mg/L	2.2
Pb, mg/L	2
Si, mg/L	37

APPENDIX B: MASS BALANCES

CAUSTIC CRACK MASS BALANCES

TABLE 42: CAUSTIC CRACK MASS BALANCE

Stream Number		1	2	3	4	5	6	7	8
Stream description		Monazite Concentrate	Nitric Acid @60%HNO_3	Nitric Leach output	Apatite leach filter cake	Fresh caustic	Recycled caustic	Caustic Crack Output	Repulp Water
Solids mass	tpa	7635.7		6246.2	6121.00	3235.22		4600.01	
%solids	%w/w	45%		28.1%	90%	100%		32%	
solution/water	tpa	9332.5	9124.4	16007.8	680.01		5480.51	10593.76	4194.20
solids density	t/m^3	2.5		2.8	2.80	2.00		2.50	
solution/water density	t/m^3	1	1.5	1.25	1.00		1.30	1.40	1.00
total density	t/m^3	1.4	1.5	1.5	2.37	2.00	1.30	1.62	1.00
solids volume	m^3/a	3054.3		2230.8	2186.07	1617.61		1840.00	
solution volume	m^3/a	9332.5	6082.9	12806.3	680.01		4215.78	7566.97	4194.20
total volume	m^3/a	12386.8	6082.9	15037.3	2866.08	1617.61	4215.78	9406.97	4194.20
total mass	tpa	16968.2	9124.4	22254.1	6801.01	3235.22	5480.51	15193.77	4194.20
continous/batch	_	Batch	Batch	Batch	batch	batch	batch	batch	batch
ThO2	tpa	453.6		453.6	437.06			437.06	
TREO	tpa	3130.6		3130.6	3099.33			3099.33	

Stream Number		9	10	11	12	13
Stream description		Repulped Slurry	Caustic Filtrate	Feed to evaporator	TSP crystallization output	Caustic Filter Cake
Solids mass	tpa	4600.04			2271.40	4600.04
%solids	%w/w	25%			29%	80%
solution/water	tpa	14787.96	14787.96	11830.37	5480.51	1150.00
solids density	t/m^3	2.50			2.50	2.50
solution/water density	t/m^3	1.35	1.35	1.35	1.35	1.00
total density	t/m^3	1.52	1.35	1.35	1.56	1.92
solids volume	m^3/a	1840.02			908.56	1840.02
solution volume	m^3/a	10954.04	10954.04	8763.23	4059.64	1150.00
total volume	m^3/a	12794.06	10954.04	8763.23	4968.20	2990.02
total mass	tpa	19388.00	14787.96	11830.37	7751.91	5750.04
continous/batch	_	batch	batch	batch	batch	batch
ThO2	tpa	437.06	0.87	0.70	0.70	436.36
TREO	tpa	3099.33	6.20	4.96	4.96	3093.13

Stream Number		14	15	16	17
Stream description		Repulp Water	Hydrochloric Acid @32% HCl	HCl selective leach output	Selective Leach PLS
Solids mass	tpa			1470.80	
%solids	%w/w			8.1%	
solution/water	tpa	7392.87	6512.90	16742.81	16742.81
solids density	t/m^3			2.00	
solution/water density	t/m^3	1.00	1.40	1.20	1.20
total density	t/m^3	1.00	1.40	1.24	1.20
solids volume	m^3/a			735.40	
solution volume	m^3/a	7392.87	4652.07	13952.34	13952.34
total volume	m^3/a		4652.07	14687.74	13952.34
total mass	tpa	7392.87	6512.90	18213.61	16742.81
continuous/batch	_	batch	batch	batch	batch
ThO2	tpa				
TREO	tpa			3093.13	2783.82

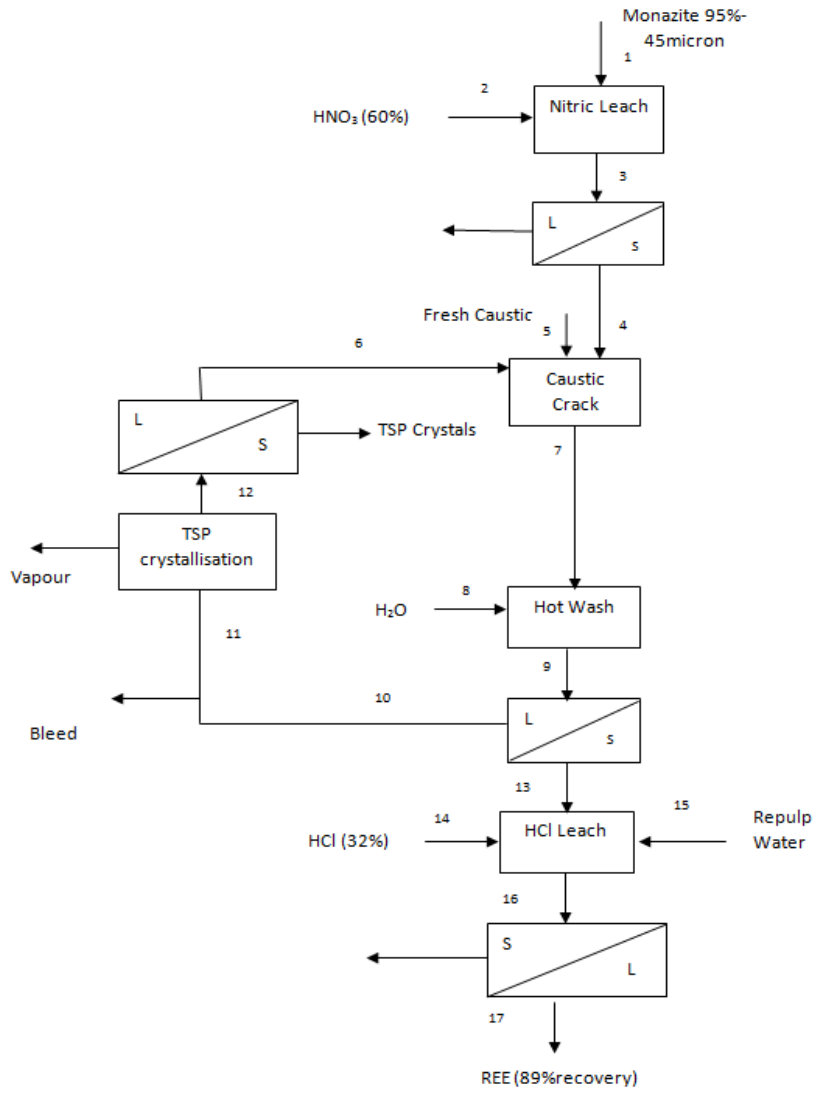

FIGURE 36: FLOW SHEET FOR THE CAUSTIC CRACK INDICATING STREAM NUMBERS AS PER THE MASS BALANCE

SULPHURIC ACID BAKE MASS BALANCES*

TABLE 43: SULPHURIC ACID BAKE MASS BALANCE

Stream Number		1	2	3	4	5
Stream description		Monazite concentrate	Dried Monazite Concentrate	Sulphuric Acid (98%)	Acid Bake Feed	Baked product
Solids mass	tpa	7500	7500		7500	15897
%solids	%w/w	60%	100%		38.50%	100%
solution/water	tpa	5000		12000	12000	3281
solids density	t/m^3	2.8	2.8		2.8	1.1
solution/water density	t/m^3	1		1.8	1.8	
total density	t/m^3	1.6	2.8	1.8	2.1	1.1
solids volume	m^3/a	2678	2678		2678	15140
solution volume	m^3/a	5000		6666	8571	
total volume	m^3/a	7678	2678	6666	11249	15140
total mass	tpa	12500	7500	12000	19500	19178
continous/batch	_	batch	batch	batch	batch	batch
ThO2	tpa	431	431		431	431
TREO	tpa	3061	3061		3061	3061

Stream Number		6	7	8	9	10
Stream description		Water	Water leach Ouput	Water leach PLS	Dry Sodium Sulphate	Double Salt PPt Ouput
Solids mass	tpa		1403		7573	7623
%solids	%w/w		3.50%		100%	14.20%
solution/water	tpa	23845	38340	38340		45970
solids density	t/m^3		0.54		2.7	0.57
solution/water density	t/m^3	1	1.25	1.3		1.2
total density	t/m^3	1	1.2	1.3	2.7	1
solids volume	m^3/a		2595		2805	13373
solution volume	m^3/a	23845	30672	30672		31956
total volume	m^3/a	23845	33267	30672	5610	45329
total mass	tpa	23845	39743	38340	15147	53593
continous/batch	_	batch	batch	batch	batch	batch
ThO2	tpa		431	427		427
TREO	tpa		3061	3030		3030

Stream Number		11	12	13	14	15
Stream description		Double Salt PPT Solids	Caustic	Double Salt Conversion out put	Double Salt Conversion Filtrate	Double Salt Conversion Solids
Solids mass	tpa	7623		3836		3836
%solids	%w/w	70%		28.10%		80%
solution/water	tpa	3267	6057	9824	9824	959
solids density	t/m^3	0.57		1.38	1.38	1.38
solution/water density	t/m^3	1	1.4	1.2	1.2	1.2
total density	t/m^3	0.6	1.4	1.2	1.2	1.4
solids volume	m^3/a	13373		2779		2779
solution volume	m^3/a	3267	4326	8187	8187	799
total volume	m^3/a	16640	4326	10966	8187	3578
total mass	tpa	10890	6057	13660	9824	4795
continous/batch	_	batch	batch	batch	batch	batch
ThO2	tpa	213		213	0.4	213
TREO	tpa	2909		2909	6**	2903

Stream Number		16	17	18	19
Stream description		Repulp Water	Hydrochloric Acid	HCl Selective leach Output	Selective leach PLS
Solids mass	tpa			515	
%solids	%w/w			3.40%	
solution/water	tpa	5000	6113	14458	14458
solids density	t/m^3			1.4	
solution/water density	t/m^3	1	1.4	1.2	1.2
total density	t/m^3	1	1.4	1.2	1.2
solids volume	m^3/a			365	
solution volume	m^3/a	5000	4367	12048	12048
total volume	m^3/a	5000	4367	12413	12048
total mass	tpa	5000	6113	14973	14458
continuous/batch	_	batch	batch	batch	batch
ThO2	tpa			213	14
TREO	tpa			2903	2728

*This mass balance does not take into account wash efficiencies ** no rare earth hydroxide is expected to go into solution due to extremely alkaline pH environment and therefore probably assay detection limit

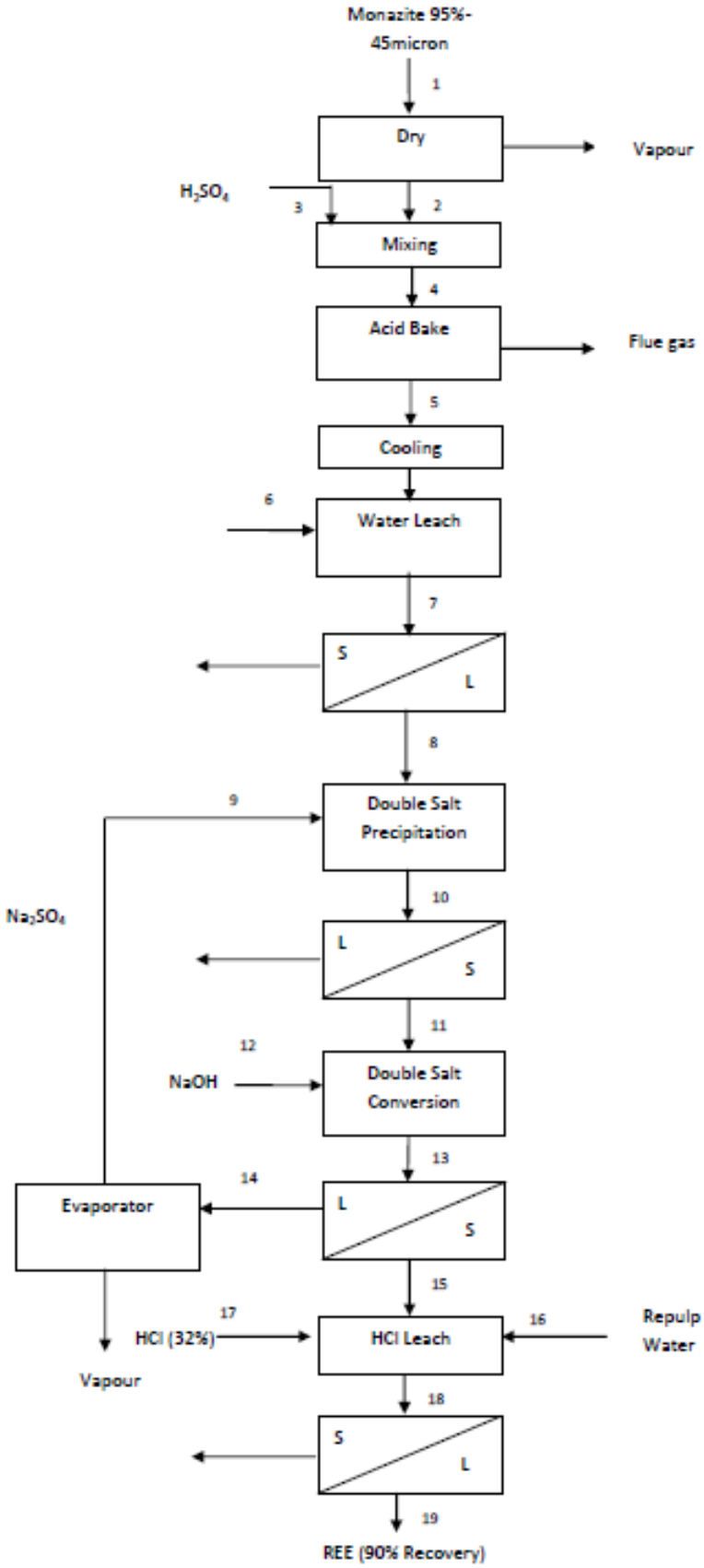

FIGURE 37: FLOW SHEET FOR THE SULPHURIC ACID CRACK INDICATING STREAM NUMBERS AS PER THE MASS BALANCE

EQUIPMENT SIZING EXAMPLE

Let us use the sizing of the double salt precipitation vessel as an example:

As can be seen from Figure 37, two streams flow into this vessel i.e. stream 8 and stream 9. From the mass balance it can be deduced that the total volume in will be:

Total Volume **into** vessel= Volume of stream 8+ Volume of stream 9

=30672+5610

=36282 m^3/annum

Based on the assumptions in Table 9, we can see that the amount of batches is 1862.

The volume per reactor is thus 36282 m^3per annum/1862= 19.48m^3 per batch going into this reactor. However, this 19m^3 was then assumed to be filled to 80% capacity. This results in 23.75m^3. Thus a 25m^3 was chosen because the supplier manufactures tanks of this magnitude.

But, let us look at the material going out of the vessel:

Total Volume **out** of vessel= Volume of stream 10

=45329m^3/annum

Based on the assumptions in Table 9, we can see that the amount of batches is 1862. The volume per reactor is thus 45329 m^3 per annum/1862= 24.34m^3 per batch going into this reactor. However, this 24.34m^3 was then assumed to be filled to 80% capacity. This results in 30m^3.

Thus between the 25m^3 and 30m^3, the 30m^3 as it is the greater of the two.